Innovative processes for the production of new nanocomposite materials by electrospinning technique

Benito Eduardo Valarezo Valdez

Department of Chemical and Food Engineering

Ph.D. Course in Chemical Engineering
(IV Cycle-New Series)

Innovative processes for the production of new nanocomposite materials by electrospinning technique

Supervisor
Prof. Vittoria Vittoria

Ph.D. student
Eduardo Valarezo

Scientific Referees
Prof. Ernesto Reverchon
Prof. Omar Malagón

Ph.D. Course Coordinator
Prof. Paolo Ciambelli

To my dear family…

Acknowledgments

Son tantos los nombres que deberían incluirse en esta interminable lista, tantas aportaciones, unas grandes otras pequeñas, aportaciones en todos los ámbitos desde lo económico hasta lo sentimental y lo espiritual, todas igual de importantes, mi temor mas grande es dejar sin nombrar a alguno de ustedes, por lo que digo gracias, gracias a todos.

A Dios, gracias por cuidarme
A mi esposa Diana, por ser mi amor
A mis hijos Renata y Jean Paul, que son mi inspiración
A mis padres Yolanda y Noe, por darme la vida
A mis hermanos Angel, Carmen, María, Hugo y Carlos
A mis compañeros, amigos,…..

A la Universidad Técnica Particular de Loja, en especial al Dr. Omar Malagón por permitir y apoyar este ambicioso sueño y a todos mis compañeros del Departamento de Química por haber dado un nuevo sentido a la palabra compañerismo.

Un agradecimiento especial a la Profesora Vittoria Vittoria que me enseño que no existe problema sin solución, a Loredana, Valeria y todo el personal del Laboratorio I4 que me hicieron sentir como en casa.

Al Profesor Ernesto Reverchon que me enseño que es posible plasmar las ideas en equipos innovativos, a Renata Adami por abrir una ventana y dejarme ver la calidez del pueblo italiano, a Mariarosa Scognamiglio, Miguel Meneses y a todo el equipo del Laboratorio T9.

A La Secretaría Nacional de Educación Superior, Ciencia, Tecnología e Innovación de Ecuador por el apoyo financiero.

Eduardo

Publications list

- **Valarezo E.,** Stanzione M., Tammaro L., Cartuche L., Malagón O. and Vittoria V., (2012). Preparation, characterization and antibacterial activity of poly(ε-caprolactone) electrospun fibers loaded with amoxicillin for controlled release in biomedical applications. *Journal of Nanoscience and Nanotechnology*, *In Press*.

- **Valarezo E.,** Tammaro L., Malagón O. and Vittoria V., (2012). Tunable delivering of amoxicillin from poly(lactic acid)/poly(ε-caprolactone) blend fibers: preferred encapsulation of amoxicillin in polylactide. *Journal of Applied Polymer Science*, submitted.

- **Valarezo E**., Tammaro L., González S., Malagón O. and Vittoria V., (2012). Fabrication and sustained release properties of poly(ε-caprolactone) electrospun fibers loaded with layered double hydroxide nanoparticles intercalated with amoxicillin. *Applied Clay Science*, *In Press*.

- Stanzione M., **Valarezo E**. and Vittoria V., (2011). Controlled release of amoxicillin encapsulated into PCL electrospun nano fibers for biomedical applications. *Nanodrug Delivery: from the bench to the patient, Consiglio Nacionale delle Ricerche*, 10-13 October, Rome, Italy.

- **Valarezo E.,** Stanzione M., Tammaro L., Cartuche L., Malagón O. and Vittoria V., (2012). Encapsulation of amoxicillin into poly(ε-caprolactone) electrospun fibers for biomedical applications. *XIII Simposio Latinoamericano de Polímeros, XI Congreso*

Iberoamericano de Polímeros y V Conferencia Andina PVC y Sustentabilidad (SLAP 2012), 23-26 September, Bógota, Colombia.

- **Valarezo E.,** Tammaro L., Cartuche L., Malagón O. and Vittoria V., (2012). Uso de la técnica "electrospinning" para la producción de materiales poliméricos nanocompuestos. *XIII Simposio Latinoamericano de Polímeros, XI Congreso Iberoamericano de Polímeros y V Conferencia Andina PVC y Sustentabilidad (SLAP 2012)*, 23-26 September, Bógota, Colombia.

Index

II

Figures Content

Table Content

x

Abstract

The technical parameters for electrospinning solutions of biodegradable polymers poly(ε-caprolactone), poly(lactic acid) and their composites with active molecules were defined and set up. A trial-and-error approach has been employed by varying solution properties and processing parameters to obtain uniform defect-free fibers. Amoxicillin drug was intercalated in layered double hydroxide nanoparticles by coprecipitation and then the modified nanohybrid was successfully encapsulated at different concentrations into poly(ε-caprolactone) matrix by the electrospinning technique. Non-woven fibrous mats were fabricated and characterized in terms of morphology, *in vitro* release and antibacterial properties.

Blends of poly(lactic acid) and poly(ε-caprolactone), loaded with different amounts of amoxicillin were electrospun to investigate the release behaviour and obtain a controlled and tuneable release. Morphology and thermal behaviour were found dependent on the component ratio as well as on the incorporated drug amount.

Introduction

Electrospinning is a versatile method to process solutions or melts, mainly of polymers, into continuous fibers with diameters ranging from a few micrometers to a few nanometers. This technique is applicable to virtually every soluble or fusible polymer. The polymers can be chemically modified and can also be tailored with additives ranging from simple carbon-black particles to complex species such as enzymes, viruses, and bacteria. Electrospinning appears to be straightforward, but is a rather intricate process that depends on a multitude of molecular, process, and technical parameters. The method provides access to entirely new materials, which may have complex chemical structures. Electrospinning is not only a focus of intense academic investigation; the technique is already being applied in many technological area. The Electrospinning is currently the only technique that allows the fabrication of continuous fibers with diameters down to a few nanometers. The method can be applied to synthetic and natural polymers, polymer alloys, and polymers loaded with chromophores, nanoparticles, or active agents, as well as to metals and ceramics. Fibers with complex architectures, such as core–shell fibers or hollow fibers, can be produced by special electrospinning methods. It is also possible to produce structures ranging from single fibers to ordered arrangements of fibers. Electrospinning is not only employed in university laboratories, but is also increasingly being applied in industry. The scope of applications, in fields as diverse as optoelectronics, sensor technology, catalysis, filtration, and medicine, is very broad.

Electrospun nanofibers are broadly applied in biomedical applications, as tissue engineering scaffolds, in wound healing, drug delivery, filtration, as affinity membrane, in immobilization of enzymes, small diameter vascular graft implants, healthcare, biotechnology, environmental engineering, defense and security, and energy storage and generation and in various researches that are on-going (Ramakrishna et al., 2006). Since the early 1980's, electrospun polymer nanofibers have already been proposed for vascular and breast prostheses applications(Bhardwaj and Kundu, 2010). A number of US patents have been issued on fabrication methods and

techniques for these prostheses such as, covering vascular prostheses, and for breast prosthesis has been disclosed in a US patent. Reviewing the number of patents, we can see that approximately two-thirds of all electrospinning applications are in the medical field. Of the remaining patents, one-half deals with filtration applications, and all other applications share the remaining half. Owing to application of these nanofibers in diverse fields, various research and developments are going in the fields of electrospinning (Burger et al., 2006).

In the recent literature shows the tendency to the production of nanofibers nanocomposite for biomedical applications, applications are becoming more specific, so it should work with biodegradable polymers with specific characteristics and suitable properties, likewise the drug should be chosen carefully for our future research will have repercussions.

The aim of this work is to study and optimize electrospinning process for the production of nanofibers and nanocomposites nanofibers.

The principal objective of the work is the production of micro and nanofibers of polymers loaded with active molecules.

For the production of micro-and nanofiber nanocomposite are several parameters that should be taken into account, also take into consideration the drug release profiles and the biodegradability of the polymer. This work will focus on the following point: study of different polymer solution parameters (Concentration, viscosity, conductivity, surface tension, dielectric constant); study of different processing conditions (voltage, federate, temperature, diameter of needle, distance between tip and collector); study of ambient parameters (humidity, type of atmosphere, pressure); product characterizations (solid state characterization, drug loading, release profiles); mathematical modelling of release kinetics of a selected systems of interest.

Chapter I

Electrospinning

I.1 Introduction

In the late 1500s William Gilbert set out to describe the behaviour of magnetic and electrostatic phenomena. His work is an early example of what would become the modern scientific method (Gilbert, 1600). He received funding from Queen Elizabeth I, whereupon he moved to London, caught bubonic plague, and passed away. He had, however, already distinguished between the magnetic forces arising from a lodestone (natural magnet) and the electrostatic forces arising from rubbed amber. One of his more obscure observations was that when a suitably charged piece of amber was brought near a droplet of water it would form a cone shape and small droplets would be ejected from the tip of the cone the first recorded observation of electrospraying.

The first description of a process recognisable as electrospinning was in 1902 when J. F. Cooley filed a United States patent entitled "Apparatus for electrically dispersing fibres" (Cooley, 1902). In his patent he describes a method of using high voltage power supplies to generate yarn. Even at this early stage it was recognised that to form fibres rather than droplets the (i) fluid must be sufficiently viscous, (ii) solvent volatile enough to evaporate to allow regeneration of the solid polymer, and (iii) electric field strength within a certain range.

The next significant academic development was achieved by John Zeleny, who published work on the behaviour of fluid droplets at the end of metal capillaries in 1914 (Zeleny, 1914). His work began the efforts to mathematically model the behaviour of fluids under electrostatic forces. Between 1964 and 1969, Sir Geoffrey Ingram Taylor produced the theoretical underpinning of electrospinning (Taylor, 1964, 1966, 1969).

Taylor's work on electrostatics was performed during his retirement after a broad career including modelling of turbulent mixing of air at the Arctic, significant contributions to the fields of fluid mechanics and solid mechanics via work on the Manhattan Project and development of supersonic aircraft. Taylor's work contributed to electrospinning by mathematically modelling the shape of the cone formed by the fluid droplet under the effect of an electric field; this characteristic droplet shape is now known as the Taylor cone. He further worked with J.R. Melcher to develop the 'leaky dielectric model' for conducting fluids (Melcher and Taylor, 1969).

In parallel to the academic work of Zeleny and Taylor came a sequence of patents, starting with the design by Cooley who separated the charging device from the spinning head (Cooley, 1902). In the same year, Morton patented a simpler low-throughput machine (Morton, 1902). Melt spinning and air-blast assist were proposed by Norton (Norton, 1936) then a sequence of constant pressure feed high-throughput machines by Anton Formhals was filed between 1934 and 1944 to produce continuous fine fibres for use on standard textile machinery (Formhals, 1934, 1938, 1939, 1940, 1943, 1944). Gladding also proposed the use of the process to produce staple (discontinuous fibres) (Gladding, 1939).

Electrospinning was re-discovered in 1995 in the form of a potential source of nano-structured material by Doshi and Reneker who, whilst investigating electrospraying, observed that fibres could easily be formed with diameters on the nanometre scale(Doshi and Reneker, 1995). Huang and co-workers noted that between 1995 and 2000 fewer than 10 journal papers were published annually, but from 2000 onwards the number of papers per year grew, reaching over 50 by 2002 and reflecting the growing interest in electrospinning by, at least, the academic community (Huang et al., 2003).

Since 1995 there have been further theoretical developments of the driving mechanisms of the electrospinning process. Reznik and co-workers describe extensive work on the shape of the Taylor cone and the subsequent ejection of a fluid jet (Reznik et al., 2004). The work by Hohman and co-workers investigates the relative growth rates of the numerous proposed instabilities in an electrically forced jet once in flight. Also important has been the work by Yarin and co-workers that endeavours to describe the most important instability to the electrospinning process, the bending (whipping) instability(Yarin et al., 2001). The term 'electrospinning' was first coined in 1995 by Doshi and Reneker (Doshi and Reneker, 1995).

For improvement in the applicability of these fibers, various new innovations electrospinning are being used. These innovations include coaxial electrospinning, mixing and multiple electrospinning, core shelled electrospinning, blow assisted electrospinning and others.

2

Coaxial electrospinning includes fabrication of nanofibers from two polymers which utilizes coaxial capillary spinneret and as a result a core of one polymer and shell of the other are formed (Sun et al., 2003). With this technology, some polymers which are difficult to process are coelectrospun and form a core inside the shell of other polymer. This method gains attention as it provides novel properties and functionalities of nanoscale devices through the combination of polymeric materials in the axial and radial direction. The electrospun nanofibers are also used as drug delivery vehicles, but due to large surface area and high porosity, a significant burst release is observed. Coaxial method is commonly used for controlling the burst release of drugs, as the shell of the polymer acts as diffusion barrier for drugs. Other new innovations will also offer various advantages. Blowing-assisted electrospinning helps in spinning of high molecular weight polymers which was otherwise difficult to spin by solution electrospinning. Recently, there has been wide interest in using the nanofibrous membranes as tissue engineering scaffolds. A nanoscale fibrous scaffold more closely mimics the extracellular matrix than macroscale scaffolds and provides a three dimensional (3D) environment. With nanofibrous scaffolds, cell adhesion, proliferation and differentiation of several types of cells have been observed including bone marrow stem cells too. As a tissue engineering scaffolds, nanofibers of various polymers can be used for osteogenesis, wound healing, skin regeneration. Therefore, an electrospun nanofibrous scaffold holds great potential to be used for tissue engineering applications in future. A recent research has demonstrated the use of nanofibers in making nanowires as the incorporation of carbon nanotubes within the fibrous structure provides anisotropic properties such as electrical and thermal conductivity (Hunley and Long, 2008). With the advent of copolymerization and polymer mixtures, attainment of the desired physical and biological properties of nanofibrous mesh has become possible now. There is on-going research for the improvement of nanofiber properties and the scale up of this process. In future electrospun nanofibers will prove to be a promising candidate for a wider range of applications (Bhardwaj and Kundu, 2010).

I.2 Electrospinning Process

The process of electrospinning, namely utilizing electrostatic forces to generate polymer fibers, traces its roots back to the process of electrospraying, in which solid polymer droplets are formed rather than fibers. In fact, a number of processing parameters must be optimized in order to generate fibers as opposed to droplets, and a typical electrospinning apparatus can be used to form fibers, droplets, or a beaded structure depending on the various processing parameters, such as distance between source and collector. In recent work, a greater understanding of processing

parameters has led to the formation of fibers with diameters in the range of 100-500 nm, typically referred to as nanofibers. The development of nanofibers has led to resurgence in interest regarding the electrospinning process due to potential applications in filtration, protective clothing, and biological applications such as tissue engineering scaffolds, and drug delivery devices (Sill and von Recum, 2008).

A typical electrospinning setup consists of a capillary through which the liquid to be electrospun is forced; a high voltage source with positive or negative polarity, which injects charge into the liquid; and a grounded collector. A syringe pump, gravitational forces, or pressurized gas are typically used to force the liquid through a small-diameter capillary forming a pendant drop at the tip. An electrode from the high voltage source is then immersed in the liquid or can be directly attached to the capillary if a metal needle is used. The voltage source is then turned on and charge is injected into the polymer solution. Increasing the electric field strength causes the repulsive interactions between like charges in the liquid and the attractive forces between the oppositely charged liquid and collector to begin to exert tensile forces on the liquid, elongating the pendant drop at the tip of the capillary. As the electric field strength is increased further a point will be reached at which the electrostatic forces balance out the surface tension of the liquid leading to the development of the Taylor cone. If the applied voltage is increased beyond this point a fiber jet will be ejected from the apex of the cone and be accelerated toward the grounded collector. While the fiber jet is accelerated through the atmosphere toward the collector it undergoes a chaotic bending instability, thereby increasing the transit time and the path length to the collector and aiding in the fiber thinning and solvent evaporation processes. Yarin et al. have suggested that this bending instability is due to repulsive interactions between like charges found in the polymer jet (Yarin et al., 2001). Doshi and Reneker had hypothesized that charge density increases as the fiber jet thins, dramatically increasing radial charge repulsion which causes the fiber jet to split into a number of smaller fibers when a critical charge density is met (Doshi and Reneker, 1995). However, in more recent studies high-speed photography has been used to image the unstable zone of the fiber jet, revealing that a whipping instability causes the single fiber to bend and turn rapidly giving the impression that the fiber is splitting (Shin et al., 2001a).

The solid polymer fibers are then deposited onto a grounded collector. Depending on the application a number of collector configurations can be used, including a stationary plate, rotating mandrel, solvent (e.g. water), etc. Typically the use of a stationary collector will result in the formation of a randomly oriented fiber mat. A rotating collector can be used to generate mats with aligned fibers, with the rotation speed playing an important role in determining the degree of anisotropy. Additionally, Liu and Hsieh found that

4

both the conductivity and the porosity of the collector play an important role in determining the packing density of the collected fibers (Liu and Hsieh, 2002).

The parameters affecting electrospinning and the fibers may be broadly classified into processing parameters, solution parameters and ambient parameters. With the understanding of these parameters, it is possible to come out with setups to yield fibrous structures of various forms and arrangements. It is also possible to create nanofiber with different morphology by varying the parameters.

I.2.1 Processing parameters

Despite electrospinning's relative ease of use, there are a number of processing parameters that can greatly affect fibers formation and structure. Grouped in order of relative impact to the electrospinning process, these parameters are applied voltage, polymer flow rate, capillary-collector distance, collector geometry, collector material, diameter of pipette orifice/needle and temperature. Furthermore, all parameters can influence the formation of bead defects.

I.2.1.1 Applied voltage

The strength of the applied electric field controls formation of fibers from several microns in diameter to tens of nanometers. Suboptimal field strength could lead to bead defects in the spun fibers or even failure in jet formation. Deitzel et al. examined a polyethylene oxide (PEO)/water system and found that increases in applied voltage altered the shape of the surface at which the Taylor cone and fiber jet were formed (Deitzel et al., 2001). At lower applied voltages the Taylor cone formed at the tip of the pendent drop; however, as the applied voltage was increased the volume of the drop decreased until the Taylor cone was formed at the tip of the capillary, which was associated with an increase in bead defects seen among the electrospun fibers.

I.2.1.2 Flow rate

The flow rate will determine the amount of solution available for electrospinning. For a given voltage, there is a corresponding flow rate if a stable Taylor cone is to be maintained. When the flow rate is increased, there is a corresponding increase in the fiber diameter or beads size, this is apparent as there is a greater volume of solution that is drawn away from the needle tip (Rutledge et al., 2000; Zong et al., 2002).

I.2.1.3 Capillary-collector distance

While playing a much smaller role, the distance between capillary tip and collector can also influence fiber size by 1-2 orders of magnitude. Additionally, this distance can dictate whether the end result is electrospinning or electrospraying. Doshi and Reneker found that the fiber diameter decreased with increasing distances from the Taylor cone (Doshi and Reneker, 1995).

I.2.2 Solution parameters

In addition to the processing parameters a number of solution parameters play an important role in fiber formation and structure. In relative order of their impact on the electrospinning process these include polymer concentration, solvent volatility, solvent conductivity, surface tension, molecular weight and solution viscosity and dielectric effect of solvent (dielectric constant ε).

I.2.2.1 Polymer concentration

At concentrations allowing adequate chain entanglement, continuous uniform nanofibers can be electrospun from polymer solutions in a strong enough electric field (Deitzel et al., 2001; Pornsopone et al., 2005). The concentration of polymer in solution often determines if it wills electrospin at all and generally has a dominant effect on the fiber diameter, as well as fiber morphology (Demir et al., 2002).

I.2.2.2 Solvent volatility

Invariably, it is the evaporation of solvent from the jet that yields a solid polymer nanofiber at the collector plate. Ideally, all traces of solvent must be removed by the time the nanofiber hits the collector. If not, the wet fibers may fuse together to form a melded or reticular mat. Sometimes a flat ribbon-like nanofibers derived from the fluid–filled, incompletely dry nanofiber due to slow subsequent evaporation of solvent and collapse of the tube, are obtained (Koombhongse et al., 2001).

I.2.2.3 Solution conductivity

Electrospinning involves stretching of the solution caused by repulsion of the charges at its surface. Thus if the conductivity of the solution is increased, more charges can be carried by the electrospinning jet. The conductivity of the solution can be increased by the addition of ions.

6

Moreover, most drugs and proteins form ions when dissolved in water. As previously mentioned, beads formation will occur if the solution is not fully stretched. Therefore, when a small amount of salt or polyelectrolyte is added to the solution, the increased charges carried by the solution will increase the stretching of the solution. As a result, smooth fibers are formed which may otherwise yield beaded fibers. The increased in the stretching of the solution also will tend to yield fibers of smaller diameter (Zong et al., 2002).

I.2.3 Ambient Parameters

The effect of the electrospinning jet surrounding is one area which is still poorly investigated. Any interaction between the surrounding and the polymer solution may have an effect on the electrospun fiber morphology. Ambient parameters include humidity, type of atmosphere and pressure. High humidity for example was found to cause the formation of pores on the surface of the fibers. Since electrospinning is influenced by external electric field, any changes in the electrospinning environment will also affect the electrospinning process.

Chapter II

Composite nanofibers

II.1 Nanofibers

Nanofibers are defined as fibers with diameters on the order of 1000 nanometers. They can be produced by a variety of techniques such as phase separation, self-assembly, drawing, melt fibrillation, template synthesis, interfacial polymerization, solution spinning and electrospinning. Nanofibers reduce the handling problems mostly associated with the nanoparticles. Nanoparticles can agglomerate and form clusters, whereas nanofibers form a mesh that stays intact even after regeneration. Nanofibers are used in medical applications, which include drug and gene delivery, artificial blood vessels, artificial organs and medical facemasks (Chang, 2009).

The nanofibers produced by electrospinning technique are commonly called electrospun fibers or electrospun nanofibers. They can be used in several applications: nonwoven fabrics, reinforced fibres, support for enzymes, drug delivery systems, fuel cells, conducting polymers and composites, photonics, sensorics, medicine, pharmacy, wound dressings, filtration, tissue engineering, catalyst supports, fibre mats serving as reinforcing component in composite systems, and fibre templates for the preparation of functional nanotubes, to name just a few.

The accumulation of non-woven or aligned fibers produces the so called fibrous mats (Charernsriwilaiwat et al., 2010), fibrous fabrics (Chegoonian et al., 2012) or fibrous membranes (Chen et al., 2011). For instance, a pore structured electrospun nanofibrous membrane used as a wound dressing can promote the exudation of fluid from the wound, so as to prevent either build-up under the covering or wound desiccation. The electrospun nanofibrous membrane shows controlled liquid evaporation, excellent oxygen permeability and promoted fluid drainage capacity, while still inhibiting exogenous microorganism invasion because its ultrafine pores. Fibre mats

serving as reinforcing component in composite systems, and fibre templates for the preparation of functional nanotubes (He et al., 2008).

Nanofibers will also eventually find important applications in making nanocomposites. This is because nanofibers can have even better mechanical properties than micro fibers of the same materials, and hence the superior structural properties of nanocomposites can be anticipated. Moreover, nanofiber reinforced composites may possess some additional merits which cannot be shared by traditional (microfiber) composites (Huang et al., 2003).

II.2 Nanocomposite

A nanocomposite is a multiphase solid material where one of the phases has one, two or three dimensions of less than 100 nm, or structures having nano-scale repeat distances between the different phases that make up the material (Ajayan et al., 2006).

The synthesis of polymer nanocomposites is an integral aspect of polymer nanotechnology. By inserting the nanometric inorganic compounds, the properties of polymers improve and hence this has a lot of applications depending upon the inorganic material present in the polymers. Polymer nanocomposites are materials in which nanoscopic inorganic particles, typically 10-100 Å in at least one dimension, are dispersed in an organic polymer matrix in order to dramatically improve the performance properties of the polymer (Lagashetty and Venkataraman, 2005). Systems in which the inorganic particles are the individual layers of a lamellar compound - most typically a smectite clay or nanocomposites of a polymer (such as nylon) embedded among layers of silicates – exhibit dramatically altered physical properties relative to the pristine polymer. Polymer nanocomposites represent a new alternative to conventionally filled polymers. Because of their nanometer sizes, filler dispersion nanocomposites exhibit markedly improved properties when compared to the pure polymers or their traditional composites. These include increased modulus and strength, outstanding barrier properties, improved solvent and heat resistance and decreased flammability.

There are three types of nanocomposites, depending on how many dimensions of the dispersed particles are in the nanometer range can be distinguished (Alexandre and Dubois, 2000). Particles with three dimensions in the order of nanometers are typically isodimensional, such as spherical silica nanoparticles obtained by in situ sol-gel

10

methods (Mark, 1996; Reynaud et al., 1999) or by polymerization promoted directly from their surface (Reynaud et al., 1999; Von Werne and Patten, 1999). They also include semiconductor nanoclusters (Herron and Thorn, 1998) and others (Reynaud et al., 1999). Nanotubes or whiskers (with dimensions in the nanometer scale and the third forming a larger elongated structure), for example, carbon nanotubes or cellulose whiskers (Chazeau et al., 1999; Favier et al., 1997), are extensively studied as reinforcing phases yielding materials with exceptional properties. The third type of nanocomposites is characterized by only one dimension in the nanometer range. In this case the material is present in the form of sheets of one to a few nanometers thick and hundreds to thousands nanometers long. This family of composites is referred to as polymer-layered crystal nanocomposites (Mojumdar and Raki, 2005).

Depending on the nature of the components used (layered structure, organic ions/polymer matrix) and the method of preparation, three main types of composites composites may be obtained when a layered structure is associated with a polymer (Alexandre and Dubois, 2000).

If the polymer is unable to intercalate between the layered sheets, a phase-separated composite is obtained, whose properties stay in the same range as traditional microcomposites. Beyond this classical family of composites, two types of nanocomposites can be distinguished. An 'intercalated' structure in which a single (and sometimes more than one) extended polymer chain is intercalated between the inorganic layers resulting in a well-ordered multilayer morphology built up with alternating polymeric and inorganic layers. When the layers are completely and uniformly dispersed in a continuous polymer matrix, an 'exfoliated or delaminated' structure is obtained.

II.3 Composite Nanofibers

It is a general practice in polymer technology to compound inorganic (and sometimes even organic) fillers into a polymer matrix to either reduce the cost of a formulation or to improve its mechanical properties. Fillers used in the latter case are reinforcing fillers and must be of small enough average particle size and of adequate surface compatibility with the matrix to effectively play this crucial role. Ideally, the particle size should be smaller than the interchain distances in the polymer matrix to avoid the introduction of points of local stress into the material. For instance, in elastomers only filler particles smaller than about a micrometer result in significant levels of

reinforcement, with better composite properties obtained at even smaller particle sizes. Larger particles of filler (>10 microns) typically reduce the mechanical properties of composites. Qualitatively, the mechanism of reinforcement in composites is via the transfer of stresses propagating through the polymer to the higher-modulus filler particles. High specific surface area and larger aspect ratio of the filler as well as good compatibility between the filler and polymer will determine the efficiency of load transfer and invariably the degree of reinforcement. Reinforcing fillers are often surface treated to alter their chemistry (e.g., silica might be treated with, 1% by weight of aminosilane) to allow better wetting or closer interaction of filler with the polymer. Carbon nanotubes and carbon fibers have been extensively researched to improve their function as potential reinforcing fillers in polymer composites (Andrady, 2008).

Composite materials owe their exceptional mechanical and other useful properties to the existence of an extensive interface fraction localized at the phase boundary between filler and bulk resin. The larger the fractional interface, the more pronounced will be its influence on the properties of the composite. With a compatible filler material the interface is more complex than a simple two-dimensional contact region between the particle and polymer. The interface "layer" formed around the particle has a finite thickness, and within it the material properties are very different from those in the bulk (Pukánszky, 2005).

II.3.1 Polymer–clay composites

A majority of studies on composite nanofibers reinforced with clays has been on montmorillonite (MMT), a clay with plate-like particles having a chemical composition of hydrated sodium calcium aluminum magnesium silicate hydroxide $(Na,Ca)_{0.33}(Al,Mg)_2(Si4O10)(OH)_2.nH2O$ (value of n varies with the degree of hydration). The platelets of the clay have a high modulus (170GPa), a high aspect ratio (1000nm x75–100nm), a surface area of 750 m^2 per g, are hydrophilic, and occur in aggregated form or as tactoids. These have to be dispersed into individual platelets to exploit their high surface area in reinforcing polymers (Hong et al., 2005).

II.3.2 Drug-loaded fibers

The kinetics of release of the drug is controlled by the semicrystalline nature of the polymer as well as by the morphology of the polymer/drug composite. Three basic morphological models (Figure II.1) for drug-loaded polymers (or polymer particles), first proposed by Kissel et al. (Kissel et al., 1993), apply to drug-loaded nanofibers as well (Verreck et al., 2003):

12

a. Drug dissolved in the polymer matrix at the molecular level.

b. Drug distributed in the polymer matrix as crystalline or amorphous particles.

c. Drug enclosed in the polymer matrix yielding a core of the drug encapsulated by a polymer layer (similar to a reservoir device).
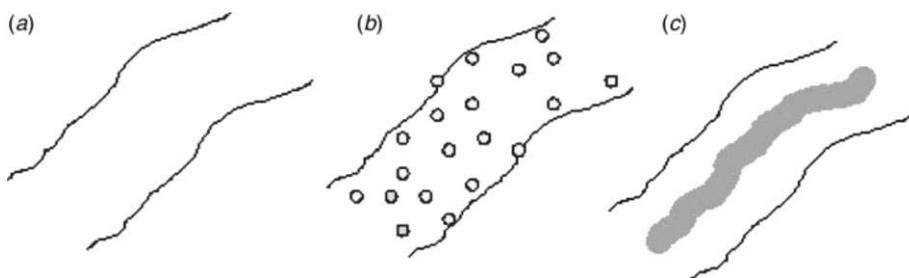
Figure II.1 *Illustration of the three morphological models of drug-loaded polymer nanofibers.*

II.3.2.1 Drug delivery

The simplest configuration of a controlled release device is where a drug is either dissolved in high concentration or suspended as particles in a monolithic polymer such as a cylindrical polymer fiber (Andrady, 2008). The release of the drug from it may occur via:

1. Diffusive transfer through the polymer matrix to the surrounding tissue.

2. Release of the dissolved or suspended drug due to slow biodegradation or erosion of the surface layers of the fiber.

3. Slow release of covalently bonded drug via hydrolytic cleavage of the linkages.

4. Rapid delivery of the drug due to dissolution of the fiber.

In vitro dissolution has been recognized as an important element in drug development. Under certain conditions it can be used as a surrogate for the assessment of Bioequivalence. Several theories / kinetics models describe drug dissolution from immediate and modified reléase dosage forms. There are several models to represent the drug dissolution profiles where f_t (fraction of drug dissolved in time t) is a function of t (time) related to the amount of drug dissolved from the pharmaceutical dosage system. The quantitative interpretation of the values obtained in the dissolution assay is facilitated by the usage of a generic equation that mathematically translates the dissolution curve in function of some parameters related with the pharmaceutical dosage forms. In some cases, that equation can be deduced

by a theoretical analysis of the process, as for example in zero order kinetics. In most cases, with tablets, capsules, coated forms or prolonged release forms that theoretical fundament does not exist and sometimes a more adequate empirical equations is used. The kind of drug, its polymorphic form, cristallinity, particle size, solubility and amount in the pharmaceutical dosage form can influence the release kinetic (Ei-Arini and Leuenberger, 1995; Salomon and Doelker, 1980). A water-soluble drug incorporated in a matrix is mainly released by diffusion, while for a low water-soluble drug the self-erosion of the matrix will be the principal release mechanism. To accomplish these studies the cumulative profiles of the dissolved drug are more commonly used in opposition to their differential profiles. To compare dissolution profiles between two drug products model dependent (curve fitting), statistic analysis and model independent methods can be used (Costa and Sousa Lobo, 2001).

The quantitative interpretation of the values obtained in dissolution assays is easier using mathematical equations which describe the release profile in function of some parameters related with the pharmaceutical dosage forms. Some of the most relevant and more commonly used mathematical models describing the dissolution curves are:

Zero order:	$Q_t = Q_0 + K_0 t$	(II.1)
First order:	$\ln Q_t = \ln Q_0 + K_1 t$	(II.2)
Second order:	$Q_t / Q_\infty (Q_\infty - Q_t) K_2\, t$	(II.3)
Hixson–Crowell	$Q_0^{1/3} - Q_t^{1/3} = K_s t$	(II.4)
Weibull	$\log[-\ln(1 - (Q_t / Q_\infty))] = b \times \log t - \log a$	(II.5)
Higuchi	$Q_t = K_H \sqrt{t}$	(II.6)
Baker–Lonsdale	$(3/2)[1 - (-1(Q_t / Q_\infty))^{2/3}] - (Q_t / Q_\infty) = Kt$	(II.7)
Korsmeyer–Peppas	$Q_t / Q_\infty = K_k\, t^n$	(II.8)
Quadratic	$Q_t = 100(K_1\, t^2 + K_2\, t)$	(II.9)
Logistic	$Q_t = A / [1 + e^{-K(t - y)}]$	(II.10)
Gompertz	$Q_t = A\, e^{-e - K(t - y)}$	(II.11)
Hopfenberg	$Q_t / Q_\infty = 1 - [1 - k_0\, t / C_0 a_0]$	(II.12)

where Q_t is the amount of drug dissolved in time t, Q_0 is initial amount of drug in the solution (most times, $Q_0 = 0$), K_0 is the zero order release constant, K_1 is the first order release constant, Q_∞ is the amount of drug released at an infinite time, K_2 is the second order release constant, K_s is a constant incorporating the surface–volume relation, the scale parameter, a, defines the time scale of the process. The shape parameter, b, characterizes the curve as either exponential ($b = 1$) (Case 1), sigmoid, S-shaped, with upward curvature followed by a turning point ($b.1$) (Case 2), or parabolic, with a

14

higher initial slope and after that consistent with the exponential ($b > 1$) (Case 3), where K_H is the Higuchi dissolution constant, the release constant, k, corresponds to the slope, K_k is the Korsmeyer–Peppas release constant, n is the release exponent, indicative of the drug release mechanism, Peppas (Peppas, 1985) used this n value in order to characterize different release mechanisms, concluding for values for a slab, of $n = 0.5$ for Fick diffusion and higher values of n, between 0.5 and 1.0, or $n = 1.0$, for mass transfer following a non-Fickian model (Table II.1). In the case of a cylinder, k_0 is the erosion rate constant, C_0 is the initial concentration of drug in the matrix and a_0 is the initial radius for a sphere or cylinder or the half-thickness for a slab (Costa and Sousa Lobo, 2001).

The drug transport inside pharmaceutical systems and its release sometimes involves multiple steps provoked by different physical or chemical phenomena, making it difficult, or even impossible, to get a mathematical model describing it in the correct way. These models better describe the drug release from pharmaceutical systems when it results from a simple phenomenon or when that phenomenon, by the fact of being the rate-limiting step, conditions all the other processes.

Table II.1 *Interpretation of diffusional release mechanisms from polymeric films*

Release exponent (n)	Drug transport mechanism	Rate as a function of time
0.5	Fickian diffusion	$t^{-0.5}$
$0.5 < n < 1.0$	Anomalous transport	t^{n-1}
1.0	Case-II transport	Zero order release
Higher than 1.0	Super Case-II transport	t^{n-1}

The release models with major appliance and best describing drug release phenomena are, in general, the Higuchi model, zero order model, Weibull model and Korsmeyer–Peppas model. The Higuchi and zero order models represent two limit cases in the transport and drug release phenomena, and the Korsmeyer–Peppas model can be a decision parameter between these two models. While the Higuchi model has a large application in polymeric matrix systems, the zero order model becomes ideal to describe coated dosage forms or membrane controlled dosage forms.

Chapter III

Methods of investigation and Materials

III.1 Methods

III.1.1 Differential Scanning Calorimetry (DSC)

DSC measurements were carried out using a Mettler DSC 822/400 thermal analyzer instrument having sub-ambient capability. About 2-3 mg sample was placed in an aluminium pan and heated at a rate of 10 °C/min from 0 to 250 °C in a nitrogen atmosphere.

III.1.2 Thermogravimetric Analysis (TGA)

Thermoanalytical characterizations were performed by a Mettler TC-10 thermobalance operating at 5 °C/min heating rate, under air flow, from 25 to 800 °C. Degradation temperature (T_d) is reported as the midpoint of the degradation step.

III.1.3 X-ray Diffraction (XRD)

XRD data were collected using an automatic Bruker diffractometer (equipped with a continuous scan attachment and a proportional counter), with the nickel filtered Cu Kα radiation (λ = 1.54050 Å) and operating at 40 kV and 40 mA. The diffraction scans were recorded at 2θ = 2-40°, step scan 0.03° of 2θ and 3s of counting time.

III.1.4 Scanning Electron Microscopy (SEM)

The morphology and the diameter of the electrospun nanofibers were analysed by a scanning electron microscope (SEM Mod. LEO 420, Assing, Italy). All samples were sputter coated with gold (Agar Automatic Sputter Coater Mod.B7341, Stansted, UK) at 40 mA for 180 s prior the analysis. The fibers diameter distribution was determined by Sigma SacnPro 5. About 500 fibers were considered, taking their dimensions respect to the reference bar of SEM image.

III.1.5 Ultraviolet Spectroscopy (UV-VIS)

The in vitro study of amoxicillin release was performed by measuring the absorbance at 228 nm using an ultraviolet spectrophotometer (model UV-2401, SHIMADZU). The tests were performed using rectangular specimen of 25 cm^2 placed into 25 mL of physiological saline solution, stirred at room temperature and 100 rpm in an orbital shaker (VDRL MOD. 711+, Asal S.r.l.). The release medium was withdrawn at fixed time intervals and replenished with fresh medium.

III.1.6 High Energy Ball Milling (HEBM)

Milling was carried out using a Retsch PM100 planetary milling at 600 rpm, PCL with amoxicillin was prepared by mixing 3.8 g of PCL with 0.2 g of AMOX in a 50 mL Retsch stainless steel vessel with five 10 mm diameter stainless. Milling was performed in 1.5 min intervals, followed by a 10 s pause.

III.1.7 Mechanical properties

The Young's modulus, tensile strength and the strain at break of the fibers were measured using a dynamometric apparatus INSTRON (model 4301). The instrument is interfaced to a PC with a software "Series IX" for data acquisition. The measurements were carried out at room temperature at a deformation rate of 10 mm/min. The length, thickness and width were measured for each sample (approximately $20 \times 10 \times 0.03$ mm).

III.1.8 Antibacterial activities in vitro

The inhibitory activity of the electrospun nanofibers charged with different concentrations of AMOX was evaluated by the disc diffusion method according to the specifications of the document M2-A9 from the

Clinical and Laboratory Standards Institute (Clinical and Laboratory Standards Institute, 2006b). A criogenic (-80 °C) reserve of each strain was used to make the overnight broth culture. An aliquot of the criogenic reserve of *S. aureus* and *E. coli* was inoculated in two 7 ml Tryptic soy broth tubes while *E. faecalis* was inoculated in 7 ml BHI broth. Each bacteria was adjusted to 0,5 McFarland in 0,9% sodium chloride solution previous to the inoculation in MHA plates. Three membranes in shape of disc of 6 mm diameter were placed onto MHA plates. The procedure was repeated three times per bacteria. The plates were inverted face down and incubated at 35 °C for 24 hours. AMOX work solution (1mg/mL) was used as positive control(Clinical and Laboratory Standards Institute, 2006a), three 6 mm diameter wells were made in three MHA plates, one per strain, 25 μl of the AMOX work solution was injected in each well. The activity against the same three bacteria was evaluated using the agar well diffusion method as described by Boyanova et al. (Boyanova et al., 2005) and Kroiss et al. (Kroiss et al., 2010). As negative control, five 6 mm diameter discs of nanofibers without AMOX were sterily placed onto one MHA plate and incubated under the same conditions above. All data were statistical analyzed by means of Student's t-test with α 0,05.

III.2 Materials

III.2.1 Poly(ε-caprolactone) (PCL)

Poly(ε-caprolactone) (PCL) is a semi-crystalline biodegradable polyester with a glass transition temperature of about −60°C and a low melting point of around 60°C, which could be a handicap in some applications. Therefore, PCL is generally blended (Averous et al., 2000) or modified (e.g., copolymerisation, crosslink (Tan et al., 2012)). Two main pathways to produce polycaprolactone have been described in the literature: the polycondensation of a hydroxycarboxylic acid: 6-hydroxyhexanoic acid, and the ring-opening polymerisation (ROP) of a lactone: ε-caprolactone (ε-CL) in the presence of aluminium isopropoxide (Albertsson and Varma, 2002; Chiellini and Solaro, 1996; Okada, 2002). Figure III.1 gives the chemical structure of this polyester.
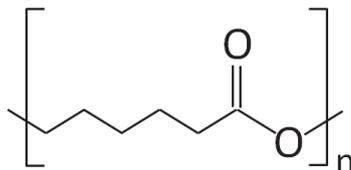
Figure III.1 *Chemical structure of Poly(ε-caprolactone)*

This synthetic polymer is currently used in a number of biomedical applications due to its mechanical properties, miscibility with a large range of other polymers, biocompatibility (Kim et al., 2004b), biodegradability, good drug permeability and slow biodegradability (Lannutti et al., 2007). PCL is widely used in the manufacture of speciality polyurethanes. Polycaprolactones impart good water, oil, solvent and chlorine resistance to the polyurethane produced. This polymer is often used as an additive for resins to improve their processing characteristics and their end use properties (e.g., impact resistance). Being compatible with a range of other materials, PCL can be mixed with starch to lower its cost and increase biodegradability or it can be added as a polymeric plasticizer to Polyvinyl chloride (PV). But, it finds also some application based on its biodegradable character in domains such as controlled release of drugs, soft compostable packaging. Polycaprolactone is also used for splinting, modeling, and as a feedstock for prototyping systems.

PCL is considered a non-toxic and a tissue compatible material (Gunatillake and Adhikari, 2003). It is being investigated as a scaffold for tissue repair via tissue engineering, GBR membrane. It has been used as the hydrophobic block of amphiphilic synthetic block copolymers used to form the vesicle membrane of polymersomes. A variety of drugs have been encapsulated within PCL beads for controlled release and targeted drug delivery which have been peer reviewed (Surendran et al., 2012).

Tokiwa and Suzuki have discussed the hydrolysis of PCL and biodegradation by fungi. They have shown that PCL can be easily enzymatically degraded (Tokiwa and Suzuki, 1977). According to Bastioli, the biodegradability can be clearly claimed but the homoplymer hydrolysis rate is very low (Bastioli, 1998). The presence of starch can significantly increase the biodegradation rate of PCL. PCL is degraded by hydrolysis of its ester linkages in physiological conditions (such as in the human body) and has therefore received a great deal of attention for use as an implantable biomaterial. In particular it is especially interesting for the preparation of long term implantable devices, owing to its degradation which is even slower than that of polylactide (Ibrahim et al., 2009).

III.2.2 Poly(lactic acid) (PLA)

Polylactic acid or polylactide (PLA) is a thermoplastic aliphatic polyester derived from renewable resources, such as corn starch (in the United States), tapioca roots, chips or starch (mostly in Asia), or sugarcane (in the rest of the world). It can biodegrade under certain conditions, such as the presence of

oxygen and without the presence of oxygen. This is a biodegradable polymer with different biomedical applications because of its mechanical properties and biocompatibility (Kim et al., 2004b). Figure III.2 shows the chemical structure of this polymer.
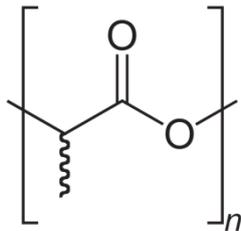
Figure III.2 *Chemical structure of Poly(lactic acid)*

There are several industrial routes to produce poly(lactic acid). Two main monomers are used: lactic acid, and the cyclic di-ester, lactide. The most common route to poly(lactic acid) is the ring-opening polymerization (ROP) of lactide with various metal catalysts (typically tin octoate) in solution, in the melt, or as a suspension. The metal-catalyzed reaction tends to cause racemization of the poly(lactic acid), reducing its stereoregularity compared to the starting material (Södergård and Stolt, 2010). Another route to produce poly(lactic acid) is the direct condensation of lactic acid monomers.

Poly(lactic acid) can be processed by extrusion, injection molding, film and sheet casting, spinning, providing access to a wide range of materials. Being able to degrade into innocuous lactic acid, poly(lactic acid) is used as medical implants in the form of screws, pins, rods, and as a mesh. Depending on the exact type used, it breaks down within the body within 6 months to 2 years. This gradual degradation is desirable for a support structure, because it gradually transfers the load to the body (e.g. the bone) as that organ heals. PLA can also be used as a compostable packaging material, either cast, injection molded, or spun. Cups and bags have been made of this material. In the form of a film, it shrinks upon heating, allowing it to be used in shrink tunnels. It is useful for producing loose-fill packaging, compost bags, food packaging, and disposable tableware. In the form of fibers and non-woven textiles, PLA also has many potential uses, for example as upholstery, disposable garments, awnings, feminine hygiene products, and diapers (Auras et al., 2010).

III.2.3 Amoxicillin (AMOX)

Amoxicillin (AMOX) (figure III.3) is a bacteriolitic, β-lactam antibiotic used to treat bacterial infections caused by susceptible microorganisms, one of the most common antibiotic for children (Ahymah Joshy et al., 2011; Songsurang et al., 2011). It was also used before surgery to prevent infections. Recently a study on mice indicated successful delivery using intraperitoneally injected amoxicillin-bearing microparticles, showing a growing interest in the controlled delivery of this drug. AMOX is used to treat infections caused by bacteria in ear, lung, nose, urinary tract and skin infections. It was also used before surgery to prevent infections(Ahymah Joshy et al., 2011).
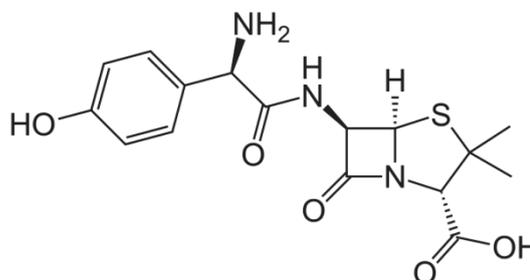
Figure III.3 *chemical structure of Amoxicillin*

III.2.3 Layered double hydroxide (LDH)

Layered double hydroxides (LDHs), also known as hydrotalcite-like compounds (figure III.4) or anionic clays, have received much attention in the past decades due to their vast applicability. An LDH is created when a fraction of the divalent cations in a brucite-like lattice are isomorphously replaced by trivalent cations, introducing a positive charge in the layers. This charge is electrically balanced by anions located in the interlayer region, along with hydration water molecules. Given the wide range of compounds with LDH structure that may be prepared, they are represented by the general formula: $[M^{II}_{(1-x)} M^{III}_{x} (OH)_{2}] (A^{n-})_{x/n} \cdot mH_2O$, where M^{II} includes: Mg^{2+}, Co^{2+}, Cu^{2+}, Ni^{2+}, Zn^{2+}, etc.; M^{III} may be Al^{3+}, Cr^{3+}, Ga^{3+}, Fe^{3+}; and A^{n-} might be any organic and/or inorganic anion. Many ternary LDHs involving mixtures of different M^{II} and/or M^{III} may also be prepared (Duan and Evans, 2006; Rives, 2001).
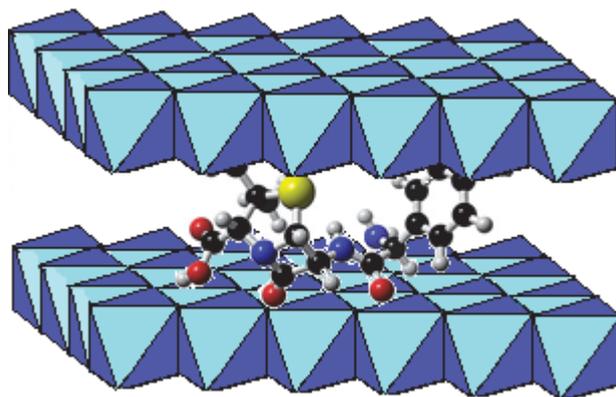
Figure III.4 *Layered crystal structure of hydrotalcite-like compounds*

Inorganic or organic anions can be introduced between hydroxide layer by ion exchange or precipitation. LDHs containing magnesium and aluminum have already been used as an antacid and antipepsin agent; therefore, LDH is quite biocompatible. Novel biohybrids of LDH and biomolecules [ATP or nucleoside monophosphate] are designed and organized artificially on nanometer scale to provide opportunities for reservoir and delivery carriers of functional biomolecules in gene therapy and drug delivery (Nalawade et al., 2009).

The MgAl LDH can also be used to incorporate and disperse one or more reducible transition metal cations in the layers, when partially replacing Mg^{2+} and/or Al^{3+} cations; the layers then have the general formula [Mg_{1-x-y} $Me_x Al_y (OH)_2$]. These reducible cations, when they are indeed located in the layers and not as separate metal hydroxide or oxide entities, are imbedded in a mostly basic matrix. The transition metal may also induce a certain degree of acidity. Accordingly, it is possible to modulate the basic strength of a series of ternary layered double hydroxide clays, depending on the nature of the cations in the layers. Bifunctional catalysts may thus be obtained in the form of mixed oxides containing highly disperse, small crystals of the reducible metal oxides (Valente et al., 2010).

LDHs are also known for their ability to adsorb negatively charged species and/or pollutants, which is mainly due to their large surface area, high anion-exchange capacities and flexible interlayer space. In this sense, LDHs have been tested as additives for the removal of sulfur oxides (SO_x) from FCC units used in petroleum refining industries. Mg-Al-Fe LDHs with added CeO_2 were found to be most effective, due to their basic/redox characteristics (Cantú et al., 2005). Additionally, LDHs have been successfully tested in the removal of pollutants, such as the herbicide 2,4-

dichlorophenoxiacetic acid (2,4-D), from aqueous solutions. Furthermore, Mg-Zn-Al LDHs, with varying amounts of zinc, were demonstrated to have semiconducting properties (5.43-3.85 eV band gap energy) and were able to photocatalytically degrade 2,4-D and phenol. The activity was superior to previous reports on the degradation of these compounds by different solids (Valente et al., 2009). Other Zn-containing LDHs have also been tested as photocatalysts (Mantilla et al., 2010).

Other scientific and technological applications of LDHs are worth mentioning, such as hybrid composites, antacids, flame retardants and PVC additives. Several research groups worldwide have focused their attention in the intercalation of biological species and organic compounds between the layers in order to use LDHs in diverse fields as drug delivery carriers, sensing devices, etc (Desigaux et al., 2005).

Traditionally, LDHs are synthesized by the coprecipitation of metallic salts with a concentrated alkaline solution. Several alternative methods have been proposed, depending on the intended application. For instance, an environmental–friendly method has been developed for industrial–scale production of multimetallic LDHs. This method does not require one to wash the slurries in order to eliminate undesirable counter-ions, as is generally done during LDH synthesis. All the reactants become part of the final product; thus, no waste is generated during catalyst preparation. The amount of water employed is reduced to a minimum, and large-scale production of catalysts is easy and economic.

Also, an alternative that has received some attention in the last few years is the sol-gel method; a proposal of a general sol-gel method for the synthesis of LDHs with various chemical compositions was presented recently (Prince et al., 2009). This method has several advantages over other synthetic procedures. It is a simple way to obtain nanoscaled particles, which have proved to be important for many of the new applications of LDHs; for instance, for the successful casting of LDH thin films. Also, high-purity products can be obtained; and the conditions throughout the process are mild, thus enabling an eventual intercalation of delicate organic molecules and biological species. Furthermore, the sol-gel method allows accurate control over structural and textural properties of the products; materials with high specific surface area and narrow pore size distribution can be obtained.
The LDH family is quite promising in the field of materials chemistry, as mumerous applications have been found; new applications are being studied continuously. The advancement in their various synthetic procedures and the optimization of the desired properties are essential for these endeavors and in the successful transference of scientific knowledge to functional technology (Valente and Prince, 2010).

Chapter IV

Poly(ε-caprolactone) electrospun fibers

IV.1 Introduction

In the last decades the successes reached by modern medicine are undoubtedly of great importance for the human life. The growing use of scientific discoveries from other branches of science such as chemistry and physics are strongly improving the quality of the medical practices of the past, not always supported by scientific knowledge.

In the field of material science and engineering a challenge to biomedical applications, and in particular of tissue engineering, is currently the design of synthetic matrices that can mimic the structure and biological functions of the natural extracellular matrix (ECM) (Bohner et al., 2005; Butscher et al., 2011; Mathieu et al., 2006; Sun et al., 2005; Zeltinger et al., 2001). Human cells can attach and organize well around fibers with diameters smaller than those of the cells. In this regard, nanoscale fibrous scaffolds can provide an optimal template for cells to seed, migrate and grow (Sabir et al., 2009; Valenta and Auner, 2004; Whang et al., 1995).

The utilization of biomaterials – both natural and synthetic – is enabling to develop scaffolds specifically designed for many medical applications (Brekke and Toth, 1998; Callaghan, 1997; Chapekar, 2000; Cheung et al., 2007; Dimar and Glassman, 2007 ; Oh et al., 2003). The production methods for preparing such devices are wide ranging, and each method has its unique characteristics. Of particular interest in tissue engineering is the creation of reproducible and biocompatible three-dimensional scaffolds resulting in bio-matrix composites useful for various applications, as medical prostheses,

drug delivery and tissue template. In each specific application the ability to shape materials on different length scales, including the nanoscale is of the utmost importance.

Recently electrospinning (Doshi and Reneker, 1995), able to produce non-woven membranes of nanofibres, characterized by a high surface-to-volume ratio, has been demonstrated as a successful means of producing scaffolds having many of the desirable and controllable properties (Bashur et al., 2006; Dalton et al., 2006; Leung and Ko, 2011; Noh et al., 2006; Patel et al., 2009; Qi et al., 2008; Taepaiboon et al., 2007; Tammaro et al., 2009b; Teo and Ramakrishna, 2006). It is applicable to a wide variety of polymers and composite polymers, both natural and synthetic. In this technique polymer nanofibers are produced from an electrostatically driven jet of polymer solution or melt. The discharged polymer solution jet undergoes a whipping process wherein the solvent evaporates and the highly stretched polymer fiber deposits on a grounded target. A number of experimental parameters control the fiber diameter and morphology. The nanofibers, with diameters ranging from microns down to hundreds of nanometers or less, can be fabricated into a variety of forms such as membranes, coatings and films, and therefore serve in several applications.

Furthermore, depending on the specific polymer being used, a wide range of fabric properties such as strength, weight and porosity, surface functionality etc. can be achieved.

This novel fiber spinning technique provides as well the capacity to encapsulate into the nano-fibers small insoluble particles as well as soluble drugs for a topical controlled release. The encapsulation of drugs into nano fibers can be tailored to obtain: a) more efficient release systems; b) decrease of side effects; c) improved selective toxicities (Chen et al., 2010; Romeo et al., 2007; Suganya et al., 2011; Wei et al., 2010; Wu et al., 2010b; Yang et al., 2011; Zamani et al., 2010).

However not necessarily the parameters for spinning the pure polymer can be applied for encapsulating the drugs, and therefore all the procedures, both in the absence and with drugs, have to be separately and carefully set up.

The release properties can be tuned by varying the drug concentration, the presence of the drug inside or outside the polymeric fibers, the fiber diameter and distribution. Moreover release profiles of entrapped drugs can be finely tuned by controlling either the drug diffusion or the degradation rate of the polymer matrix through molecular weight and distribution, material composition and porosity of the carriers.

Electrospun polymer nanofibers have been designed for pharmaceutical compositions either integrating the drug and carrier materials into one kind of fiber containing both components or electrospinning the carrier material into a tubular form in which the drug particles are encapsulated. A possible

limit of these systems is a rapid exit of the drug, making it available for a too short period.

In the present chapter we present the preparation by electrospinning of new carriers, obtained by encapsulating an antibiotic drug, amoxicillin into a biodegradable poly ε-caprolactone.

IV.2 Preparation of electrospun fibers

IV.2.1 Electrospinning Procedure

Fibrous membranes of PCL were prepared by electrospinning of its solution in acetone (17.5 wt% PCL). PCL/AMOX fibers with 3, 5 and 7 (wt %) of amoxicillin were obtained by electrospinning of their mixed solution in acetone (17.5 wt% total polymer concentration). These solutions were prepared by first dissolving the exact amount of PCL required to obtain the fully polymer solution in acetone as the solvent. Then the filler AMOX was slowly added to the acetone polymer solution, stirred vigorously for 1 h until complete dissolution.

Electrospinning of PCL fibers was carried out at room temperature at a constant voltage of 30 kV (HV Power Supply, Gamma High Voltage Research, Ormond, FL). A copper wire was mounted in the spinneret having an inner diameter of 0.8 mm and used as the positive electrode. Grounded aluminium foil was used as the counter electrode and mounted at a distance of 30 cm from the spinneret. Continuous PCL fibers were collected on the aluminium foil in the form of a fibrous mat. Electrospinning conditions were optimized to produce PCL nano fibrous mats composed of individual fibers 0.75 μm in diameter and without bead formation. In the following, fibers obtained by electrospinning will be coded as PCL-A*n* where *n* is the amount (worded as weight percentage) of AMOX present.

IV.2.2 High Energy Ball Milling (HEBM) experiments

Powders composed of 3.8 g PCL and 0.2 g of AMOX were milled in a Retsch PM100 planetary milling at 600 rpm. The powders were milled in a 50 mL Retsch stainless steel vessel with five stainless steel balls of 10 mm of diameter. We used two milling time, 3 and 6 minutes, with 1.5 min intervals, followed by a 10 s pause. In the following, electrospun samples obtained by milling the powders of PCL and AMOX will be coded as PCL-A5M*m* where *m* is the milling time.

IV.3 Morphology and structure of the pure and filled samples

Many internal as well as external parameters do influence the electrospinning process and, as a consequence, the fiber morphology. Indeed it is difficult to isolate the effect of each parameter since they all are interrelated. For this reason, typically a trial-and-error approach has been employed by varying the solution properties and spinning parameters until uniform defect-free fibers are obtained.

According to previous results (Romeo et al., 2007; Tammaro et al., 2009a) we chose acetone as solvent for PCL and PCL loaded with different concentrations of amoxicillin (AMOX). Since the drug is insoluble in acetone, in another set of experiments, it was subjected to high energy ball milling procedure (Sorrentino et al., 2005) to reduce the powder dimensions. In Figure IV.1 SEM micrographs of amoxicillin pristine (Figure IV.1a) and after 3 min milling with PCL (Figure IV.1b), and the crystal dimension distribution are shown.
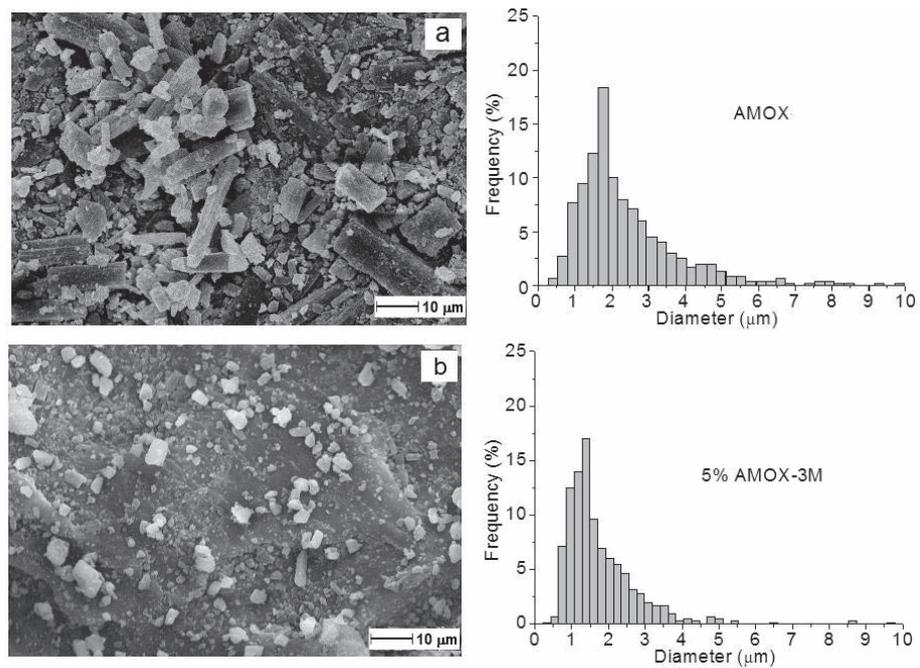
Figure IV.1 *SEM micrographs and crystal dimension of amoxicillin pristine (a) and after milling with PCL (b)*

Pure amoxicillin is seen to be a highly crystalline material with a flat rod shape of dimensions ranging between 1 and 3 micron and centred at about 2

micron. This crystalline shape is still maintained when the granules of amoxicillin are milled with PCL and the dimensions are reduced to values centred at about 1.5 micron.

The SEM micrographs and diameter distribution of the obtained fibrous membranes of PCL (Figure IV.2a), and PCL charged with Amoxicillin at 3% (Figure IV.2b), 5% (Figure IV.2c), and 7% (Figure IV.2d) are show in figure IV.2.
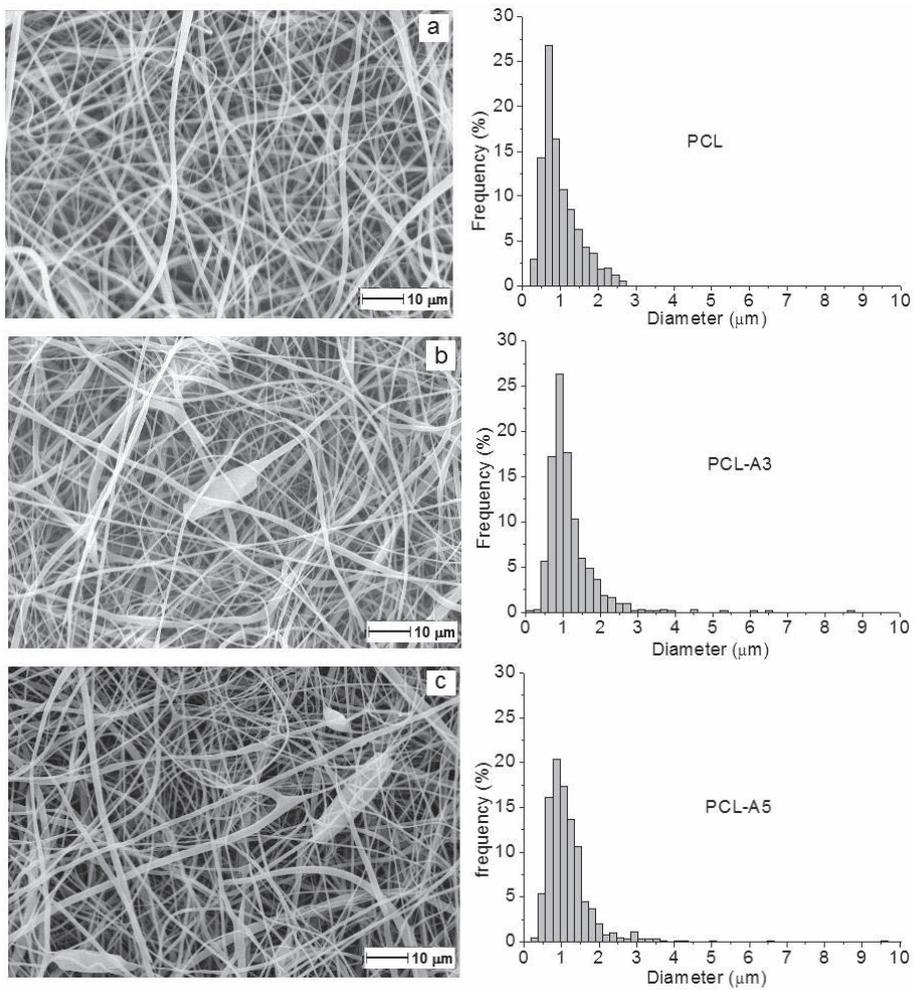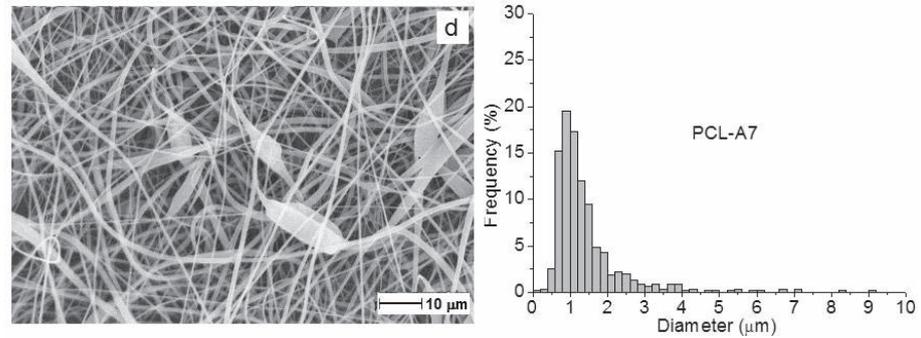
Figure IV.2 *SEM micrographs and diameter distribution of PCL (a), PCL-A3 (b), PCL-A5 (c), PCL-A7 (d)*

The nanofibrous structure of pristine PCL sample composed of individual, uniform, and randomly oriented fibres with an average diameter ranging around 0.8 micron is evident. The addition of amoxicillin at different concentrations of 3%, 5% and 7% caused no noticeable change in the morphology. Moreover it resulted in electrospun nanofibers with very similar or slightly higher average diameter around 0.8-1.2 micron, in comparison with pure PCL, although a prevailing number of fibers with higher dimensions is observable. Some rare beads appear, possibly due to clusters of the AMOX molecules on the surface of the microfibers.

In Figure IV.3 SEM micrographs and fibre dimension distributions are shown for PCL electrospun with 5% of AMOX milled for 3 min (Figure IV.3a) and 6 min (Figure IV.3b). We observe that, in spite of reduced dimensions of the crystalline AMOX, the fiber dimension distribution is slightly shifted toward higher dimensions, centred at 1.0 micron, yet maintaining a similar fibrous structure. Definitively the milled samples are not very much different from the others, indicating a scarce influence of the milling procedure.
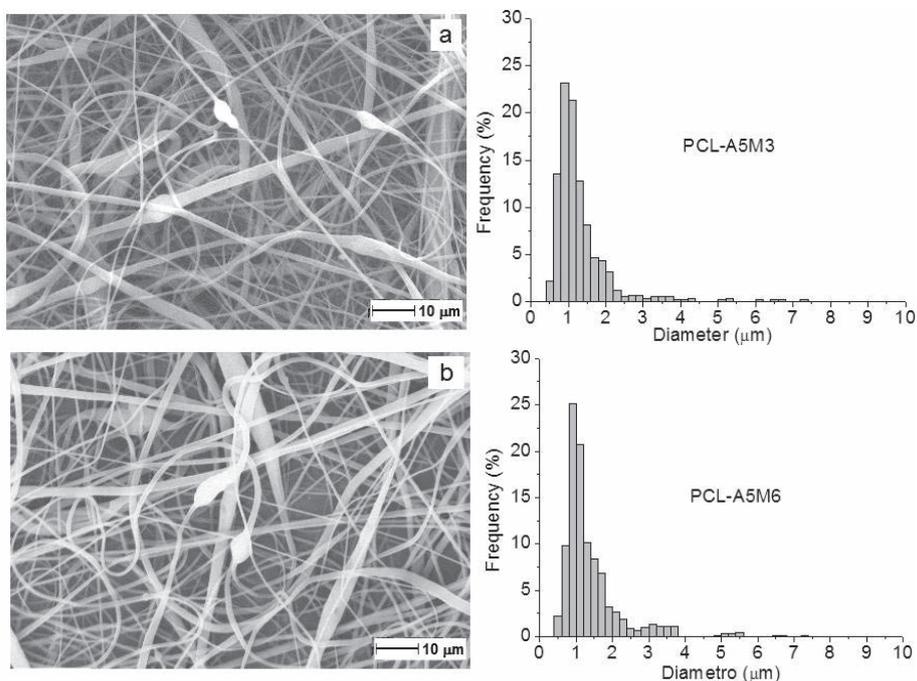
Figure IV.3 *SEM micrographs and diameter distribution of PCL-A5M3 (a) and PCL-A5M6 (d)*

The X-ray diffractograms were performed to investigate the crystalline structure of the membranes, and are reported in Figure IV.4. The AMOX powders are very crystalline (Figure IV.4a), showing the most intense peaks at 12.5°, 15°, 18° and 19.5° of 2θ. The pristine PCL (Figure IV.4c), spun from the 17.5 % solution in acetone and PCL with 3% (Figure IV.4d), 5% (Figure IV.4e) and 7% (Figure IV.4f). The pristine electrospun PCL and all the filled samples show the crystalline structure of PCL well developed with the main diffraction peaks appearing at 21.4° of 2θ and 23.8° of 2θ. Interestingly, observing the diffractograms of the filled AMOX with PCL we can notice that even in the most concentrated sample, that is the 7% AMOX (Figure IV.4f) the crystalline peaks of AMOX do not appear at all. We suggest that the AMOX, encapsulated into the PCL fibers, is not allowed to crystallize and exists as amorphous molecular aggregates or solid solution into the fibers. This result has been already found (Ahymah Joshy et al., 2011; Songsurang et al., 2011) and is confirmed by the following thermal properties.
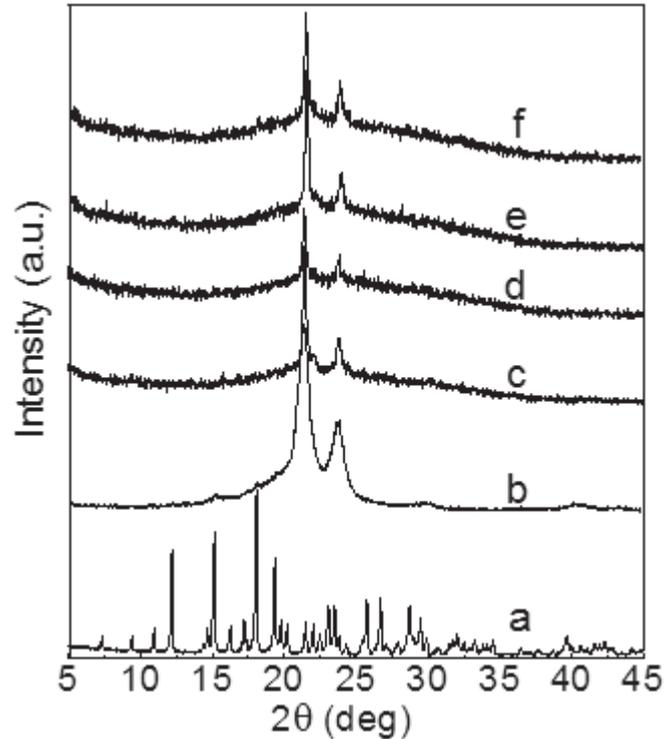
Figure IV.4 *XRD diffractograms of pure AMOX (a), and after milling 3 min with PCL (b), PCL (c), PCL-A3 (d), PCL-A5 (e), and PCL-A7(f).*

IV.4 Mechanical properties

Amoxicilline at 3%, 5% and 7%, as well as milled amoxicilline at 5% were electrospun with PCL solution in acetone and all the experimental conditions for obtaining the membranes are reported in Table IV.1. The mechanical properties of pristine and composite membranes were measured and the principal mechanical parameters are reported in Table IV.1, too. Young's modulus, stress at break and strain at break of the pristine PCA fiber are slightly reduced in the charged membranes and this reduction is the more the higher the AMOX concentration. However the reduction is not drastic and stress at break and strain at break of all samples are adequate for biomedical applications as implantable release systems.

Table IV.1 *Processing parameters and mechanical properties of fibers fabricated by electrospinning (voltage: 30 kV, distance: 30cm, flow rate: 4 mL/h).*

Sample	PCL+AMOX (wt%)	AMOX/PCL (wt/wt-%)	HEBM (min)	Young's modulus (MPa)	Stress at break (MPa)	Strain at break (%)
PCL	17.5	-	-	3.25	0.698	71.3
PCL-A3	17.5	3	-	2.88	0.685	61.9
PCL-A5	17.5	5	-	2.42	0.483	55.2
PCL-A7	17.5	7	-	2.37	0.516	41.7
PCL-A5M3	17.5	5	3	2.45	0.518	58.7
PCL-A5M6	17.5	5	6	2.51	0.482	54.9

IV.5 Thermal properties

In Figure IV.5 the Differential Scanning Calorimetry (DSC) curves are shown. The crystalline AMOX (Figure IV.5a) shows the melting peak very broad and centred at 130°C (Songsurang et al., 2011). Pure PCL shows the melting temperature (T_m) at about 60°C (Figure IV.5b) with a melting enthalpy (ΔH_m) of 75.58 J/g. The melting curves of the filled membranes are very similar to pristine PCL, with the peak at about the same temperature and a lower melting enthalpy. No peak of AMOX melting is apparent, even at the highest concentration of 7%. This is a further evidence that AMOX does not crystallize into the PCL membranes. The DSC thermal parameters are reported in Table IV.2.
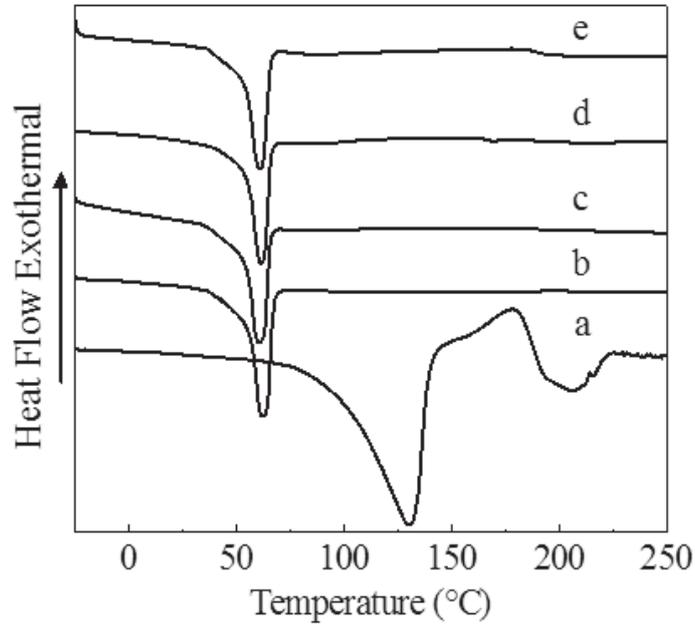
Figure IV.5 *Differential Scanning Calorimetry (DSC) curves of pure AMOX (a), PCL (b), PCL-A3 (c), PCL-A5 (d), and PCL-A7(e).*

In Figure IV.6 the thermogravimetric curves of AMOX powders, pristine PCL electrospun membrane and the membranes filled with 3% and 5% and 7% AMOX concentrations are shown. Beside the 10% for the loss of water at around 100°C the weight loss of AMOX occurs in two main steps; the first centred around 250°C regarding about 30% of the weight loss, and the second centred around 660°C regarding 75% of the weight loss. PCL thermally degrades to volatile products above 300 °C and ends above 500 °C. It appears that the introduction of even very small amounts (about 3 wt %) of AMOX slightly increases the thermal stability of the filled samples, changing the inflection point from 385°C of pure PCL to 386°C , 387°C and 388°C for 3%, 5% and 7% AMOX membrane respectively (Table IV.2). This is an evidence of a good interaction between PCL and the AMOX species.

34
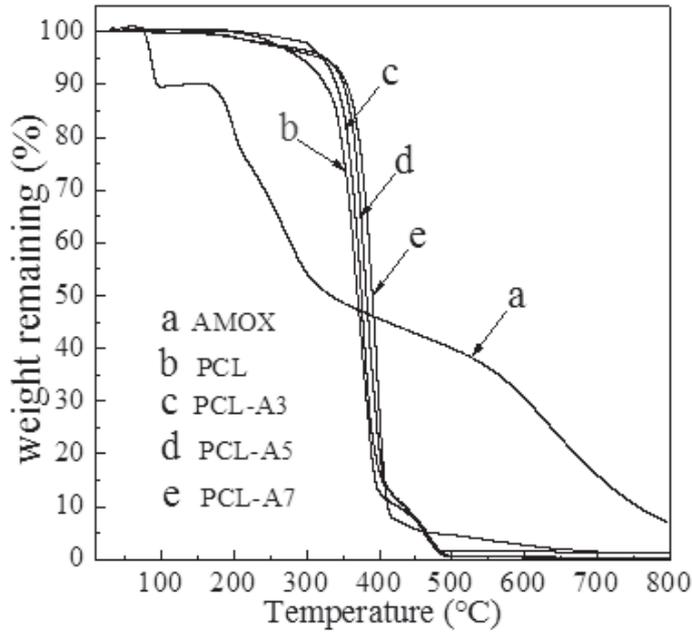
Figure IV.6 *Thermogravimetric curves of pure AMOX(a), PCL(b), PCL-A3(c), PCL-A5(d), and PCL-A7(e).*

All the thermal parameters are reported in Table IV.2. These results show that increasing the amount of AMOX in the semi-crystalline PCL nanofibers caused a reduction in the crystallinity degree (X_c).

Table IV.2 *Thermal parameters of pure AMOX, PCL and filled PCL.*

Sample	T_m ($\circ$C)	ΔH_m (J/g)	X_c (%)	Midpoint temperature ($\circ$C)
AMOX	130.6	-	-	306
PCL	62.5	75.6	51.8	385
PCL-A3	61.8	69.1	45.9	386
PCl-A5	61.7	68.6	44.7	387
PCL-A7	61.6	68.4	43.6	388

IV.6 Drug release studies

Local delivery of drugs sustained for many days is preferred to systemic administration due to the advantages of these delivery systems, such as: i) improving the effectiveness of drug and selective targeting; ii) decreasing the side effects; iii) reducing the frequency of administration. Therefore following the encapsulation procedures of an antibiotic molecule into a biocompatible polymer, it is of utmost importance to investigate the release profiles, depending on the many parameters that it is possible to modulate for the specific applications.

The most important parameters that it is possible to modulate for a local controlled release from elecrospun membranes can be considered: a) drug concentration; b) drug location (inside and/or outside the fibers); c) diameter of the fibers, which in turn determines the membrane porosity and membrane thickness; d) biodegradation time of the polymeric matrix, that can be quicker than drug diffusion or can simultaneously occur, contributing to the delivery. In the present case we chose a polymer, PCL, whose biodegradation is very slow, and therefore we can modulate other parameters without considering its influence. We investigated the effect of varying the concentration of AMOX, whose location is mainly inside the PCL fibers and the membrane thickness. The influence of milling was also investigated.

In forthcoming papers we will consider the other parameters (fiber diameter and polymeric matrix biodegradation time) with the aim to reach a complete correlation picture for the release of the antibiotic specie AMOX from electrospun polymeric membranes.

IV.6.1 Influence of AMOX concentration

In Figure IV.7 the release of AMOX at different concentrations, monitored up to 40 days is shown, as absolute concentration (C_t, mg/L) (Figure IV.7a) and as % of the maximun achievable concentration (Figure IV.7b). As explained in the experimental part, we took membranes of same thickness that is 30 μm and the same weight and dimensions, and therefore we can calculate the maximum quantity of amoxicilline present to be released.

All curves present mainly two stages: a first stage, quick as a"burst", followed by a successive slow second stage. Release kinetics were examined by Korsmeyer-Peppas and Higuchi equations (Costa and Sousa Lobo, 2001). The calculated kinetic release parameters are show in Table IV.3.

The initial burst, found in many controlled-release systems for AMOX (Ahymah Joshy et al., 2011; Said et al., 2011), has been described as caused by a number of mechanisms, including surface desorption, pore diffusion, or the lack of a diffusion front barrier regulating the diffusive process. For

36

customized release processes it must be carefully addressed and controlled, since, depending on application, it may be an optimal mechanism of delivery, as in wound treatment, whereas in others it is undesirable, since the drug can exceed the toxic limits. Indeed, although favorable in some limited situations, under most of the cases burst delivery is considered a negative effect, and many methods have been developed to prevent or minimize this effect. A system for controlled release would be ideal if it could be processed in a single step to encapsulate high drug loading and show no burst release. Another important observation is that adsolute concentration of AMOX released in the time is highest for the most concentrated sample while this sample shows the lowest percentage respect to the maximum achievable quantity.
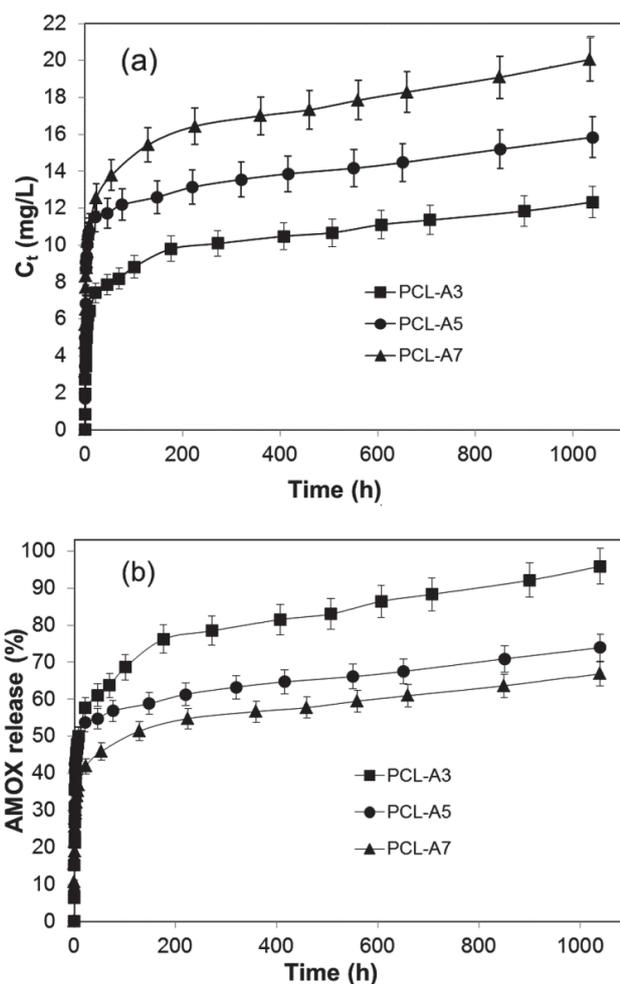
Figure IV.7 *In vitro release profiles of AMOX from PCL-A3, PCL-A5 and PCL-A7, absolute concentration (C_t, mg/L) (a) and as % drug release (b).*

Therefore if we consider the % of AMOX released in the burst, derived from Figure IV.7b, it decreses on increasing the AMOX concentration in the membrane. If we report the burst percentage as a function of the membrane loading (3%, 5%, and 7%) we obtain the behavior shown in Figure IV.8. We observe that the % delivered in the first stage (burst) linearly decreases on increasing the AMOX loading into the membrane; it is therefore possible to extrapolate to zero, obtaining the minimum concentratio for not observing the "burst". This concentration results 15%. This would mean that for concentrations of AMOX higher than 15% the burst possibly does not influence the release, that would be linear with time from the early beginning of the phenomenon.
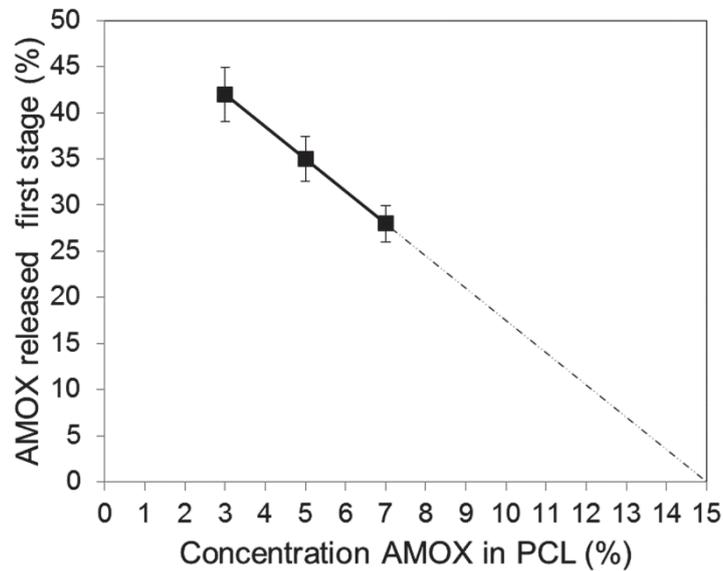
Figure IV.8 *Behavior of the first stage (- - -, extrapolate values)*

IV.6.2 Influence of milling

With the aim to investigate the influence of milling of the AMOX powders on the release properties we chose the 5% concentration membranes with a thickness of 30 μm of the not milled powders and the AMOX powders milled for 3 and 6 minutes, Figure IV.9 show the results. We observe the same behavior, that is an initial burst followed by a slow release. Two interesting points can be put in evidence: i) the fraction of AMOX released in the burst is lower for the milled samples (Table IV.3); ii) the rate of release in the second stage is similar for either sample. Therefore the milling influences only the first stage. We suggest that a better
38

interaction between AMOX and PCL, created by the milling process, allows a less fraction on the surface with a preference for the AMOX to reside inside the fibers. 3 minutes are sufficient and no further change is observable for longer milling times.
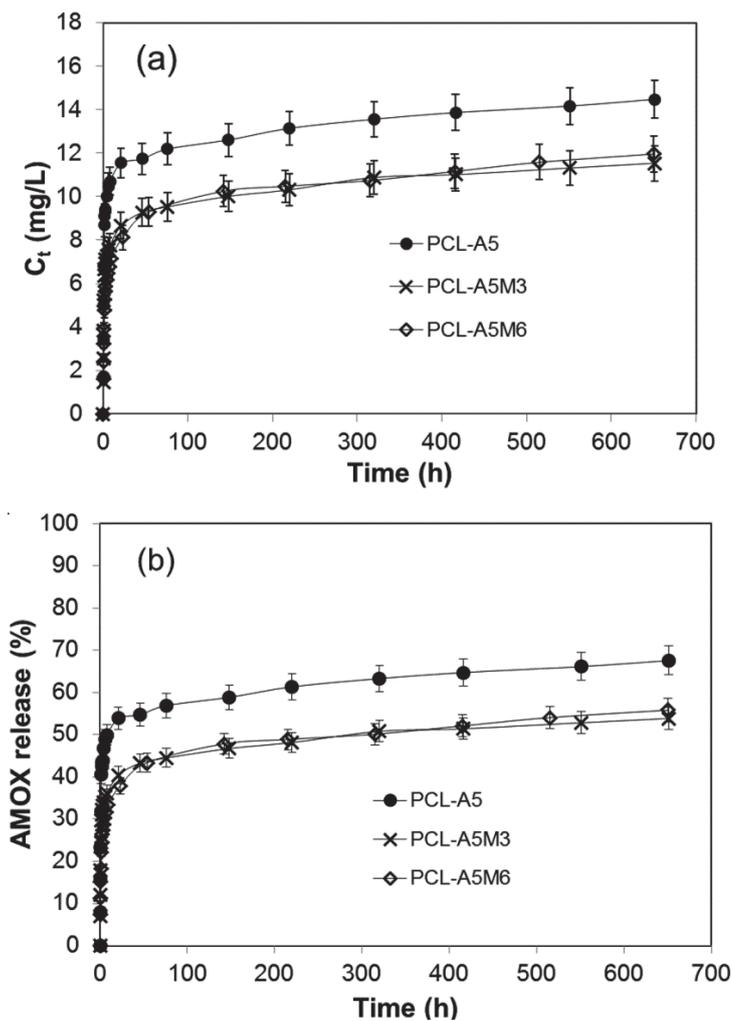
Figure IV.9 *In vitro release profiles of Amoxicillin from PCL-A5, PCL-A5M3 and PCL-A5M6, absolute concentration (C_t, mg/L) (a) and as % of the maximun achievable concentration (b).*

IV.6.3 Influence of membrane thickness

For investigating the influence of the membrane thickness in Figure IV.10 the release profiles of AMOX concentration of 7% in membranes 30 μm, 45 μm and 60 μm, as absolute concentration (C_t, mg/L) (Figure IV.10a) and as % of the maximun achievable concentration (Figure IV.10b) are shown.
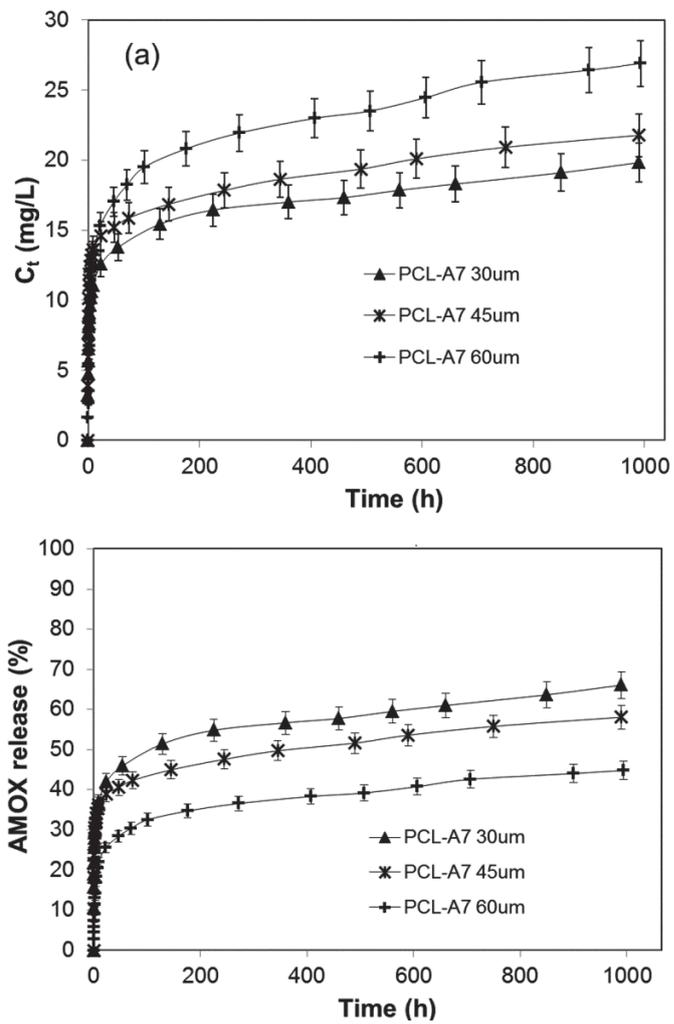
Figure IV.10. *In vitro release profiles of MOX from PCL-A7 30 μm, 45 μm and 60 μm membranes, absolute concentration (C_t, mg/L) (a) and as % drug release (b).*

40

The three curves show the same behavior, that is an initial burst, followed by a slower release. However the initial burst decreases on increasing the membrane thickness, as % respect to the maximum quantity to be delivered, indicating that in our case the burst is mainly a surface phenomenon. If we report the percentage of release in the burst, as a function of the membrane thickness we obtain a linear behavior that extrapolates to zero for membrane thickness higher than 110 μm. This means that for these membranes the burst becomes irrelevant. This is an important result to control the burst, too.

The second stage release kinetics was examined by Korsmeyer-Peppas equation:

$$\frac{M_t}{M_\infty} = K_k t^n \qquad\qquad (IV.1)$$

where M_t/M_∞ is the drug fraction released at time t, K_k is a constant depending on the structural and geometric characteristic of the system, n is the diffusional coefficient related to the release mechanism (Costa and Sousa Lobo, 2001; Zamani et al., 2010).
Higuchi equation was olso used:

$$\%Q_t = K_H t^{1/2} \qquad\qquad (IV.2)$$

where $\%Q_t$ is the amount in % of drug released in time t, K_H is the constant depending on the design variables of the system (Costa and Sousa Lobo, 2001; Said et al., 2011).

The largest r^2 values were obtained for the Korsmeyer-Peppas equations, with values of n from 0.122 to 0.132. Because of AMOX release present two stages, all formulations followed non-Fickian diffusion mechanism (Said et al., 2011). In the second stage release was attributed mainly to the diffusion or permeation of the drug through PCL matrix.

Table IV.3 *Initial burst effect and kinetic parameters of AMOX release from PCL electrospun nanofibers using Korsmeyer-Peppas and Higuchi equation.*

Sample	Initial burst (%)	Korsmeyer-Peppas parameters			Higuchi parameters	
		k_k	n	r^2	k_H	r^2
PCL-A3	41.53	0.374	0.132	0.996	1.952	0.950
PCL-A5	35.65	0.314	0.128	0.983	1.222	0.924
PCL-A7	27.80	0.272	0.126	0.994	1.149	0.933
PCL-A5M3	31.08	0.255	0.122	0.997	1.042	0.929
PCL-A5M6	28.80	0.253	0.124	0.989	1.073	0.933

IV.7 Antibacterial activity in vitro

Antibacterial activity of the membranes filled with 3% and 5% and 7% AMOX concentrations are reported in Table IV.4.

Table IV.4 *Inhibition zone in mm ± SD of AMOX at different concentrations in PCL membranes (the results show the media of 9 repetions ± SD)*

Disc diffsuion method	E. coli	S. aureus	E. faecalis
PCL-A3	7,67 ± 0,52	30,78 ± 0,44	21,00 ± 0,00
PCL-A5	7,60 ± 0,55	29,78 ± 1,09	20,25 ± 0,46
PCL-A7	9,78 ± 0,97	32,78 ± 0,44	22,11 ± 0,60
PCL	-	-	-
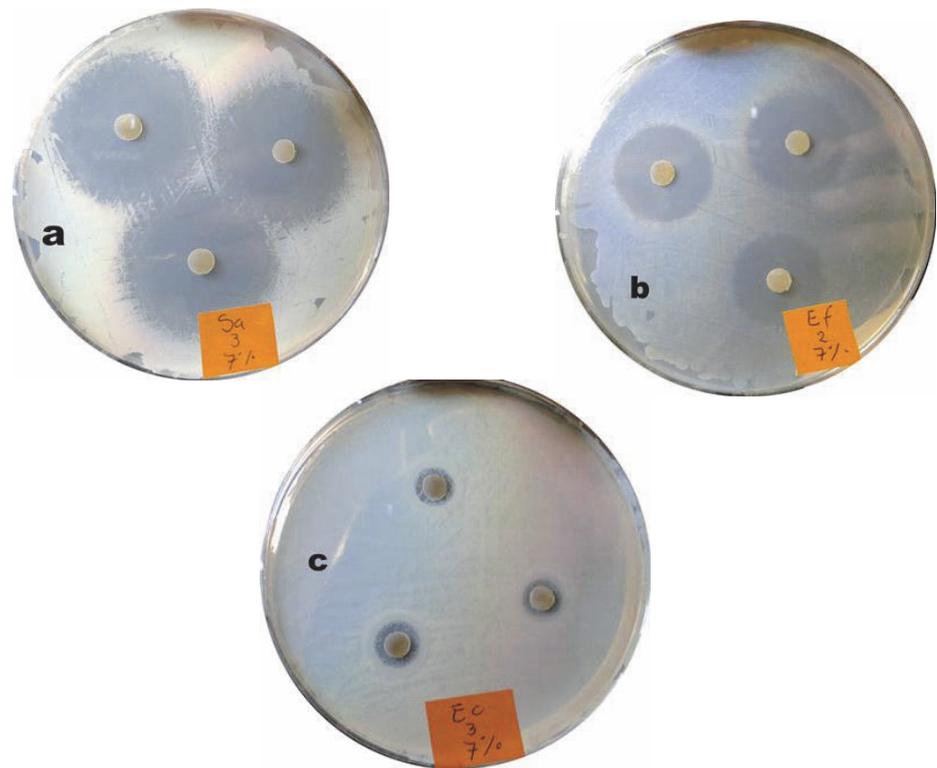
Figure IV.11 *Inhibitory effect of PCL-A7 against three human patogenic bacteria by means of disc diffusion, Staphyococcus aureus (a), Enterococcus faecalis (b), and Escherichia coli (c).*

42

The inhibitory effect of PCL-A7 against three human patogenic bacteria by means of disc diffusion, *Staphyococcus aureus* (Figure IV.11a), *Enterococcus faecalis* (Figure IV.11b), and *Escherichia coli* (Figure IV.11c) is shown in Figure IV.11. The inhibition zone around the discs also named inhibition halo can be clearly visualized in the figure. The plates a, b and c, show the inhibition halos around 6 mm PCL discs of PCL-A7.

Comparing the three bacteria for the highest concentration, that is 7% (Figure IV.11), *S. aureus* results largely the most sensible to AMOX with a maximum of 32,68 ± 0,44 mm, *E. faecalis* shows an intermediate behavior (22,11 ± 0,60 mm) and *E. Coli* is the less inhibited (9,78 ± 0,97 mm). Less evident is the influence of AMOX concentration, although a slight increse on increasing the concentration can be observed. The explanation can be related to that in the first 24 hours the quantity the Amox released is quasi similar for all the samples.

Chapter V

Electrospun fibers loaded with LDHs nanoparticles

V.1 Introduction

Nano-micro scale structured polymeric matrices are very promising devices in controlled drug delivery phenomena due to their ability of hosting and protecting drugs against chemical and physiological triggers, afterward allowing their release according to many tuneable parameters. Controlled drug delivery using a polymeric system indicates that the release of the drug has to occur in a predetermined manner so that the potential for both under and overdosing can be eliminated (Asane et al., 2008; Bawa et al., 2009; Huang et al., 2009; Kumari et al., 2010; Raemdonck et al., 2009; Stevanovic and Uskokovic, 2009; Zilberman and Elsner, 2008).

The release can be either immediate, or constant, or cyclic or even triggered by the surrounding environment, according to different and specific necessities (Brannon-Peppas, 1997). The release properties can be tuned by controlling either the drug diffusion or the degradation rate of the polymer matrix through molecular weight and distribution, material composition and porosity of the carriers. Providing that biodegradable components are incorporated in the matrix structure, controlled drug release profile will be achievable by taking advantage of altering their degradation rate and swelling profile (Ghasemi-Mobarakeh et al., 2008; Kumbar et al., 2008).

One of the most studied problems of drug controlled release is wound dressing, which is essential for the prevention of infection. An ideal candidate for dressing of infectious wounds should deliver sufficiently high concentration of antibiotics to the wound site; mimic the structure and biological function of native extracellular matrix proteins, which provide

support and regulate cellular activities; maintain the normal state of differentiation within the cellular compartment; be biocompatible and/or biodegradable; and have no adverse effects on the surrounding tissue (Elsner and Zilberman, 2009; Kontogiannopoulos et al., 2011; Liu et al., 2010; Meng et al., 2011; Peng et al., 2008; Teo et al., 2011; Yoo et al., 2008).

Among the numerous methods that have been adopted to face this problem, many research groups have successfully used electrospinning to encapsulate drugs and proteins into the fiber matrix and also in the preparation of grafts for tissue engineering applications. Due to high encapsulation efficacy and structural stability of the electrospun fibers, it has been studied extensively by many researchers for drug carrier applications (Chew et al., 2005; Kenawy et al., 2002; Wu et al., 2010a; Xu et al., 2011; Zeng et al., 2003; Zeng et al., 2005).

However, the incorporation of low molecular weight active molecules into polymer matrices has the disadvantage that the migration and the release of the molecule cannot be easily predicted and controlled. To face these problems we have recently proposed a method for fixing active molecules (antiinflammatory, antibiotic, and antimicrobial) into an inorganic compound able to hold them, allowing a very slow and controlled release in selected conditions (Sammartino et al., 2005; Tammaro et al., 2007; Tammaro et al., 2009a).

In particular, layered double hydroxide (LDHs), or hydrotalcite like compounds, have been considered as active molecule delivery vehicles, because of their anion exchange properties(Aguzzi et al., 2007). These compounds, also known as "anionic clays" have the general formula [M$(II)_{(1-x)}$M$(III)_x$(OH)$_2$](A$^{x/n}$) $\cdot$ mH$_2$O where M(II) is a divalent cation such as Mg, Ni, Zn, Cu or Co and M(III) is a trivalent cation such as Al, Cr, Fe or Ga, A^{n-} an anion of charge n such as CO$_3^{2-}$, Cl$^-$, NO$_3^-$ or organic anions(Ardanuy and Velasco, 2011; Cavani et al., 1991; Costantino et al., 2008; Costantino et al., 1998; Leroux and Taviot-Gueho, 2005; Rives, 2001; Xu and Braterman, 2010).

Modified LDHs can be prepared with simple procedures, at high level of purity. They are cheap and eco-compatible and can be organically modified with a variety of organic anions, generally much more numerous than organic cations, commonly involved in the modification of cationic clays (i.e. fillosilicates). This latter characteristic will make these layered compounds a very attractive class of lamellar solids because the release of active molecules in molecule-intercalated layered materials is potentially controllable. The new trend of the research is based on the fact that the active molecular anions, fixed by ionic bonds to the inorganic lamellae, not only can improve the compatibility with the polymer matrix but can carry out the antimicrobial activity either when anchored to the lamellae, or when being slowly released in particular environments (Bugatti et al., 2010). The

46

active component may be released via a de-intercalation process, occurring because of the ion exchange or displacement reactions and will depend on the diffusion through the matrix. Therefore the release rate is related both to the rate of the de-intercalation process, depending on the electronic and steric structure of the guest molecule, and to the diffusion through the matrix, depending on the dispersion of the inorganic lamellae.

In this chapter we present the preparation by electrospinning of new carriers obtained by encapsulating LDH-amoxicillin nano-hybrids into a biodegradable polycaprolactone (PCL)

V.2 Intercalation of amoxicillin into ZnAl–LDH by coprecipitation method

20 mL of an aqueous solution of $Zn(NO_3)_2*6H_2O$ (2.5) and $Al(NO_3)_3*9H_2O$ (1.6g) were added to amoxicillin sodium solution (20 ml) in a conical flask under stirring and under a nitrogen atmosphere. After about 4 hours the pH slowly reaches the value of 7.5 by adding dropwise 1M NaOH solution. After precipitation the solid product was separated by filtration, washed several times with distilled water and dried at 50 ° C for 24h in vacuum oven. The intercalate with formula: $[Zn_{0.65}Al_{0.35}(OH)_2](C_{16}H_{18}N_3O_5S)_{0.35} \cdot 1.2\ H_2O$ and denoted as LDH/AMOX was obtained. The amoxicillin content is 54 wt% % of the total nano-hybrid weight.

V.3 Electrospun membranes preparation

V.3.1 Preparation of polymer solutions

PCL solution was prepared by dissolving in acetone, using a polymer weight/volume percentage of 17.5 wt%. PCL solutions with 3, 5 and 7 wt% of LDH-AMOX were prepared by first dissolving the amount of polymer required to obtain the fully polymer solution in acetone as the solvent. Then the nano-hybrid slowly added to the acetone polymer solution, stirred vigorously for 1 h until complete dissolution.

V.3.2 Electrospinning Procedure

Electrospinning of PCL fibers was carried out at room temperature at a high voltage of 30 kV (HV Power Supply, Gamma High Voltage Research, Ormond, FL). The spinneret used in the experiments had an inner diameter of 0.8 mm. A copper wire was mounted in the spinneret and used as the positive electrode. Grounded aluminum foil was used as the counter electrode and mounted at a distance of 30 cm from the spinneret. Continuous

PCL fibers were collected on the aluminum foil in the form of a fibrous mat. Electrospinning conditions were optimized to produce PCL nanofibrous mats composed of individual fibrils without bead formation. Pure PCL (17.5% in acetone) and composites formed by PCL (17.5% in acetone), and 3%, 5% and 7% (w_t/w_t) of LDH/AMOX (respect to the polymer) were stirred vigorously for 1 h until complete dissolution of PCL in acetone and then spun utilizing the same conditions of pristine PCL. The best processing parameters, obtained by a trial and error procedure, were: voltage 30 kV, needle-collector distance 30 cm, flow rate 4 mL/h, needle diameter 0.8 mm. Sample will be named as PLA-LDH/AMOX*n* where *n* is the amount of LDH/AMOX present (3, 5 and 7 wt%)

V.4 Nano-hybrid characterization

In Figure V.2 the X-ray diffractograms of AMOX powders and LDH/AMOX nano-hybrid are shown. The pristine AMOX powders (Figure V.2a) are very crystalline, showing the most intense peaks at 12.1, 15.1, 18.1 and 19.4° of 2θ whereas their order is lost when the anions are intercalated into the LDH lamellae. The nano-hybrid indeed (Figure V.2b) shows only a peak corresponding to the basal diffraction reflection of the hydrotalcite lamellae, appearing at 3.8° of 2θ. It corresponds to an interlayer distance of 23.2 Å, much larger than the distance when inorganic anions are intercalated, for example 7.55 Å in the case of carbonate anions (Costantino et al., 1998).

The peak is broad indicating very small and imperfect crystals of hydrotalcite with AMOX anions intercalated in the lamellae. The lower structural order has been found able to facilitate the successive dispersion into the polymeric matrix (Vittoria et al., 2011).
The two samples were analyzed by thermogravimetric analysis to confirm the nano-hybrid formation and to determine the degradation temperature (T_d) and the content of the inorganic component in the nano-hybrid material after the thermal decomposition of the organic part in air up to 800 °C.

The AMOX DSC (not shown) exhibits a first endothermic peak between 60 and 120°C with a maximum at 104 °C ($\Delta H= 347.0$ J/g), which corresponds to the dehydration of AMOX. At this endothermic peak corresponds a mass loss of 10% (Figure V.2). Then, AMOX is thermally decomposed at several stages with a total weight loss of 93%, leaving a residual mass at 800°C of 7% (Bisson-Boutelliez et al., 2010).

As shown in Figure V.2, LDH/AMOX is thermally decomposed in several mass loss steps: the first one, accompanied with an endothermic peak at about 85°C, was attributed to the loss of 5% of interlayer and adsorbed water molecules. The second mass loss stage between 90 and 290 °C, with an obvious endothermic peak, was due to dehydroxylation of the layers; the

third stage was due to the oxidative decomposition of amoxicillin anion leaving a residual mass at 800°C of 53%.

Interestingly the degradation of the AMOX anions intercalated into LDH lamellae (Figure V.1) is postponed, indicating a protection of the drug due to the encapsulation between the inorganic lamellae. This result has been already shown in many cases of intercalated organic molecules (Tammaro et al., 2009a) and results one of the reasons for intercalating drugs into the inorganic lamellae.
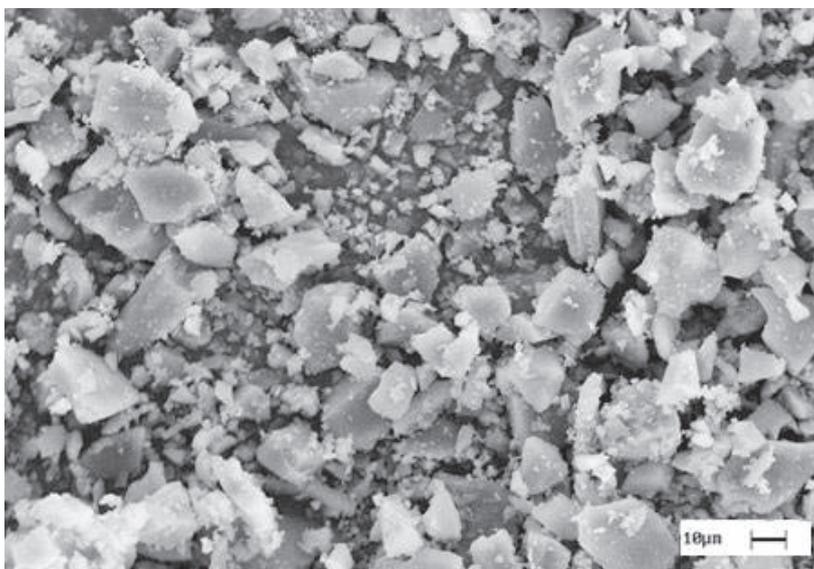
Figure V.1 *AMOX intercalated into LDH*.

V.5 Electrospun membrane characterization

Many internal as well as external parameters do influence the electrospinning process and, as a consequence, the fiber morphology. Indeed it is difficult to isolate the effect of each parameter since they all are interrelated. For this reason, typically a trial-and-error approach has been employed by varying the solution properties and the spinning parameters until uniform defect-free fibers were obtained.

According to the results of previous papers (Tammaro et al., 2009b), we chose acetone as solvent for PCL and PCL loaded with 3, 5 and 7 wt% of the nano-hybrid LDH-AMOX. The mixtures were electrospun using the processing parameters: voltage 30 kV, needle-collector distance 30 cm, flow rate 4 mL/h, needle diameter 0.8 mm.

The X-ray diffractograms were performed to investigate the crystalline structure of the membranes, and are reported in Figure V.2. The pristine PCL (Figure V.2c), spun from the 17.5 % solution in acetone and PCL with 3% (Figure V.2f), 5% (Figure V.2e) and 7% (Figure V.2d) of LDH/AMOX shows the crystalline structure of PCL well developed with the main peaks at 21.4 and 23.8° of 2θ. Interestingly, observing the diffraction patterns of PCL filled with LDH-AMOX we can notice that even in the most concentrated sample (PCL-LDH/AMOX7) the basal peak of the nano-hybrid do not appear at all. We suggest that the LDH/AMOX, is a well dispersed into the PCL fibers.
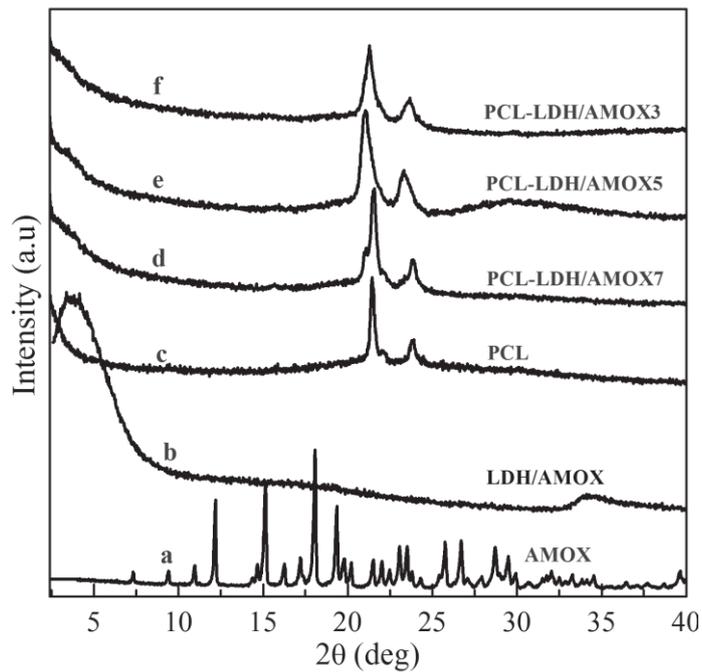
Figure V.2 *XRD diffractograms of PCL fiber, PCL loaded with LDH/AMOX fibers, AMOX and LDH/AMOX.*

SEM micrographs and the diameter distribution of the fibrous membranes of PCL (a), and PCL charged with 3% (b), 5% (c), and 7% (d) of LDH/AMOX are shown in Figure V.3.

50
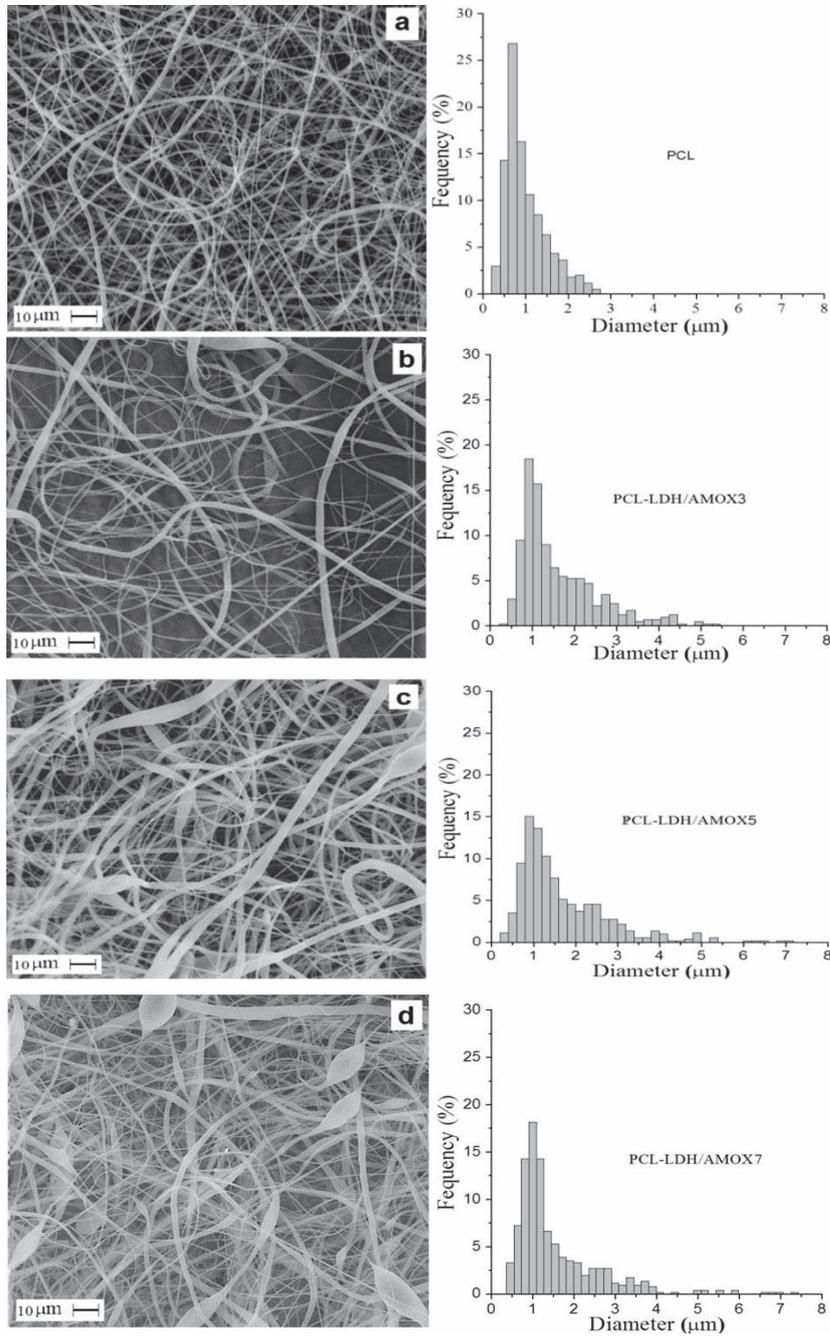
Figure V.3 *SEM micrographs and diameter distribution of PCL (a), PCL-LDH/AMOX3 (b), PCL-LDH/AMOX5 (c), PCL-LDH/AMOX7 (d).*

 The nano-fibrous structure of pristine PCL sample composed of individual, uniform, and randomly oriented fibres with an average diameter ranging around 0.8 micron is evident. The addition of LDH/AMOX at different concentrations caused no noticeable change in the morphology. Moreover it resulted in electrospun nanofibers with very similar or slightly higher average diameter around 0.8-1.2 micron, in comparison with pure PCL, although a prevailing number of fibers with higher dimensions is observable. Some rare beads appear (Figure V.3c and V.3d), possibly due to clusters of the nano-hybrid on the surface of the microfibers.

V.5.1 Thermal properties

The thermogravimetric analysis was performed to investigate the degradation temperature of the samples. The TGA curves of electrospun PCL and composites are showed in Figure V.4
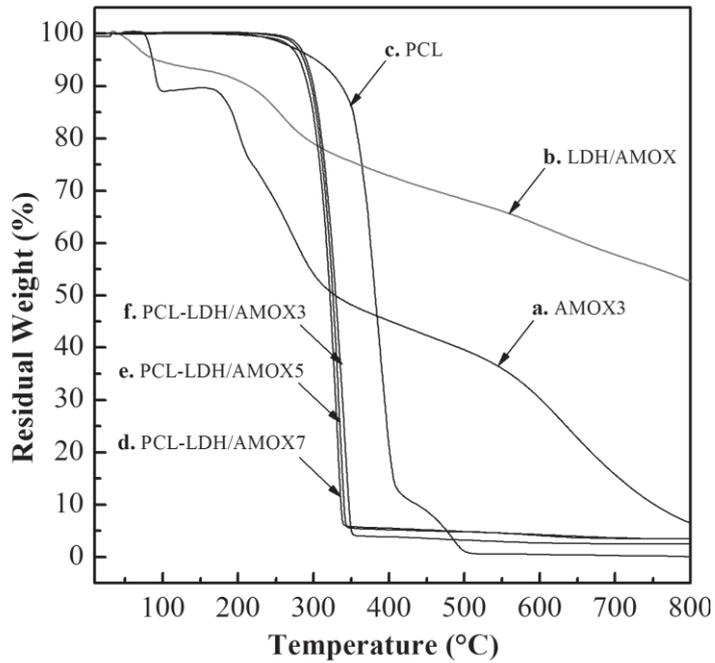
Figure V.4 *Thermogravimetric curves of PCL fiber, PCL loaded with LDH/AMOX fibers, AMOX and LDH/AMOX.*

It appears that the presence of LDH/AMOX in the composites anticipates the degradation of the polymer due to the lower degradation temperature of the nano-hybrid. The PCL melting peak slightly shifted to lower temperatures in all composites and the melting enthalpy slightly decreased. The cristallinity (Xc) of the composites is slightly lower than Xc value of alone PCL (Costantino et al., 2009).
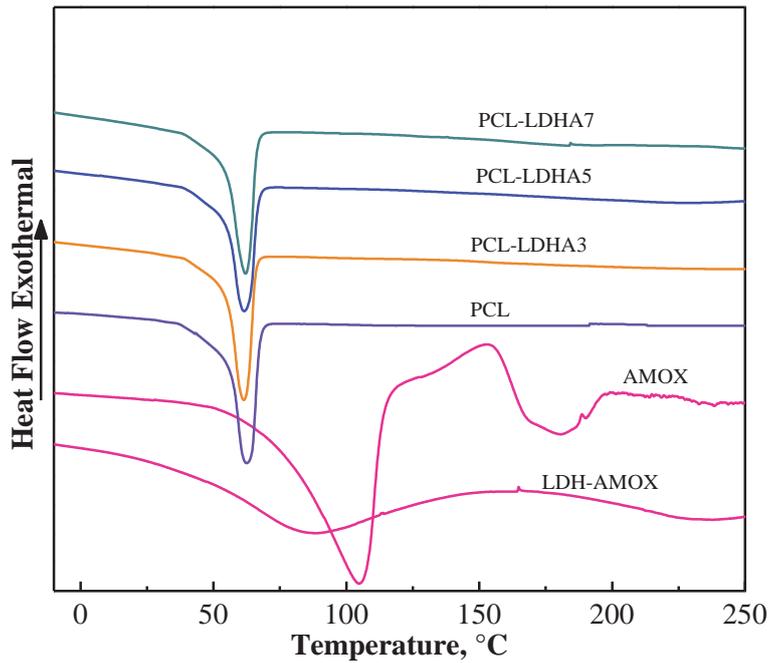
Figure V.5 *Differential Scanning Calorimetry (DSC) curves of PCL fiber, PCL loaded with LDH/AMOX fibers, AMOX and LDH/AMOX.*

Table V.1 *LDH/AMOX content and thermal parameters*

Sample	LDH/AMOX content (wt/wt %)	AMOX content (wt/wt %)	T_m (°C)	X_c (%)	ΔH_m (J/g)	$T_{midpoint}$ (°C)
LDH/AMOX	100	54	80,8	-	-	337
PCL	0	0	62.5	51.8	75.6	385
PCL-LDH/AMOX3	3	1.62	61.5	47.8	69.7	329
PCL-LDH/AMOX5	5	2.70	61.4	47.5	69.4	325
PCL-LDH/AMOX7	7	3.78	61.3	47.4	69.2	323

In Figure V.5 the Differential Scanning Calorimetry (DSC) curves are shown. The different amount of LDH/AMOX in the composites does not produce further relevant decrease in the melting peak (T_m), melting enthalpy (ΔH_m), cristallinity (X_c) and degradation temperature (Table V.1).

V.6 Drug release study

Local delivery of drugs sustained for many days is preferred to systemic administration due to the advantages of these delivery systems, such as: i) improving the effectiveness of drug and selective targeting; ii) decreasing the side effects; iii) reducing the frequency of administration. Therefore it is of utmost importance to investigate the release profiles, depending on the many parameters that it is possible to modulate for the specific applications. The most important parameters that it is possible to modulate for a local controlled release from electrospun membranes can be considered: a) drug concentration; b) drug location (inside and/or outside the fibers); c) diameter of the fibers, which in turn determines the membrane porosity and; d) biodegradation time of the polymeric matrix, that can be quicker than drug diffusion or can simultaneously occur, contributing to the delivery. In the present case we chose a polymer, PCL, whose biodegradation is very slow, and therefore we can modulate other parameters without considering its influence.

The parameter we consider in the present paper is the encapsulation of the drug into inorganic lamellae of LDH with the aim to compare the release kinetics with those obtained with AMOX directly incorporated into the PCL membranes.

In Figure V.6 the release of AMOX at different concentrations, monitored up to 40 days is shown, as absolute concentration (C_t, mg/L) (a) and as % of the maximun achievable concentration (b). As explained in the experimental part, we took membranes of same thickness that is 45 μm and the same weight and dimensions, and therefore we can calculate the maximum quantity of amoxicilline present in the nano-hybrid to be released. In this case an exchange reaction is necessary followed by a diffusion phenomenon for the AMOX to be released.

All curves present mainly two stages: a first stage, quick as a "burst", followed by a successive slow second stage. The initial burst, found in many controlled-release systems for AMOX (Ahymah Joshy et al., 2011), has been described as caused by a number of mechanisms, including surface desorption, pore diffusion, or the lack of a diffusion front barrier regulating the diffusive process (Sill and von Recum, 2008). For customized release processes it must be carefully addressed and controlled, since, depending on application, it may be an optimal mechanism of delivery, as in wound

54

treatment, whereas in others it is undesirable, since the drug can exceed the toxic limits. This initial high-rate drug release could be caused by quick release of LHD/AMOX molecules that should be deposited on surface area of nanofibers. For the delivery of antibiotic drugs, a initial burst is actually ideal since it is important to eliminate the intruding bacteria before they begin to proliferate. However, for the few organisms that may survive the initial burst, a continued release of antibiotic is necessary to prevent their further population (Shin et al., 2001b).
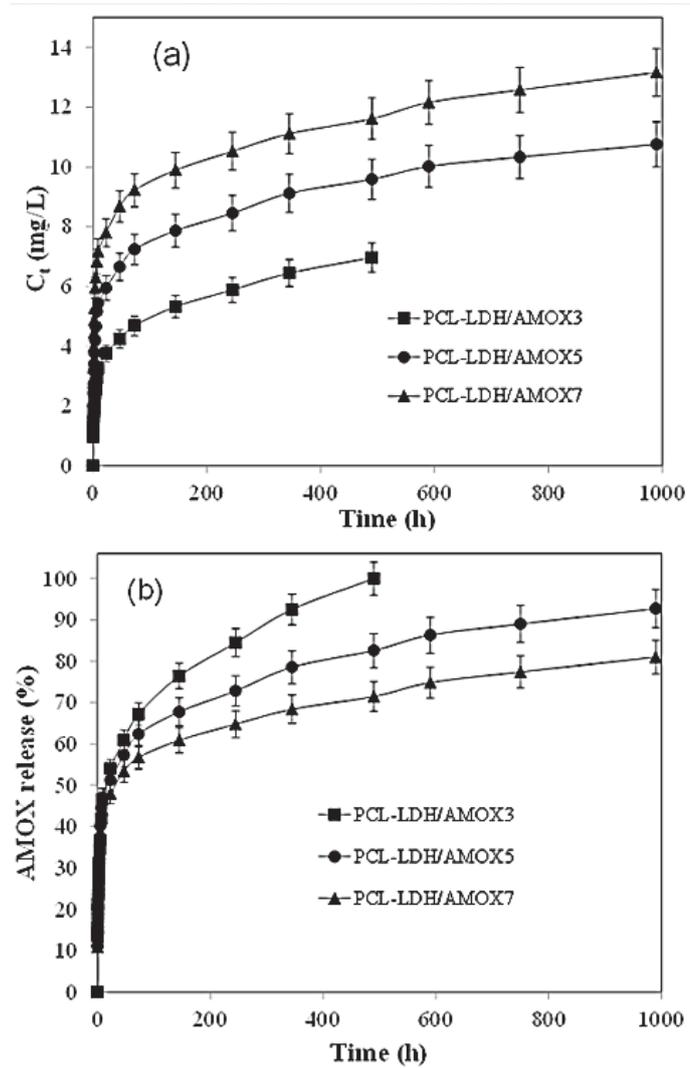
Figure V.6 *Amount of AMOX released, as absolute concentration (C_t, mg/L) (a) and as % of the maximun achievable concentration (b).*

After the initial burst we observe an increase of AMOX release, linear with time and extending for many days, depending on LDH/AMOX concentration inside the membrane. For example the complete release of AMOX from PCL-LDH/AMOX3 is observed after 20 days, whereas it is not yet completed for PCL-LDH/AMOX5 (82%) and PCL-LDH/AMOX7 (71%).

In Figure V.7 we show the fraction of AMOX released after 20 days as a function of nano-hybrid loading into the membrane, and compare the curve with that obtained for AMOX introduced alone in the membrane. We observe that the curve for the AMOX protected into the clay lays underneath the curve of the drug alone. A difference of 10% more for the last sample indicates another possibility to tune the release times, depending on the applications.
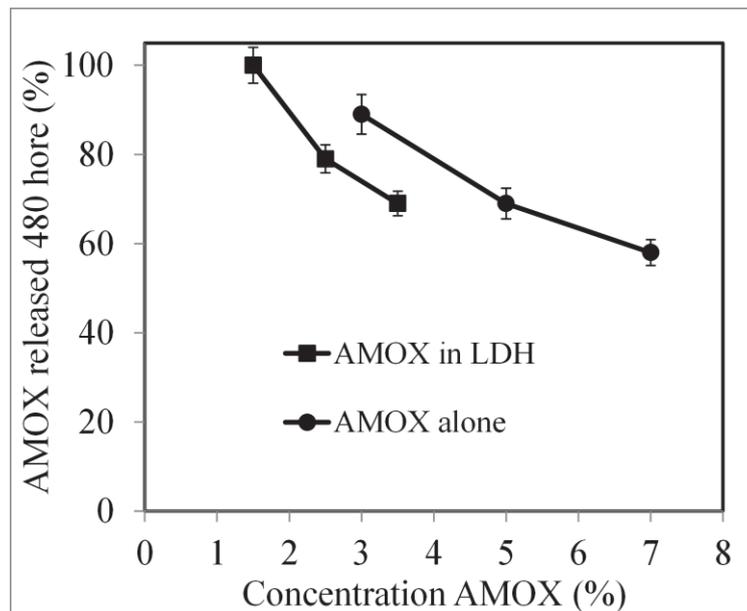
Figure V.7 *Amount of AMOX released after 20 days.*

Chapter VI

Polylactic acid electrospun fibers

VI.1 Introduction

Electrospinning is a versatile technique for preparing nano and microfibers of natural and synthetic polymers (Bhardwaj and Kundu, 2010). The accumulation of these non-woven or aligned fibers produces the so called fibrous mats (Charernsriwilaiwat et al., 2010), fibrous fabrics (Chegoonian et al., 2012) or fibrous membranes (Chen et al., 2011). Through this process it is possible to produce polymer or polymer composite fibrous mats with high surface to volume ratio (Chong et al., 2007). The solution properties, such as viscosity, concentration, surface tension and electrical conductivity as well as processing parameters, such as voltage, type of collector, solution flow rate, needle diameter and needle-collector distance can influence the properties and the morphology of the electrospun fibers (Deitzel et al., 2001; Lee and Obendorf, 2007). Solution properties and processing parameters can be optimized according to the final required characteristics.

The electrospun nanofibers were found to have wide applications in several fields such as filtration (Greiner and Wendorff, 2007), wound healing (Han et al., 2010), protective clothing (Huang and Brazel, 2003), drug delivery (Islam and Karim, 2010) and biomedical areas (Liu et al., 2008) such as scaffold for tissue engineering (Jaworek et al., 2009).

One of the most studied problems of drug controlled release is wound dressing, which is essential for the prevention of infection. An ideal candidate for dressing of infectious wounds should deliver sufficiently high concentration of antibiotics to the wound site; mimic the structure and biological function of native extracellular matrix proteins, which provide support and regulate cellular activities; maintain the normal state of differentiation within the cellular compartment; be biocompatible and/or

biodegradable; and have no adverse effects on the surrounding tissue (Elsner et al., 2011; Elsner and Zilberman, 2009; Kontogiannopoulos et al., 2011; Liu et al., 2010; Meng et al., 2011; Mi et al., 2002; Min et al., 2004; Noh et al., 2006; Peng et al., 2008; Powell et al., 2008; Rho et al., 2006; Teo et al., 2011; Yoo et al., 2008). Many of these characteristics can be fulfilled by biocompatible polymer electrospun membranes, loaded with drugs for specific applications.

In this chapter we present the preparation by electrospinning of new carriers obtained by encapsulating amoxicillin into a biodegradable Polylactic acid.

VI.2 Preparation of electrospun membranes

VI.2.1 Preparation of polymer solutions

poly(lactic acid) solution was prepared by dissolving in acetone, using a polymer percentage of 17.5 % (weight/weight). PLA with 3, 5 and 7 wt % of amoxicillin were prepared by first dissolving the amount of polymer required to obtain the fully polymer solution in acetone as the solvent. Then the filler AMOX was slowly added to the acetone polymer solution, stirred vigorously for 3 h until complete dissolution.

VI.2.2 Electrospinning Procedure

Electrospinning of PLA and their AMOX filled solutions was carried out at room temperature. The voltage used was 20 KV (HV Power Supply, Gamma High Voltage Research, Ormond, FL). A copper wire was mounted in the spinneret having an inner diameter of 0.8 mm and used as the positive electrode. Grounded aluminium foil was used as the counter electrode and mounted at a distance of 20 cm from the spinneret. Continuous polymer, polymer mixtures and composite polymer mixtures were collected on the aluminium foil in fibrous mat form. Sample will be named as PLA-A*n* where *n* is the amount of AMOX present (3, 5 and 7 wt%).

VI.3 Morphology of electrospun nanofibers

Electrospinning conditions were optimized to produce fibrous mats with bead-less fibers (Qin and Wang, 2006) (so called bead-on-string). Table VI.1 summarizes the percentages of PLA/AMOX used, the optimal electrospinning conditions applied for the different samples and the average diameter of the fibers. The average diameter of PLA fibers was 2.52 μm. The average diameter increases with increasing the amount of AMOX in the composites fibers. Since the AMOX is insoluble in acetone, it is

incorporated into the fibers as crystal particles with unchanged dimension. The presence of large AMOX crystals into the fibers (Figure VI.1) contributes to increase the average diameter.

Table VI.1 *Composition (PLA/AMOX), processing parameters and average diameter values of fibers fabricated by electrospinning (flow rate: 4 mL/h. SD: standard deviation, diameter values are means of 500 determinations).*

Sample	AMOX (wt%)	Distance (cm)	Voltage (kV)	Fiber Diameter (μm)	SD (μm)
PLA	-	20	20	2.52	0.53
PLA-A3	3	20	20	2.58	0.49
PLA-A5	5	20	20	2.66	1.17
PLA-A7	7	20	20	3.22	0.99

The Figure VI.1 shows the morphology and diameter distribution of PLA fibers, PLA loaded fibers and AMOX. The structure of fibrous mats is characterized by individual, uniform, and randomly oriented fibres. The addition of AMOX did not produce evident change in the morphology of the fibers, however, a few AMOX crystals like beads appear mainly in samples loaded with 5% and 7 wt% of AMOX (Figure VI.1d and Figure VI.1e).
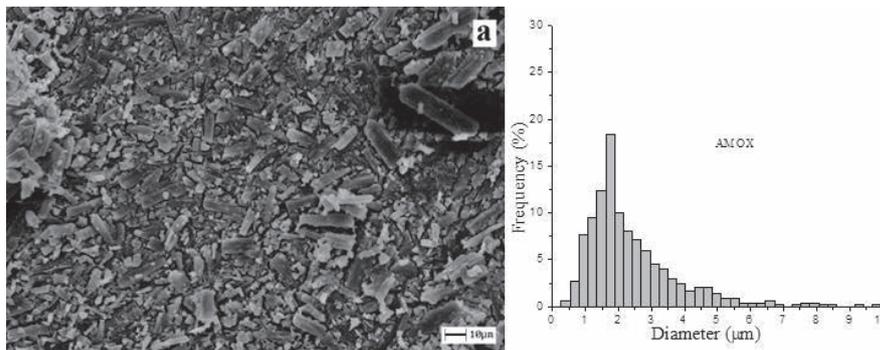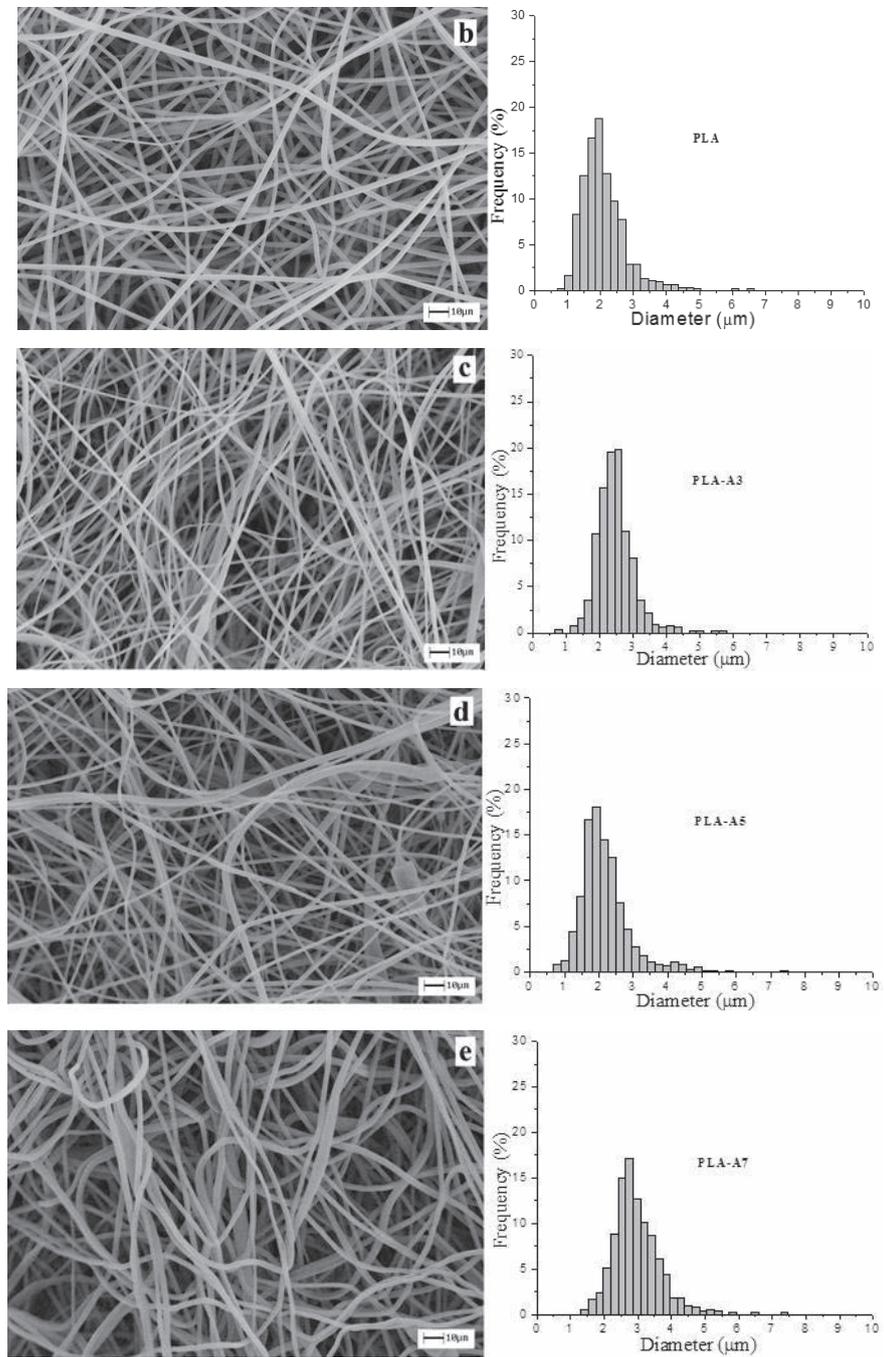
Figure VI.1 *SEM micrographs and diameter distribution of AMOX (a), PLA (b), PLA-A3 (c), PLA-A5(d) and PLA-A7(e)*

60

VI.4 Structure and thermal properties

The XRD patterns of PLA pellets, neat PLA fibers, composite fibers containing AMOX particles and original AMOX particles were shown in Figure VI.2.

The strong and sharp crystalline peaks at $2\theta = 17°$ and $19°$ correspond to the crystallographic planes of PLA pellets (Wu, 2009) are shown in Figure VI.2b

The broad pattern of the non-woven membrane (Figure VI.2c) can be attributed to the reflection of amorphous PLA, indicating that the evaporation of the solvent during electrospinning process is very rapid not allowing the polymer crystallization. The incorporation of AMOX filler, regardless of their concentration, does not induce relevant changes (Figure VI.2d, VI.2e and VI.2f)
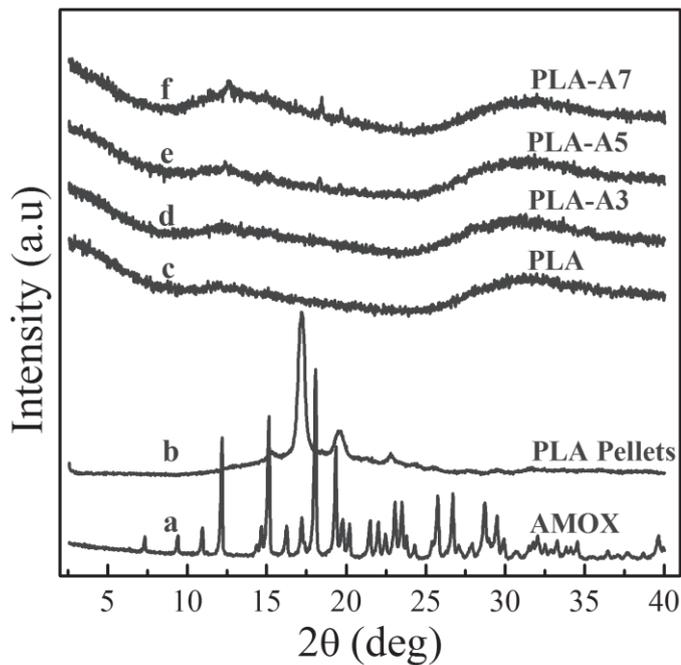
Figure VI.2 *XRD diffractograms of PLA pellets, PLA fiber, PLA loaded with AMOX fibers and AMOX.*

Table VI.2 contains the main calorimetric data obtained from the heating run of all electrospun samples. Heating traces of samples can be seen in Figure VI.3.

Table VI.2 *Thermal parameters of fibers fabricated by electrospinning (AMOX: T_m = 131 °C, Midpoint temperature = 306 °C)*

Sample	T_c (°C)	ΔH_c (J/g)	T_m (°C)	ΔH_m (J/g)	Midpoint temperature (°C)
PLA	105	17	148	25	340
PLA-A3	103	25	148	24	344
PLA-A5	103	27	147	21	345
PLA-A7	102	29	147	19	346
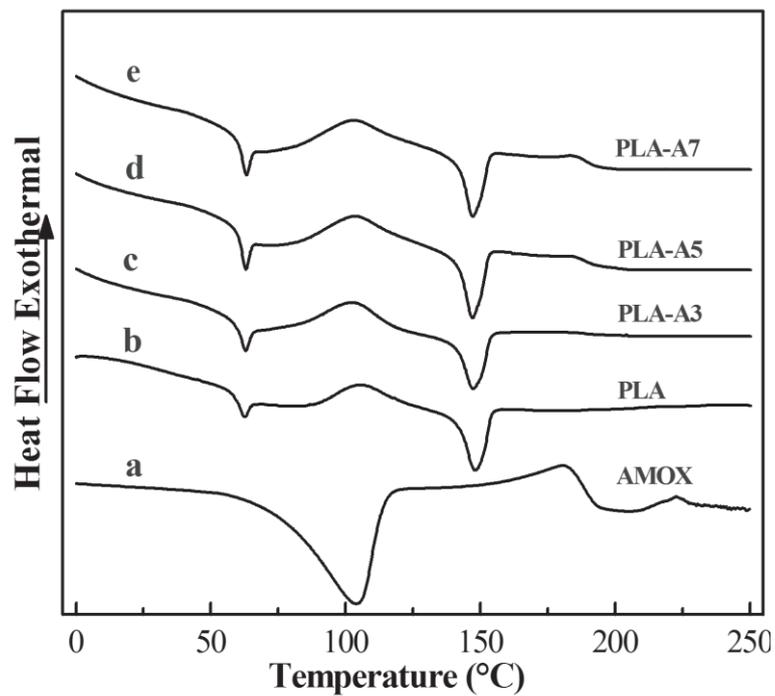
Figure VI.3. *Differential Scanning Calorimetry (DSC) curves of PLA fibers, PLA loaded with AMOX fibers and AMOX.*

The DSC curves of the electrospun samples show a broad exothermic peak (T_c: 90-120°C) indicative of the cold crystallization of polylactide, together with the corresponding melting peak (T_m: 147-150°C).

62

Polycaprolactone melting enthalpy (ΔH_m) was sometimes difficult to calculate accurately due to the overlap with polylactide enthalpy relaxation. As a consequence, the melting peak was overestimated. The PLA melting peak slightly shifted to lower temperatures in all samples and the melting enthalpy decreased when samples were loaded with AMOX. This allows inferring that the drug was well mixed into the polymeric phase.

The thermogravimetric analysis was performed to investigate the degradation temperature of the samples. The PLA and their composite samples are showed in Figure VI.4. The introduction of the AMOX does not produce further relevant decrease in the degradation temperature (Table VI.2).
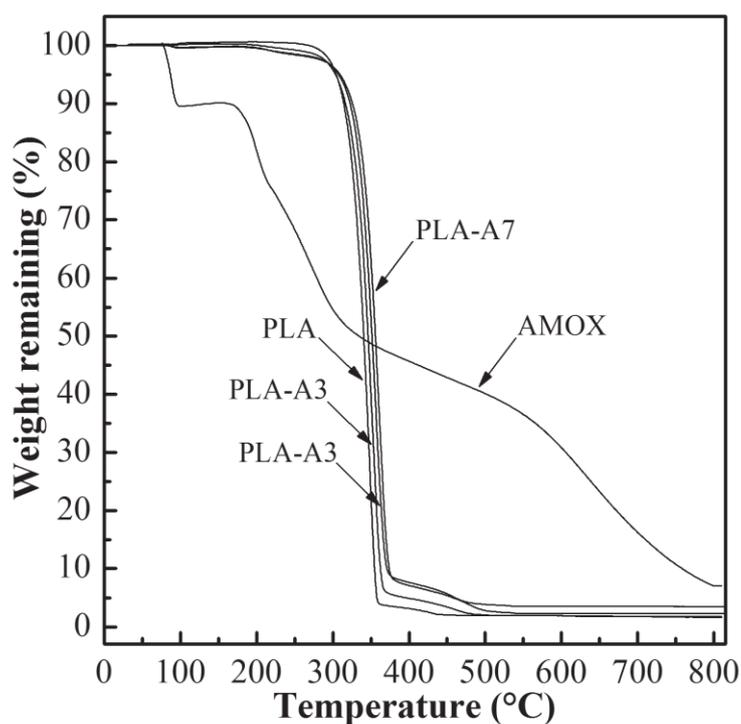
Figure VI.4 *Thermogravimetric curves of PLA fibers, PLA loaded with AMOX fibers and AMOX..*

VI.5 Drug release study

Figure VI.5 shows the release profiles of AMOX from fibrous mats containing 3, 5 and 7% w/w of drug. Samples showed a sustained release

behavior, although an initial rapid drug release was found within the first 8 h.
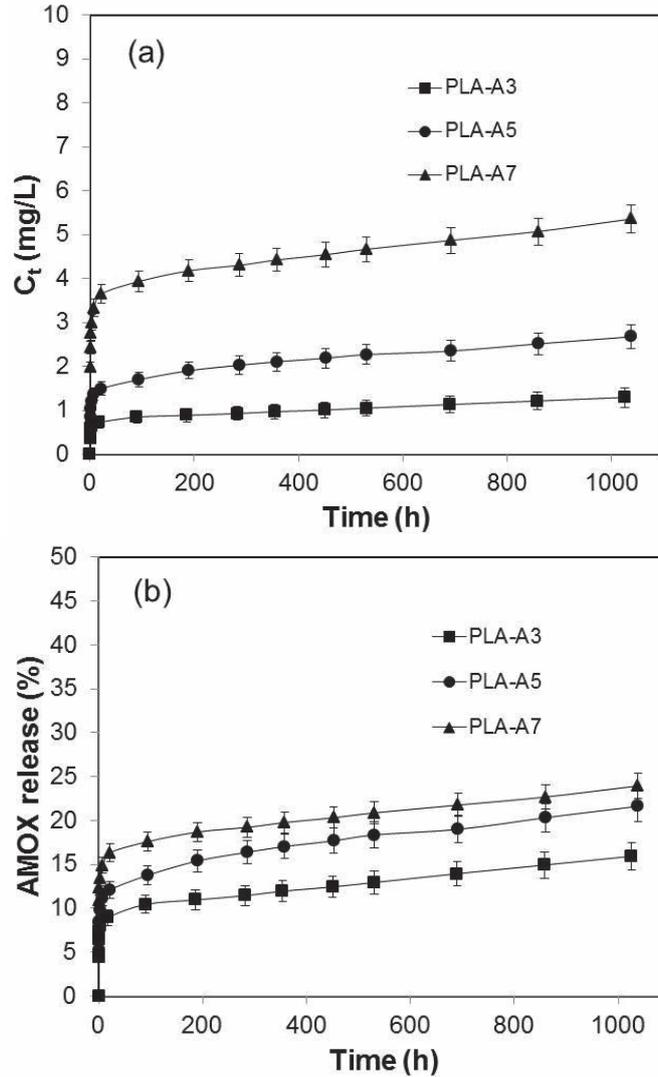
Figure VI.5 *In vitro release profiles of AMOX from PLA-A3, PLA-A5 and PLA-A7, absolute concentration (C_t, mg/L) (a) and as % drug release (b).*

The initial high-rate drug release observed at the beginning of many controlled-release processes can be caused by a number of mechanisms,

64

including surface desorption, pore diffusion, or the lack of a diffusion front barrier to regulate the diffusive process (Sill and von Recum, 2008). This initial period usually so called "burst" could be caused by quick release of AMOX molecules that should be deposited on surface area of nanofibers. For the delivery of antibiotic drugs, a initial burst is actually ideal since it is important to eliminate the intruding bacteria before they begin to proliferate. However, for the few organisms that may survive the initial burst, a continued release of antibiotic is necessary to prevent their further population (Shin et al., 2001b). Second stage shows a very slow drug release which is attribute mainly to the diffusion or permeation of the drug molecules through polymer matrix towards the release medium.

Release kinetics can be examined by several theoretical models (Costa and Sousa Lobo, 2001; Said et al., 2011; Zamani et al., 2010). In this study the second release stage was simulated by Korsmeyer-Peppas equation:

$$Q_t/Q_\infty = K_K t^n \tag{VI.1}$$

where Q_t/Q_∞ is the drug fraction released at time t, K_k is a constant depending on the structural and geometric characteristic of the system, n is the diffusional coefficient related to the release mechanism (Zamani et al., 2010).

Higuchi equation was also used:

$$\%Q_t = K_H t^{1/2} \tag{VI.2}$$

where $\%Q_t$ is the percentage of drug released at the time t, K_H is the constant depending on the design variables of the system (Said et al., 2011). The calculated kinetic release parameters are show in Table VI.3.

The largest r^2 values were obtained for the Higuchi equations. The release constants depend on the AMOX content and polymer concentration. The rate of release increases with increasing of the drug concentration and with the PCL content in the fibers.

Table VI.3 *Initial burst, kinetic parameters and release amount of AMOX in 500 h for PLA electrospun membranes.*

Sample	Korsmeyer-Peppas parameters			Higuchi Parameters		Released amount of amoxicillin (%)
	k_k	n	r^2	k_H	r^2	t=500 h
PLA-A3	0.067	0.096	0.982	0.200	0.985	12.94
PLA-A5	0.084	0.116	0.978	0.241	0.998	18.34
PLA-A7	0.095	0.121	0.976	0.343	0.996	20.86

The Table VI.3 also shows the amount (%) of AMOX released in the first 500 hours. The released percentages of AMOX increase with the drug concentration

Chapter VII

PLA/PCL blend electrospun fibers

VII.1 Introduction

Poly(lactic acid) (PLA) is a biodegradable polymer with different biomedical applications because of its mechanical properties and biocompatibility (Kim et al., 2004b). Poly(ε-caprolactone) (PCL) is a semi-crystalline biodegradable polymer broadly used in many fields, due to the good drug permeability and slow biodegradability (Lannutti et al., 2007). The compatibility of PLA and PCL has been studied to improve different properties of the resultant polymer blend. Amoxicillin (AMOX) is a bacteriolitic, penicillin like antibiotic used to treat infections caused by bacteria in ear, lung, nose, urinary tract and skin infections; one of the most common antibiotic for children. It was also used before surgery to prevent infections (Ahymah Joshy et al., 2011).

Electrospinning of biocompatible and biodegradable polymers has been employed for preparation of micro and nanofibers and composites nanofibers with different applications, one of this is the drug delivery. Blend of biocompatible and biodegradable polymer allows to improve mechanical properties and to obtain drug release system with tunable properties(Li and Xia, 2004; Liao et al., 2012; Liu and Hsieh, 2002).

The delivery of the same antibiotic from poly(lactic acid) (PLA) was found very much slower, and it was correlated to the drug concentration, too. This result, very different release kinetics of PLA and PCL, spurred us to investigate electrospun membranes obtained by blends of these two polymers, in which the fraction of PCL is varied in the entire composition interval (0-100 %), to obtain a tuneable delivery, depending on blend composition.

In the present chapter PLA/PCL and PLA/PCL/AMOX composite electrospun nanofibers were produced by electrospinning technique. For this purpose different weight ratios of the two polymers were used and different amounts of amoxicillin were loaded into PLA/PCL nanofibers.

VII.2 Preparation of electrospun membranes

VII.2.1 Preparation of polymer solutions

PLA/PCL mixtures solutions were prepared by dissolving in acetone, using a polymer percentage of 17.5 % (weight/weight). PLA/PCL mixtures solutions with 3, 5 and 7 wt % of amoxicillin were prepared by first dissolving the amount of polymer required to obtain the fully polymer solution in acetone as the solvent. Then the filler AMOX was slowly added to the acetone polymer solution, stirred vigorously for 3 h until complete dissolution.

VII.2.2 Electrospinning Procedure

Electrospinning of PLA/PCL mixtures and their AMOX filled solutions was carried out at room temperature. The voltage was varied between 20 and 30 kV (HV Power Supply, Gamma High Voltage Research, Ormond, FL). A copper wire was mounted in the spinneret having an inner diameter of 0.8 mm and used as the positive electrode. Grounded aluminium foil was used as the counter electrode and mounted at different distance (20-30 cm) from the spinneret. Continuous polymer, polymer mixtures and composite polymer mixtures were collected on the aluminium foil in fibrous mat form. Sample will be named as Pm-An where n is the amount of AMOX present (3, 5 and 7 wt%) and m is the amount of PLA in PLA/PCL mixtures (i.e. P25 is 25 wt% PLA and 75 wt% PCL)

VII.3 Morphology of electrospun nanofibers

Electrospinning conditions were optimized to produce fibrous mats with bead-less fibers (Qin and Wang, 2006) (so called bead-on-string). Table VII.1 summarizes the percentages of PLA/PCL/AMOX used, the optimal electrospinning conditions applied for the different samples and the average diameter of the fibers. A distance and a voltage lower (20 cm and 20 KV) than those used for the formation of PCL fibers (30 cm and 30 KV) are required for PLA fibers. Increasing the amount of PCL in the mixture, higher voltage and higher distance were needed for the formation of polymer mixture fibers. The average diameter of P25 was 1.51 μm. This value

68

increased with increasing the amount of PLA: 1.98 µm for P50 and 2.43 µm for P75. The average diameter increases also with increasing the amount of AMOX in the composites fibers (Figure VII.1, Figure VII.2 and Figure VII.3). Since the AMOX is insoluble in acetone, it is incorporated into the fibers as crystal particles with unchanged dimension. The presence of large AMOX crystals into the fibers contributes to increase the average diameter.

Table VII.1 *Composition (PLA/PCL/AMOX), processing parameters and average diameter values of fibers fabricated by electrospinning (flow rate: 4 mL/h. SD: standard deviation, diameter values are means of 500 determinations).*

Sample	PLA (wt%)	PCL (wt%)	AMOX (wt%)	Distance (cm)	Voltage (kV)	Fiber Diameter (µm)	SD (µm)
P75	75	25	-	25	20	2.43	0.48
P75-A3	75	25	3	25	20	2.53	0.77
P75-A5	75	25	5	25	20	2.60	1.23
P75-A7	75	25	7	25	20	2.63	1.68
P50	50	25	-	25	20	1.98	0.51
P50-A3	50	50	3	25	20	2.04	0.86
P50-A5	50	50	5	25	20	2.10	1.23
P50-A7	50	50	7	25	20	2.30	1.24
P25	25	75	-	25	25	1.51	0.46
P25-A3	25	75	3	25	25	1.97	0.72
P25-A5	25	75	5	25	25	2.05	1.09
P25-A7	25	75	7	25	25	2.22	1.10

The morphology and diameter distribution of P75 fibers and P75 fibers loaded with 3, 5 and 7% of AMOX are shown in Figure VII.1. All fibrous mats are characterized by individual, uniform, and randomly oriented fibres. The addition of AMOX did not produce evident change in the morphology of the fibers, however, a few AMOX crystals like beads appear mainly in samples loaded with 5% and 7 wt% of AMOX.
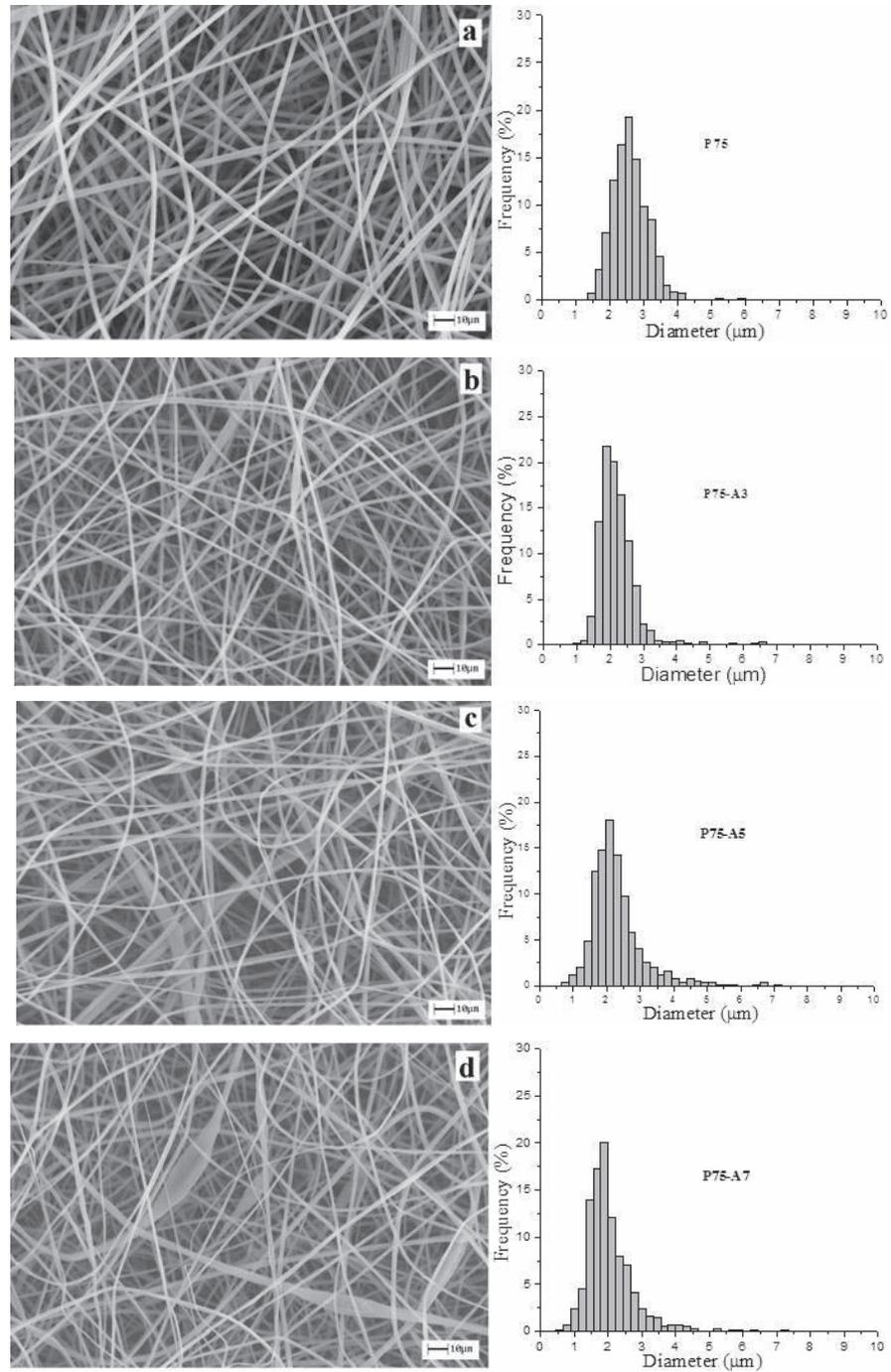
Figure VII.1 *SEM micrographs and diameter distribution P75 (a), P75-A3 (b), P75-A5 (c) and P75-A7(d).*

70

The morphology of the fibrous mats of P50, P50-A3, P50-A5 and P50-A7 are characterized by uniform, individual, randomly and non-woven fibres. The addition of AMOX did not produce evident change in the morphology of the fibers (Figure VII.2).
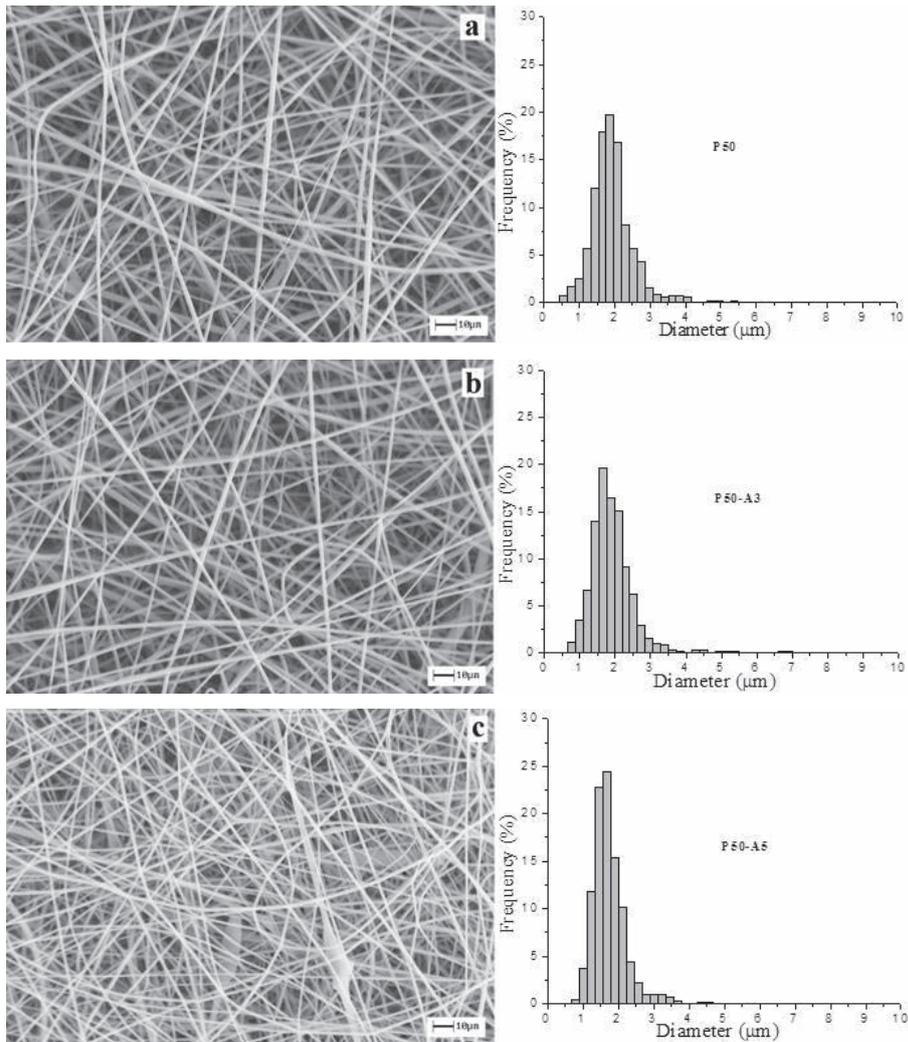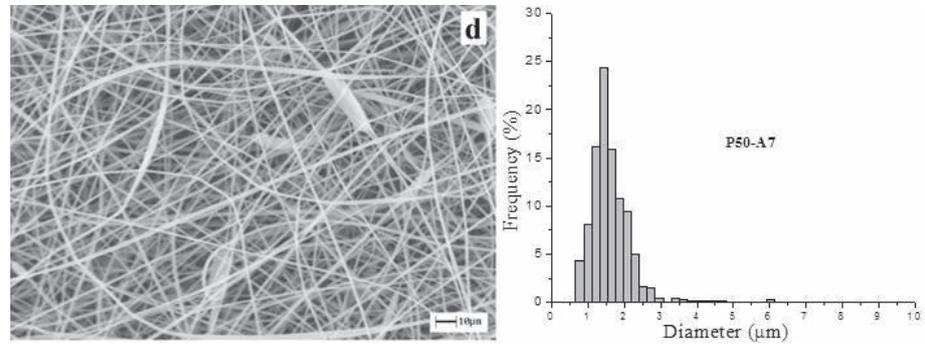
Figure VII.2 *SEM micrographs and diameter distribution P50 (a), P50-A3 (b), P50-A5 (c) and P50-A7(d).*

The Figure VII.3 shows that the structure of P75 fibrous mats is characterized by individual, uniform, and randomly oriented fibres. As in P25 and P50 the addition of AMOX did not produce evident change in the morphology of the fibers.
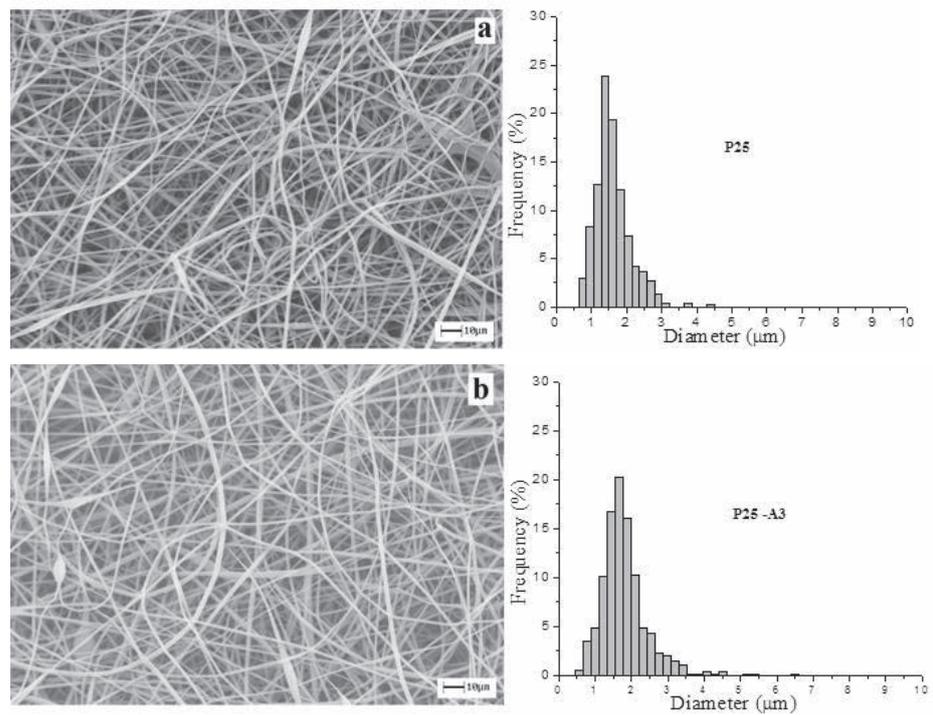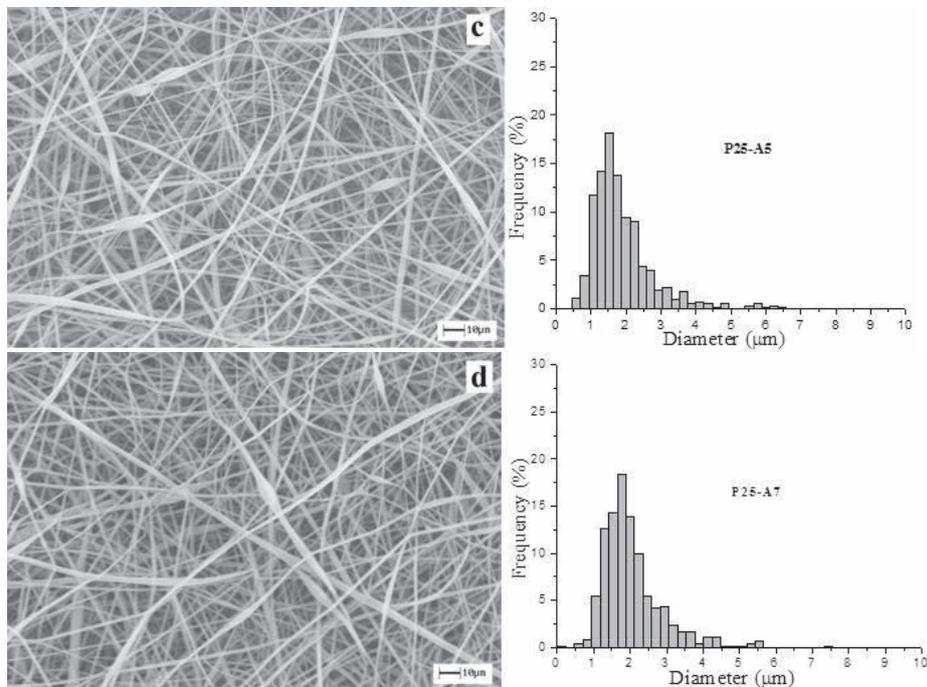
Figure VII.3 *SEM micrographs and diameter distribution P25 (a), P25-A3 (b), P25-A5 (c) and P25-A7(d).*

VII.4 Structure and thermal properties

The XRD patterns of polymer mixture fibers containing PCL and PLA, composite mixture containing AMOX particles and original AMOX particles, the neat PCL and PLA fibers were shown in Figure VII.4, Figure VII.5 and Figure VII.6

PCL shown two strong and sharp crystalline peaks at $2\theta = 21.4°$ and $23.9°$ correspond to the crystallographic planes (Kim et al., 2004a; Li et al., 2007). The broad pattern of the non-woven membrane can be attributed to the reflection of amorphous PLA, indicating that the evaporation of the solvent during electrospinning process is very rapid not allowing the polymer crystallization.
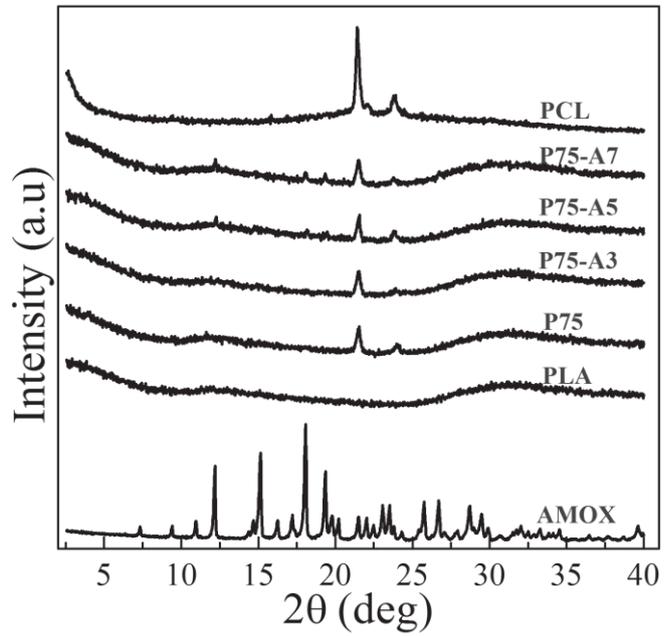
Figure VII.4 *XRD diffractograms of AMOX, PLA, P75, P75-A3, P75-A5, P75-A7 and PCL.*
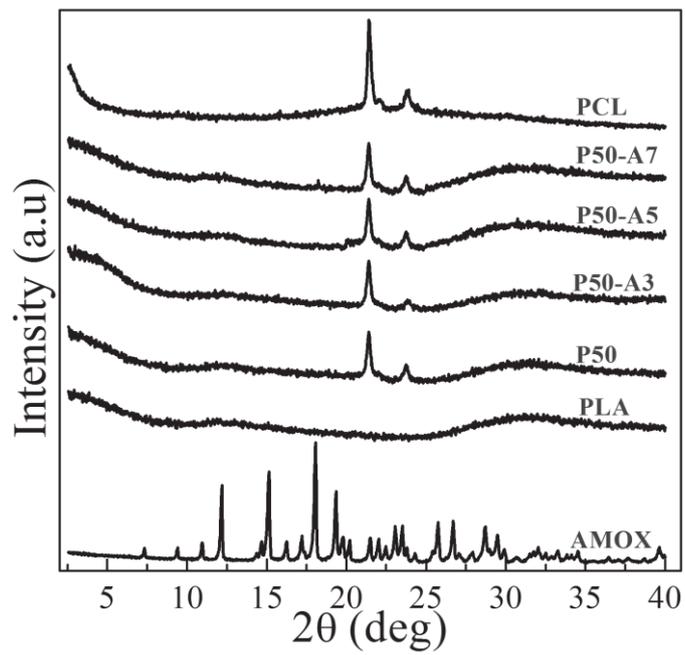
Figure VII.5 *XRD diffractograms of AMOX, PLA, P50, P50-A3, P50-A5, P50-A7 and PCL*

74

The presence of a broad pattern in all polymeric mixture and in all composite spectra demonstrates that the PLA polymer has an amorphous structure, on which the incorporation of PCL and AMOX filler, regardless of their concentration, does not induce relevant changes.
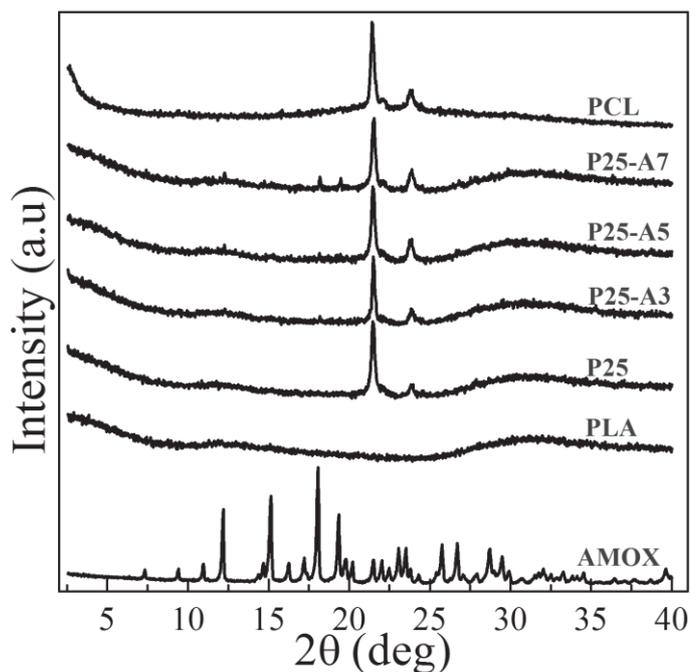
Figure VII.6 *XRD diffractograms of AMOX, PLA, P25, P25-A3, P25-A5, P25-A7 and PCL.*

For the polymer mixtures the PCL reflection intensity increases with increasing the PCL content. The fibers composite containing AMOX particles show the main peaks at 12.1, 15.1, 18.1 and 19.4° of 2θ all corresponded to the structure of AMOX particles with low intensity due to the amorphous PLA phase that overlaps the filler diffraction, apart from the diffraction peaks of PCL. These results also confirmed that the AMOX particles existed in the composite material. Polymer mixtures and composite fibers resulted as physical mixtures of the constituent components.

Table VII.2 contains the main calorimetric data obtained from the heating run of all electrospun samples. Heating traces of samples can be seen in Figure VII.7, Figure VII.8 and Figure VII.9.
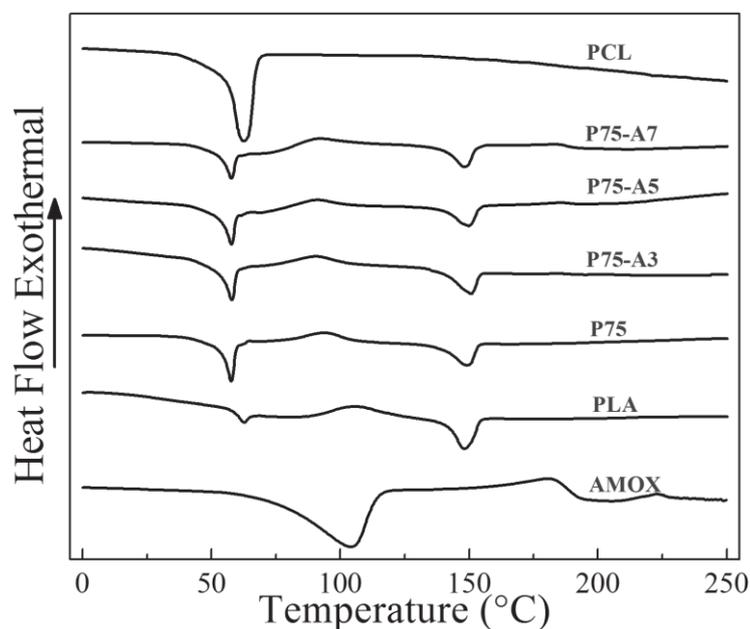
Figure VII.7 *Differential Scanning Calorimetry (DSC) curves of AMOX, PLA, P75, P75-A3, P75-A5, P75-A7 and PCL.*

The DSC curves of the electrospun samples containing both polymers show a clear endothermic peak (30-70°C) which is associated with the melting of the polycaprolactone crystalline phase and a broad exothermic peak (90-120°C) indicative of the cold crystallization of polylactide, together with the corresponding melting peak (147-150°C). Polycaprolactone melting enthalpy (ΔH_{m1}) was sometimes difficult to calculate accurately due to the overlap with polylactide enthalpy relaxation. As a consequence, the melting peak was overestimated.

The PCL melting peak slightly shifted to lower temperatures in all samples and the melting enthalpy decreased when samples were loaded with AMOX. This allows inferring that the drug was well mixed into the polymeric phase.For a given series (i.e. AMOX loaded and unloaded samples) the melting enthalpy of PCL tended to decrease with decreasing its percentage. In fact, as shown in Table VII.2, the ΔH_{m1} value of 76 J/g decreases up to 20 J/g in the sample with the lower PCL content (P75). The melting enthalpy of PLA also tended to decrease with its percentage.

76
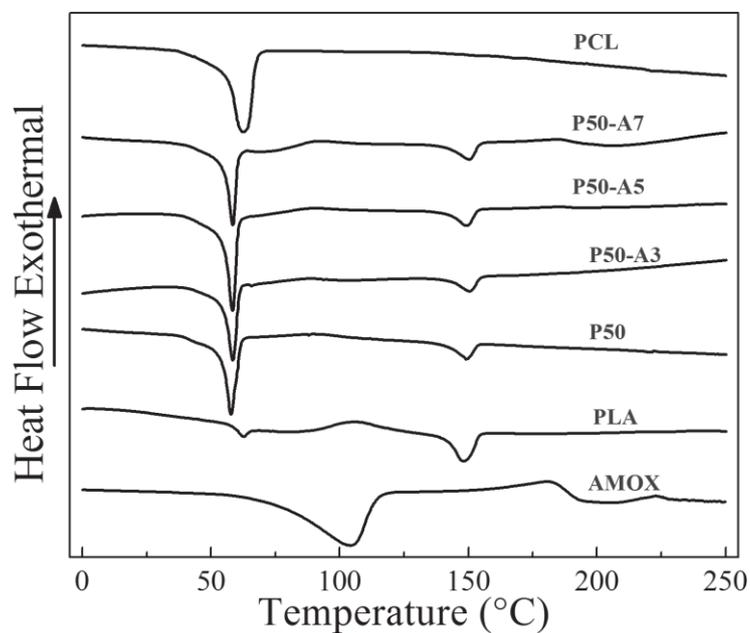
Figure VII.8 *Differential Scanning Calorimetry (DSC) curves of AMOX, PLA, P50, P50-A3, P50-A5, P50-A7 and PCL.*
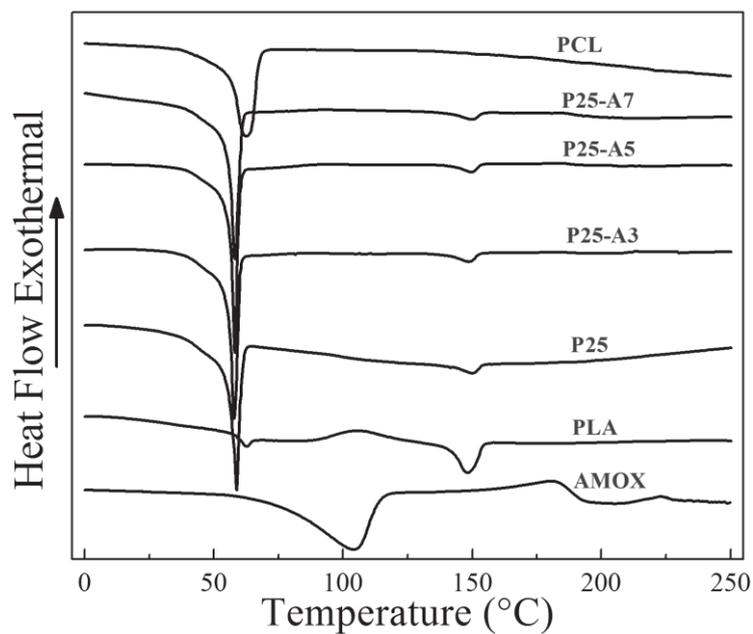
Figure VII.9 *Differential Scanning Calorimetry (DSC) curves of AMOX, PLA, P25, P25-A3, P25-A5, P25-A7 and PCL.*

In the composites polymer mixtures no AMOX melting peak is apparent, even at the highest concentration. This is an evidence that AMOX does not crystallize into the PCL membranes.

Table VII.2. *Thermal parameters of fibers fabricated by electrospinning (AMOX: $T_m = 131$ °C, Midpoint temperature = 306 °C)*

Sample	PCL		PLA				Midpoint temperature (°C)
	T_{m1} (°C)	ΔH_{m1} (J/g)	T_c (°C)	ΔH_c (J/g)	T_{m2} (°C)	ΔH_{m2} (J/g)	
PCL	62	76	-	-	-	-	385
PLA	-	-	105	17	148	25	340
P75	58	20	94	12	149	18	345
P75-A3	58	19	90	13	149	16	346
P75-A5	58	17	90	17	148	15	346
P75-A7	58	13	90	21	148	15	347
P50	58	47	89	6	150	13	350
P50-A3	58	40	89	6	150	12	350
P50-A5	58	38	89	7	150	12	353
P50-A7	58	35	88	9	150	11	354
P25	58	71	-	-	150	8	365
P25-A3	58	70	-	-	149	6	370
P25-A5	58	68	-	-	149	5	371
P25-A7	58	65	-	-	149	4	376

The thermogravimetric analysis was performed to investigate the degradation temperature of the samples. The TGA curves of pristine PCL, PLA and their mixtures (as representative of the composite samples too) are showed in Figure VII.10, Figure VII.11 and Figure VII.12. It appears that the presence of increasing amount of PLA in the mixtures anticipates either the midpoint degradation or the inflection point of PCL due to the lower degradation temperature of PLA. The introduction of the AMOX does not produce further relevant decrease in the degradation temperature (Table VII.2).
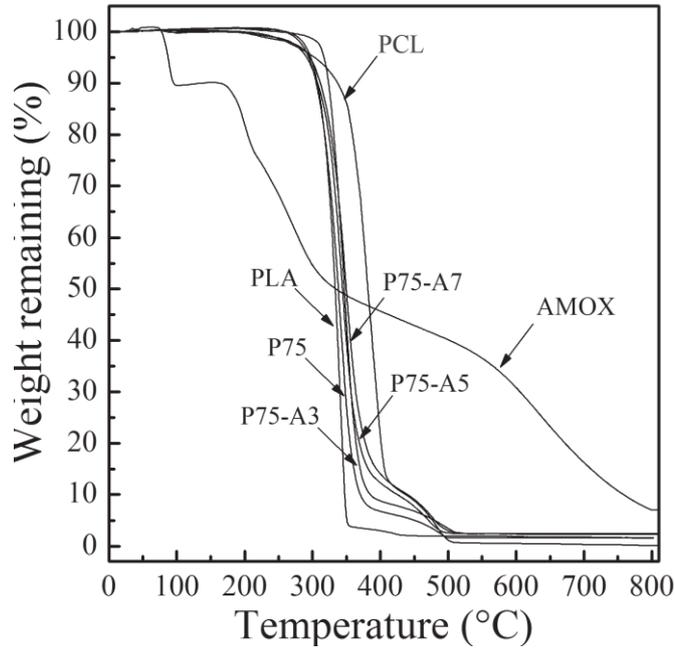
Figure VII. 10 *Thermogravimetric curves of AMOX, PLA, P75, P75-A3, P75-A5, P75-A7 and PCL.*
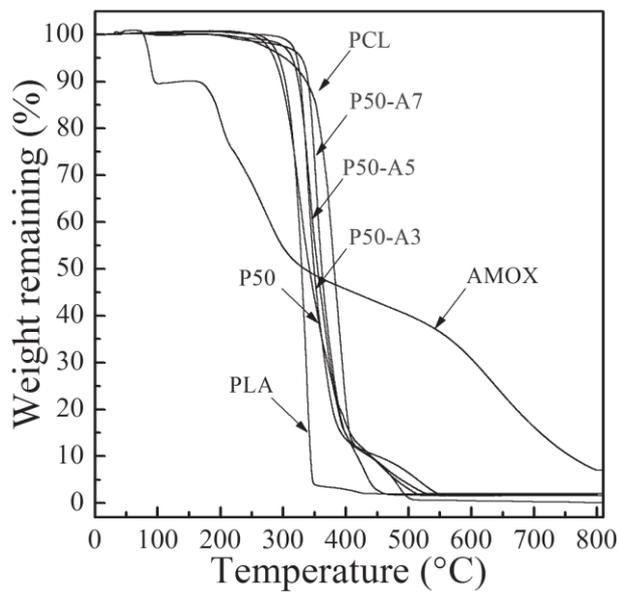
Figure VII.11 *Thermogravimetric curves of AMOX, PLA, P50, P50-A3, P50-A5, P50-A7 and PCL.*
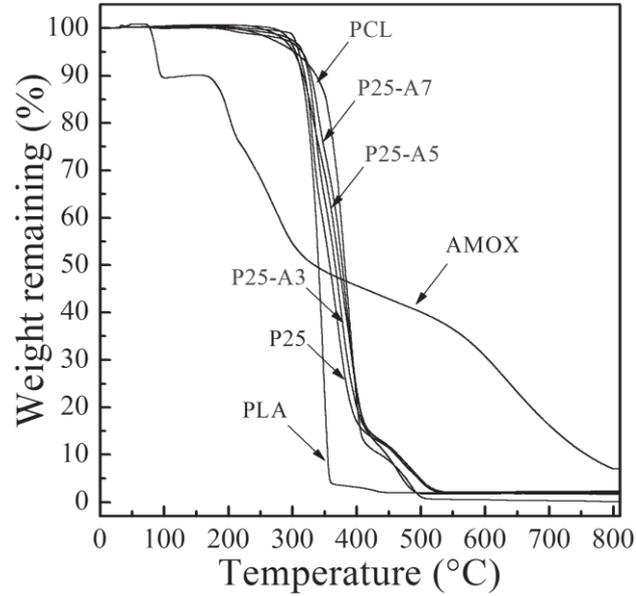
Figure VII.12 *Thermogravimetric curves of AMOX, PLA, P25, P25-A3, P25-A5, P25-A7 and PCL.*

VII.5 Mechanical properties

Mechanical properties of nanofiber mats for PLA, PCL and PLA/PCL blends, assuming a random orientation of the fibers, were tested using an Instron tester. The results of the mechanical tests are reported in Table VII.3 and plotted in Figure VII.13.

Table VII.3. *Mechanical properties of PLA, P75, P50, P25 and PCL.*

Sample	Young's modulus (MPa)	Stress at break (MPa)	Strain at break (%)
PLA	69.7 ± 8.9	3.2 ± 0.2	134.0 ± 14.1
P75	51.4 ± 5.6	2.6 ± 0.1	111.7 ± 11.3
P50	42.7 ± 4.8	1.6 ± 0.1	95.3 ± 9.2
P25	29.0 ± 3.6	1.2 ± 0.2	81.7 ± 10.3
PCL	3.1 ± 0.2	0.7 ± 0.1	66.7 ± 4.7
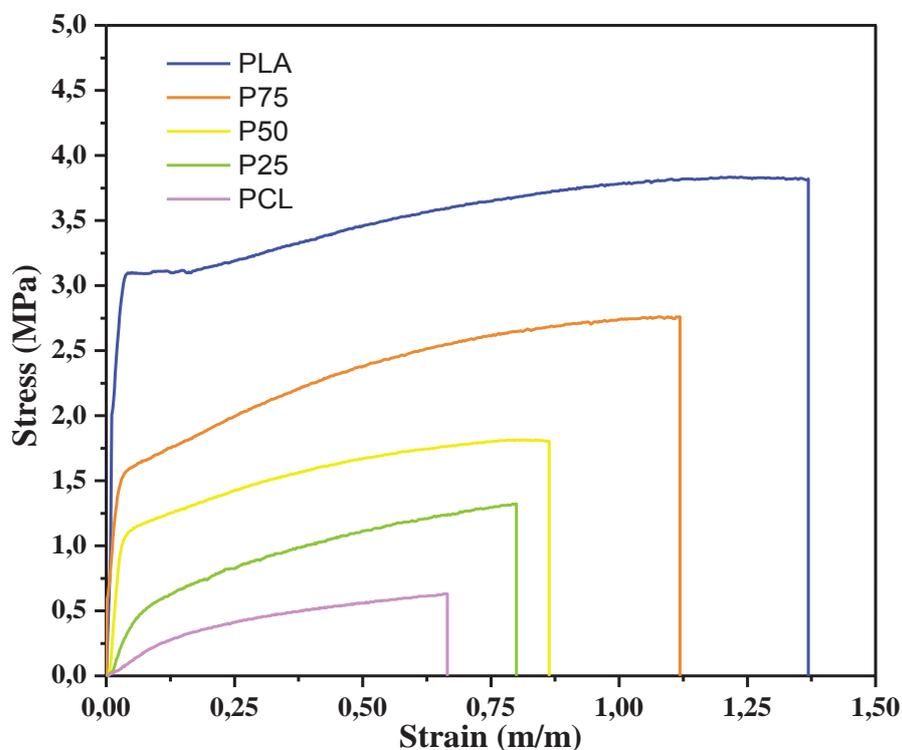
Figure VII.13 *Stress-strain curves of PLA, P75, P50, P25 and PCL.*

A general trend can be observed from Table VII.3 and Figure VII.13: the Young's modulus, stress at break and Strain at break decreased with increasing PCL content.

VII.6 Drug release study

Figure VII.14, Figure VII.15 and Figure VII.16 shows the release profiles of AMOX from fibrous mats of P75, P50 and P25 containing 3, 5 and 7% w/w of drug. Samples showed a sustained release behavior, although an initial rapid drug release was found within the first 8 h. The initial high-rate drug release observed at the beginning of many controlled-release processes can be caused by a number of mechanisms, including surface desorption, pore diffusion, or the lack of a diffusion front barrier to regulate the diffusive process (Sill and von Recum, 2008). This initial period usually so called "burst" could be caused by quick release of AMOX molecules that should be deposited on surface area of nanofibers. For the delivery of antibiotic drugs,

a initial burst is actually ideal since it is important to eliminate the intruding bacteria before they begin to proliferate. However, for the few organisms that may survive the initial burst, a continued release of antibiotic is necessary to prevent their further population (Shin et al., 2001b). Second stage shows a slow drug release which is attribute mainly to the diffusion or permeation of the drug molecules through polymer matrix towards the release medium.
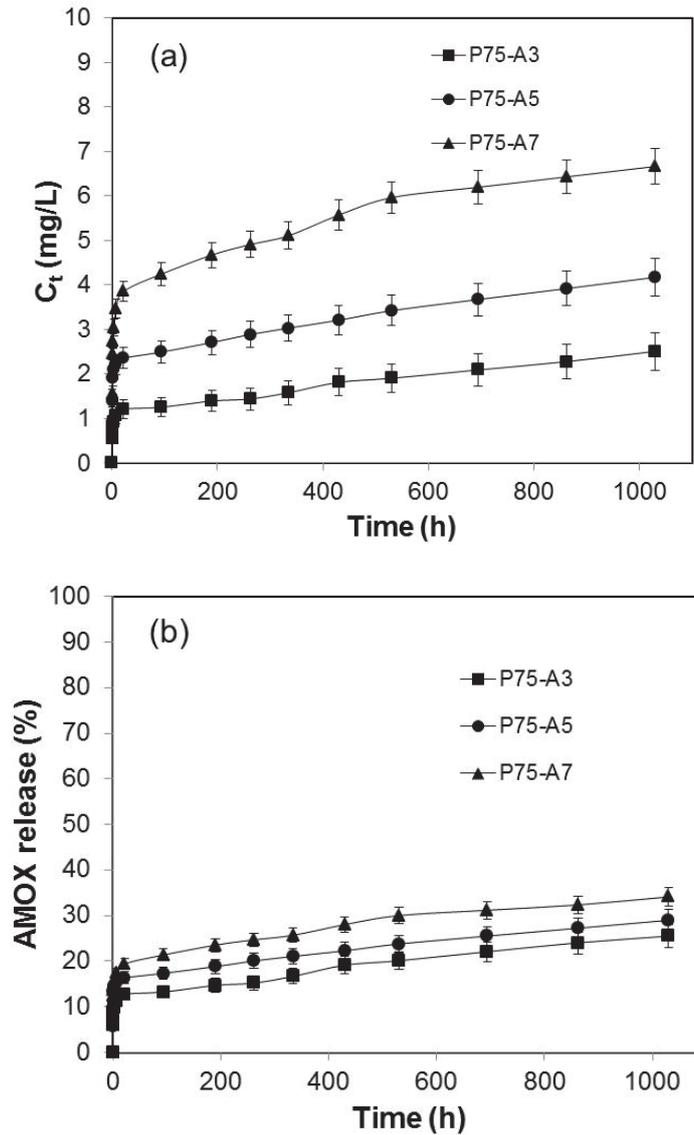
Figure VII.14 *In vitro release profiles of AMOX from P75-A3, P75-A5 and P75-A7, absolute concentration (C_t, mg/L) (a) and as % drug release (b).*

82
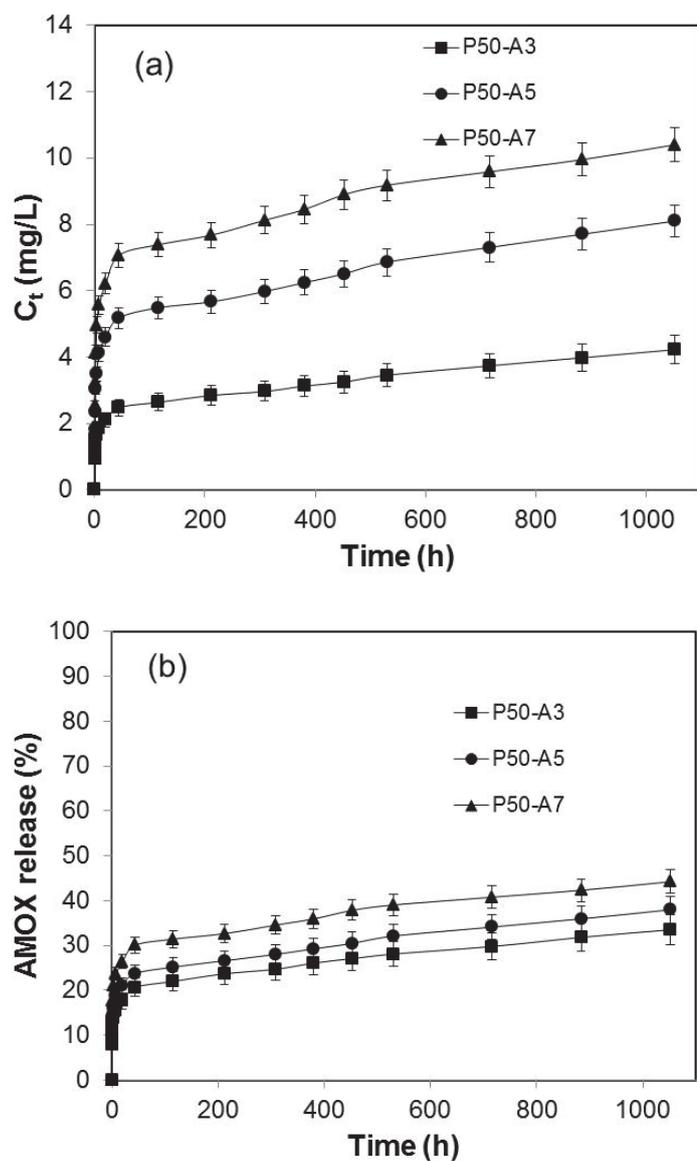
Figure VII.15 *In vitro release profiles of AMOX from P50-A3, P50-A5 and P50-A7, absolute concentration (C_t, mg/L) (a) and as % drug release (b).*
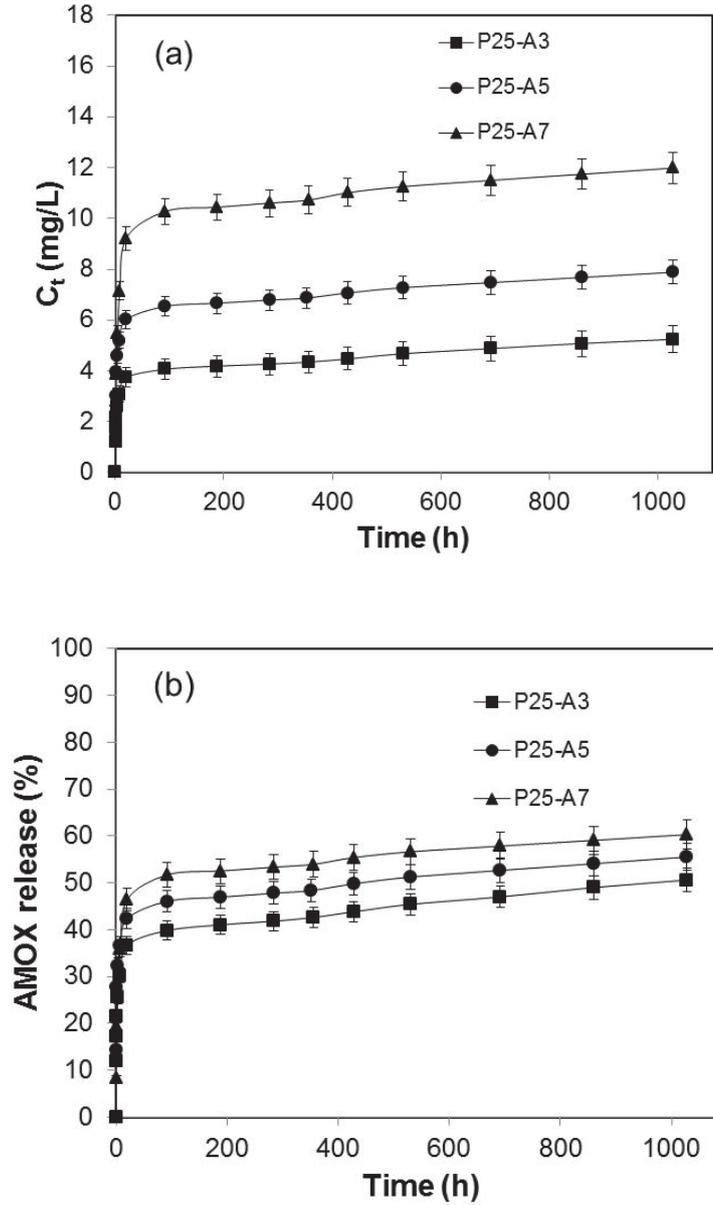
Figure VII.16 *In vitro release profiles of AMOX from P25-A3, P25-A5 and P25-A7, absolute concentration (C_t, mg/L) (a) and as % drug release (b).*

Release kinetics can be examined by several theoretical models(Costa and Sousa Lobo, 2001; Said et al., 2011; Zamani et al., 2010). In this study the second release stage was simulated by Korsmeyer-Peppas equation:

$$Q_t/Q_\infty = K_K t^n \hspace{4cm} \text{(VII.1)}$$

where Q_t/Q_∞ is the drug fraction released at time t, K_k is a constant depending on the structural and geometric characteristic of the system, n is the diffusional coefficient related to the release mechanism(Zamani et al., 2010).
Higuchi equation was also used:

$$\%Q_t = K_H t^{1/2} \hspace{4cm} \text{(VII.2)}$$

where $\%Q_t$ is the percentage of drug released at the time t, K_H is the constant depending on the design variables of the system(Said et al., 2011). The calculated kinetic release parameters are show in Table VII.4.
The largest r^2 values were obtained for the Higuchi equations. The release constants depend on the AMOX content and polymer concentration. The rate of release increases with increasing of the drug concentration and with the PCL content in the fibers.

Table VII.4 *Initial burst, kinetic parameters and release amount of AMOX in 500 h for PLA, PCL and PLA/PCL electrospun membranes.*

Sample	Korsmeyer-Peppas parameters			Higuchi Parameters		Released amount of amoxicillin (%)
	k_k	n	r^2	k_H	r^2	t=500 h
P75-A3	0.077	0.122	0.973	0.387	0.993	20.11
P75-A5	0.099	0.129	0.982	0.418	0.991	23.04
P75-A7	0.113	0.134	0.973	0.466	0.992	29.02
P50-A3	0.112	0.113	0.983	0.435	0.990	25.73
P50-A5	0.122	0.115	0.970	0.438	0.992	27.22
P50-A7	0.156	0.118	0.974	0.545	0.991	33.86
P25-A3	0.253	0.091	0.981	0.513	0.992	45.81
P25-A5	0.302	0.095	0.987	0.532	0.984	50.93
P25-A7	0.324	0.104	0.989	0.557	0.990	55.39

Table VII.4 also shows the amount (%) of AMOX released in the first 500 hours. The released percentages of AMOX increase with both the drug concentration and PCL content in the blend.
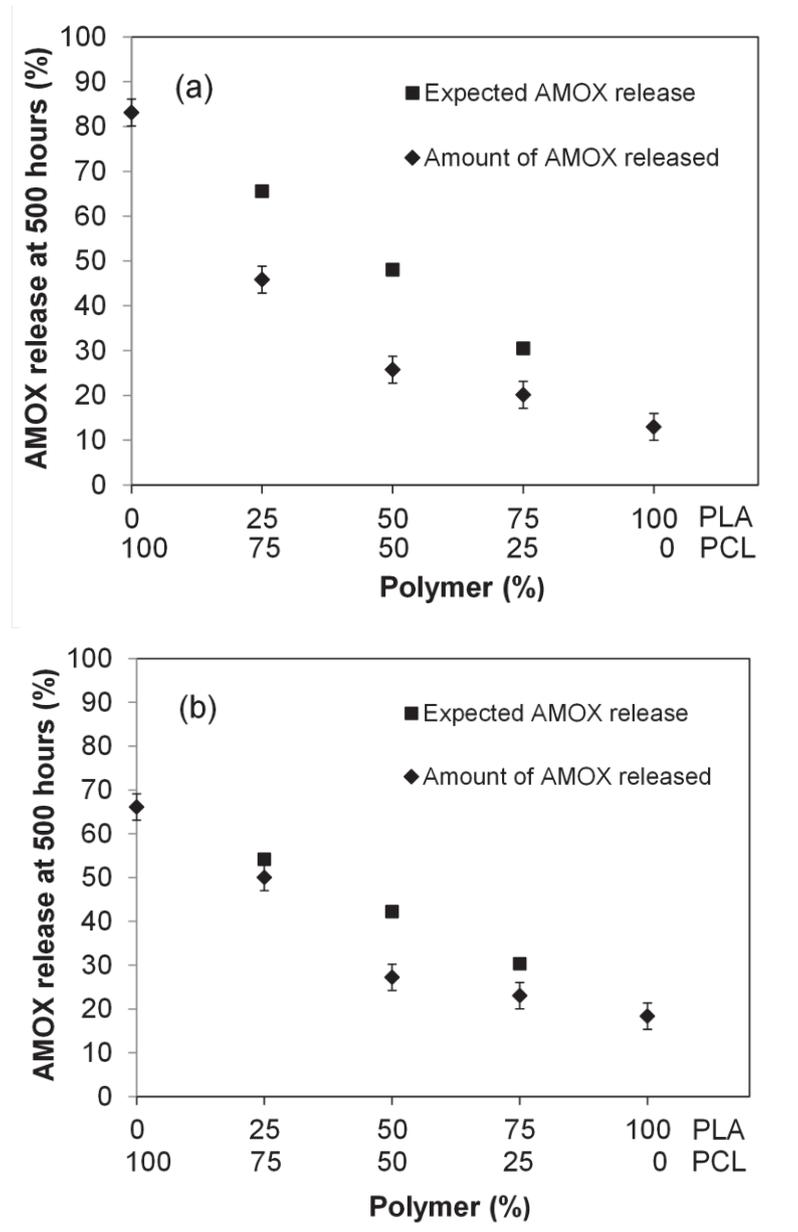
Figure VII.17 *Amount of AMOX released in 500 hours from: PCL-A3 and PLA-A3 (a), PCL-A5 and PLA-A5 (b).*

Figure VII.17 shows the amount of AMOX, released in 500 hours from samples loaded with 3% (a) and 5% of AMOX (b), as a function of phase

composition of the blends. The expected amount of AMOX released, according to the mixture rule, which is for the sample with 3%:

$$\% \text{ AMOX released} = x (12.94) + (1-x) (83.05) \qquad (VII.3)$$

where x is the content of PLA, is also shown in Figure VII.17

Figure VII.17 (a) shows that between 100 and 50% of PLA the amount of AMOX varies linearly with PCL content, whereas the dependence at PCL content of 75% is higher. The expected release, according to the mixture rule, is much higher than the experimental. This could be explained with a preferential incorporation of AMOX into PLA, which is a more polar chain respect to PCL.

Very similar results are found for the 5% AMOX blends, shown in Figure VII.17 (b). As matter of the fact the AMOX release is much lower than expected by the mixture rule at PLA content of 75% and 50%, whereas only at 25% PLA the experimental point is very near to the theoretical. Evidently, on increasing the AMOX concentration it becomes more probable to be encapsulated also in PCL, in spite of a lower interaction. This is confirmed by the 7% AMOX blends (not reported), for which the expected and calculated value coincide.

Conclusion

The aim of the thesis was the preparation and characterization of micro/nanofibers of biodegradable and biocompatible polymers (PCL and PLA), their blend and their composites with amoxicillin drug and amoxicillin intercalated in layered double hydroxide nanoparticles.

The work has been divided in several phases.

1. The technical parameters for electrospinning a solution of poly(ε-caprolactone), and poly(ε-caprolactone) filled with Amoxicilline, a bacteriolitic, β-lactam antibiotic, at different concentrations in acetone, were defined and set up. A trial-and-error approach has been employed by varying solution and processing parameters to obtain uniform defect-free fibers. The morphological analysis showed) fibers with an average diameter of 0.8 μm for the pristine poly(ε-caprolactone), whereas the fiber dimensions were slightly increased for PCL filled with amoxicilline to a mean diameter between 0.80 and 1.2 μm. X-rays suggested that the antibiotic molecules, encapsulated into the poly(ε-caprolactone) fibers, are not allowed to crystallize and are present as amorphous molecular aggregates or solid solution into the fibers. The release properties in physiological solution showed two stages for all the samples: a first stage very rapid as a "burst" and a second in which the release is slow, extending for very long time. The burst was analyzed as a function of amoxicillin concentration and thickness of the membranes, and values corresponding to absence of burst were individuated. In the second stage the release was found very slow extending up to months for the most concentrated sample. The antibacterial activity of these electrospun fibers was effective to inhibit *Staphyococcus aureus*, *Enterococcus faecalis* and *Escherichia coli,* in different proportions. The properties of these filled membranes and their capability for local delivery of antibiotics make them suitable for biomedical applications.

2. Biodegradable poly(ε-caprolactone) nanofibrous mats loaded with different concentrations of amoxicillin intercalated in layered double hydroxide were fabricated by electrospinning technique. Morphology and thermal properties of nanofibrous mats depend on drug amount incorporated. The release curves present a sustained release behavior, although an initial high-rate drug release period was found. This initial rapid drug release period was followed by a second step in which the release is slow, extending for very long time. The release time of amoxicillin intercalated in layered double hydroxide from loaded fibrous membranes was extended up to months for the most concentrated sample. The comparison of release from poly(ε-caprolactone) nanofibrous membranes of amoxicillin protected into the clay and amoxicillin alone showed that the curve for the amoxicillin protected into the clay lays underneath the curve of the drug alone. A new drug delivery system is developed with capability for controlled and local delivery of antibiotics which make this suitable for biomedical applications such as wound healing, dental treatment or skin infections.

3. Amoxicillin was successfully encapsulated at different concentrations into poly(lactic acid) by the electrospinning technique. The scanning electron microscopy evidenced the nanofibrous structure of pristine poly(lactic acid), composed of individual, uniform, and randomly oriented fibres with an average diameter ranging around 2,52 micron. The addition of amoxicillin at different concentrations of 3%, 5% and 7% caused no noticeable change in the fiber morphology. The release curves, for all samples, present mainly two stages: a first stage, quick as a "burst", followed by a successive slow stage. In the second stage the release was found very slow extending up to months.

4. Biodegradable and biocompatible poly(lactic acid)/poly(ε-caprolactone) nanofibrous mats loaded with amoxicillin were fabricated by electrospinning technique. Morphology and thermal properties of nanofibrous mats depend on the blending ratio between the two polymers as well as on the drug amount incorporated. Different release kinetics of amoxicillin of the two pristine polymers was obtained, rapid for PCL and slow for PLA, whereas for mixture of poly(lactic acid) and poly(ε-caprolactone) release kinetics depend on the blending ratio between the two polymers. The time of AMOX release from loaded fibrous membranes was extended up to months. However comparing the blend release times with those of the pristine polymers a preferential incorporation of AMOX into PLA

can be inferred. The tunable release properties of these antibiotics filled membranes and their capability for local delivery of active molecules make them suitable for biomedical applications such as dental treatment or skin infections.

References

Aguzzi C., Cerezo P., Viseras C. and Caramella C., (2007). Use of clays as drug delivery systems: Possibilities and limitations. *Appl. Clay Sci.*, **36**, 22-36.

Ahymah Joshy M. I., Elayaraja K., Suganthi R. V., Chandra Veerla S. and Kalkura S. N., (2011). In vitro sustained release of amoxicillin from lanthanum hydroxyapatite nano rods. *Curr. Appl. Phys.*, **11**, 1100-1106.

Ajayan P. M., Schadler L. S. and Braun P. V., (2006). Nanocomposite Science and Technology. Wiley, Weinheim (GE).

Albertsson A.-C. and Varma I., (2002). Aliphatic Polyesters: Synthesis, Properties and Applications

Degradable Aliphatic Polyesters, In: Springer Berlin / Heidelberg, pp. 1-40.

Alexandre M. and Dubois P., (2000). Polymer-layered silicate nanocomposites: preparation, properties and uses of a new class of materials. *Materials Science and Engineering: R: Reports*, **28**, 1-63.

Andrady A. L., (2008). Science and Technology of Polymer Nanofibers. John Wiley & Sons, New Jersey (US).

Ardanuy M. and Velasco J. I., (2011). Mg–Al Layered double hydroxide nanoparticles: Evaluation of the thermal stability in polypropylene matrix. *Appl. Clay Sci.*, **51**, 341-347.

Asane G. S., Nirmal S. A., Rasal K. B., Naik A. A., Mahadik M. S. and Rao Y. M., (2008). Polymers for Mucoadhesive Drug Delivery System: A Current Status. *Drug Dev. Ind. Pharm.*, **34**, 1246-1266.

Auras R., Lim L.-T., Selke S. E. M. and Tsuji H., (2010). Poly(Lactic Acid): Synthesis, Structures, Properties, Processing, and Applications. John Wiley & Sons, Inc., New Jersey (US).

Averous L., Moro L., Dole P. and Fringant C., (2000). Properties of thermoplastic blends: starch–polycaprolactone. *Polymer*, **41**, 4157-4167.

Bashur C. A., Dahlgren L. A. and Goldstein A. S., (2006). Effect of fiber diameter and orientation on fibroblast morphology and proliferation on electrospun poly(d,l-lactic-co-glycolic acid) meshes. *Biomaterials*, **27**, 5681-5688.

93

Bastioli C., (1998). Biodegradable materials — Present situation and future perspectives. *Macromolecular Symposia*, **135**, 193-204.

Bawa P., Pillay V., Choonara Y. E. and Toit L. C. d., (2009). Stimuli-responsive polymers and their applications in drug delivery. *Biomed. Mater.*, **4**, 022001.

Bhardwaj N. and Kundu S. C., (2010). Electrospinning: A fascinating fiber fabrication technique. *Biotechnol. Adv.*, **28**, 325-347.

Bisson-Boutelliez C., Fontanay S., Finance C. and Kedzierewicz F., (2010). Preparation and Physicochemical Characterization of Amoxicillin β-cyclodextrin Complexes. *AAPS PharmSciTech*, **11**, 574-581.

Bohner M., van Lenthe G. H., Grünenfelder S., Hirsiger W., Evison R. and Müller R., (2005). Synthesis and characterization of porous [beta]-tricalcium phosphate blocks. *Biomaterials*, **26**, 6099-6105.

Boyanova L., Gergova G., Nikolov R., Derejian S., Lazarova E., Katsarov N., Mitov I. and Krastev Z., (2005). Activity of Bulgarian propolis against 94 *Helicobacter pylori* strains in vitro by agar-well diffusion, agar dilution and disc diffusion methods. *J. Med. Microbiol.*, **54** 481-483.

Brannon-Peppas L., (1997). Polymers in Controlled Drug Delivery. *Med. Plast. Biomater.*, **4**, 34-45.

Brekke J. H. and Toth J. M., (1998). Principles of tissue engineering applied to programmable osteogenesis. *J. Biomed. Mater. Res.*, **43**, 380-398.

Bugatti V., Costantino U., Gorrasi G., Nocchetti M., Tammaro L. and Vittoria V., (2010). Nano-hybrids incorporation into poly(ε-caprolactone) for multifunctional applications: Mechanical and barrier properties. *Eur. Polym. J.*, **46**, 418-427.

Burger C., Hsiao B. S. and Chu B., (2006). NANOFIBROUS MATERIALS AND THEIR APPLICATIONS. *Annual Review of Materials Research*, **36**, 333-368.

Butscher A., Bohner M., Hofmann S., Gauckler L. and Müller R., (2011). Structural and material approaches to bone tissue engineering in powder-based three-dimensional printing. *Acta Biomaterialia*, **7**, 907-920.

Callaghan J. J., (1997). Instructional Course Lectures, The American Academy of Orthopaedic Surgeons - Periprosthetic Fractures of the Acetabulum during and following Total Hip Arthroplasty. *J. Bone Joint Surg. Am.*, **79**, 1416-1421

Cantú M., López-Salinas E., Valente J. S. and Montiel R., (2005). SOx Removal by Calcined MgAlFe Hydrotalcite-like Materials: Effect of the Chemical Composition and the Cerium Incorporation Method. *Environmental Science & Technology*, **39**, 9715-9720.

Cavani F., Trifirò F. and Vaccari A., (1991). Hydrotalcite-type anionic clays: Preparation, properties and applications. *Catal. Today*, **11**, 173-301.

References

Clinical and Laboratory Standards Institute, (2006a). Mhetods for Dilution Antimicrobial Susceptibility Tests for Bacteria that Grow Aerobically; Aproved Standard, Seventh Edition. Clinical and Laboratory Standards Institute, Pennsylvania.

Clinical and Laboratory Standards Institute, (2006b). Performance standards for Antimicrobial Disk Susceptibility Tests; Aproved Standard, Ninth Edition. Clinical and Laboratory Standards Institute, Pennsylvania.

Cooley J. F. (1902). Apparatus for electrically dispersing fluids (US, 692631).

Costa P. and Sousa Lobo J. M., (2001). Modeling and comparison of dissolution profiles. *Eur. J. Pharm. Sci.*, **13**, 123-133.

Costantino U., Ambrogi V., Nocchetti M. and Perioli L., (2008). Hydrotalcite-like compounds: Versatile layered hosts of molecular anions with biological activity. *Microporous Mesoporous Mater.*, **107**, 149-160.

Costantino U., Bugatti V., Gorrasi G., Montanari F., Nocchetti M., Tammaro L. and Vittoria V., (2009). New Polymeric Composites Based on Poly(ϵ-caprolactone) and Layered Double Hydroxides Containing Antimicrobial Species. *ACS Appl. Mater. Interfaces*, **1**, 668-677.

Costantino U., Marmottini F., Nocchetti M. and Vivani R., (1998). New Synthetic Routes to Hydrotalcite-Like Compounds − Characterisation and Properties of the Obtained Materials. *Eur. J. Inorg. Chem.*, **1998**, 1439-1446.

Chang W. N., (2009). Nanofibers: Fabrication, Performance, and Applications. Nova Science, New York (US).

Chapekar M. S., (2000). Tissue engineering: Challenges and opportunities. *J. Biomed. Mater. Res.*, **53**, 617-620.

Charernsriwilaiwat N., Opanasopit P., Rojanarata T., Ngawhirunpat T. and Supaphol P., (2010). Preparation and characterization of chitosan-hydroxybenzotriazole/polyvinyl alcohol blend nanofibers by the electrospinning technique. *Carbohydr. Polym.*, **81**, 675-680.

Chazeau L., Cavaillé J. Y., Canova G., Dendievel R. and Boutherin B., (1999). Viscoelastic properties of plasticized PVC reinforced with cellulose whiskers. *Journal of Applied Polymer Science*, **71**, 1797-1808.

Chegoonian P., Feiz M., Ravandi S. A. H. and Mallakpour S., (2012). Preparation of sulfonated poly(ethylene terephthalate) submicron fibrous membranes for removal of basic dyes. *J. Appl. Polym. Sci.*, **124**, E190-E198.

Chen H.-C., Tsai C.-H. and Yang M.-C., (2011). Mechanical properties and biocompatibility of electrospun polylactide/poly(vinylidene fluoride) mats. *J Polym Res*, **18**, 319-327.

95

Chen P., Wu Q.-S., Ding Y.-P., Chu M., Huang Z.-M. and Hu W., (2010). A controlled release system of titanocene dichloride by electrospun fiber and its antitumor activity in vitro. *Eur. J. Pharm. Biopharm.*, **76**, 413-420.

Cheung H.-Y., Lau K.-T., Lu T.-P. and Hui D., (2007). A critical review on polymer-based bio-engineered materials for scaffold development. *Composites: Part B*, **38**, 291-300.

Chew S. Y., Wen J., Yim E. K. F. and Leong K. W., (2005). Sustained Release of Proteins from Electrospun Biodegradable Fibers. *Biomacromolecules*, **6**, 2017-2024.

Chiellini E. and Solaro R., (1996). Biodegradable Polymeric Materials. *Advanced Materials*, **8**, 305-313.

Chong E. J., Phan T. T., Lim I. J., Zhang Y. Z., Bay B. H., Ramakrishna S. and Lim C. T., (2007). Evaluation of electrospun PCL/gelatin nanofibrous scaffold for wound healing and layered dermal reconstitution. *Acta Biomater.*, **3**, 321-330.

Dalton P. D., Klinkhammer K., Salber J., Klee D. and Möller M., (2006). Direct in Vitro Electrospinning with Polymer Melts. *Biomacromolecules*, **7**, 686-690.

Deitzel J. M., Kleinmeyer J., Harris D. and Beck Tan N. C., (2001). The effect of processing variables on the morphology of electrospun nanofibers and textiles. *Polymer*, **42**, 261-272.

Demir M. M., Yilgor I., Yilgor E. and Erman B., (2002). Electrospinning of polyurethane fibers. *Polymer*, **43**, 3303-3309.

Desigaux L., Belkacem M. B., Richard P., Cellier J., Léone P., Cario L., Leroux F., Taviot-Guého C. and Pitard B., (2005). Self-Assembly and Characterization of Layered Double Hydroxide/DNA Hybrids. *Nano Letters*, **6**, 199-204.

Dimar J. R. and Glassman S. D., (2007). The art of bone grafting. *Curr. Opin. Orthop.*, **18**, 226-233.

Doshi J. and Reneker D. H., (1995). Electrospinning process and applications of electrospun fibers. *J. Electrost.*, **35**, 151-160.

Duan X. and Evans D. G., (2006). Layered Double Hydroxides. Springer, Berlin Heidelberg (GE).

Ei-Arini S. K. and Leuenberger H., (1995). Modelling of drug release from polymer matrices: Effect of drug loading. *Int. J. Pharm.*, **121**, 141-148.

Elsner J. J., Egozi D., Ullmann Y., Berdicevsky I., Shefy-Peleg A. and Zilberman M., (2011). Novel biodegradable composite wound dressings with controlled release of antibiotics: Results in a guinea pig burn model. *Burns*, **37**, 896-904.

Elsner J. J. and Zilberman M., (2009). Antibiotic-eluting bioresorbable composite fibers for wound healing applications: Microstructure,

96

drug delivery and mechanical properties. *Acta Biomater.*, **5**, 2872-2883.

Favier V., Cavaille J. Y., Canova G. R. and Shrivastava S. C., (1997). Mechanical percolation in cellulose whisker nanocomposites. *Polymer Engineering & Science*, **37**, 1732-1739.

Formhals A. (1934). Process and apparatus for preparing artificial threads (US, 1975504).

Formhals A. (1938). Artificial fiber construction (US, 2109333).

Formhals A. (1939). Method and apparatus for spinning (US, 2160962).

Formhals A. (1940). Artificial thread and method of producing same (US, 2187306).

Formhals A. (1943). Production of artificial fibers from fiber forming liquids (US, 2323025).

Formhals A. (1944). Method and apparatus for spinning (US, 2349950).

Ghasemi-Mobarakeh L., Morshed M., Karbalaie K., Fesharaki M., Nasr-Esfahani M. H. and Baharvand H., (2008). Electrospun Poly (ε-Caprolactone) Nanofiber Mat as Extracellular Matrix. *Yakhteh Med. J.*, **10**, 179-184.

Gilbert W., (1600). De Magnete, Magneticisque Corporibus, et de Magno Magnete Tellure (On the Magnet and Magnetic Bodies, and on That Great Magnet the Earth). Peter Short, London (UK).

Gladding E. K. (1939). Apparatus for the production of filaments, threads, and the like (US, 2168027).

Greiner A. and Wendorff J. H., (2007). Electrospinning: A Fascinating Method for the Preparation of Ultrathin Fibers. *Angew. Chem. Int. Ed.*, **46**, 5670-5703.

Gunatillake P. A. and Adhikari R., (2003). Biodegradable synthetic polymers for tissue engineering. *Eur. Cell. Mater.*, **5**, 1-16.

Han J., Branford-White C. J. and Zhu L.-M., (2010). Preparation of poly(ε-caprolactone)/poly(trimethylene carbonate) blend nanofibers by electrospinning. *Carbohydr. Polym.*, **79**, 214-218.

He J.-H., Liu Y., Mo L.-F., Wan Y.-Q. and Xu L., (2008). Electrospun Nanofibres and Their Applications. iSmithers, Shawbury (UK).

Herron N. and Thorn D. L., (1998). Nanoparticles: Uses and Relationships to Molecular Cluster Compounds. *Advanced Materials*, **10**, 1173-1184.

Hong J. H., Jeong E. H., Lee H. S., Baik D. H., Seo S. W. and Youk J. H., (2005). Electrospinning of polyurethane/organically modified montmorillonite nanocomposites. *Journal of Polymer Science Part B: Polymer Physics*, **43**, 3171-3177.

Huang H.-H., He C.-L., Wang H.-S. and Mo X.-M., (2009). Preparation of core-shell biodegradable microfibers for long-term drug delivery. *J. Biomed. Mater. Res., Part A*, **90A**, 1243-1251.

Huang X. and Brazel C. S., (2003). Analysis of burst release of proxyphylline from poly(vinyl alcohol) hydrogels. *Chem. Eng. Commun.*, **190**, 519-532.

Huang Z.-M., Zhang Y. Z., Kotaki M. and Ramakrishna S., (2003). A review on polymer nanofibers by electrospinning and their applications in nanocomposites. *Composites Science and Technology*, **63**, 2223-2253.

Hunley M. T. and Long T. E., (2008). Electrospinning functional nanoscale fibers: a perspective for the future. *Polymer International*, **57**, 385-389.

Ibrahim N. A., Ahmad S. N. A., Yunus W. M. Z. W. and Dahlan K. Z. M., (2009). Effect of electron beam irradiation and poly(vinylpyrrolidone) addition on mechanical properties of polycaprolactone with empty fruit bunch fibre (OPEFB) composite. *eXPRESS Polymer Letters*, **3**, 226-234.

Islam M. S. and Karim M. R., (2010). Fabrication and characterization of poly(vinyl alcohol)/alginate blend nanofibers by electrospinning method. *Colloids Surf., A*, **366**, 135-140.

Jaworek A., Krupa A., Lackowski M., Sobczyk A. T., Czech T., Ramakrishna S., Sundarrajan S. and Pliszka D., (2009). Nanocomposite fabric formation by electrospinning and electrospraying technologies. *J. Electrost.*, **67**, 435-438.

Kenawy E.-R., Bowlin G. L., Mansfield K., Layman J., Simpson D. G., Sanders E. H. and Wnek G. E., (2002). Release of tetracycline hydrochloride from electrospun poly(ethylene-co-vinylacetate), poly(lactic acid), and a blend. *J. Controlled Release*, **81**, 57-64.

Kim H. W., Knowles J. C. and Kim H. E., (2004a). Development of hydroxyapatite bone scaffold for controlled drug release via poly(epsilon-caprolactone) and hydroxyapatite hybrid coatings. *J. Biomed. Mater. Res., Part B*, **70**, 240-249.

Kim K., Luu Y. K., Chang C., Fang D., Hsiao B. S., Chu B. and Hadjiargyrou M., (2004b). Incorporation and controlled release of a hydrophilic antibiotic using poly(lactide-co-glycolide)-based electrospun nanofibrous scaffolds. *J. Controlled Release*, **98**, 47-56.

Kissel T., Rummelt M. A. and Bier H. P., (1993). Wirkstofffreisetzung aus bio abbaubaren mikropartikeln. *Deutsche-Apotheker-Ztg*, **133**, 29-32.

Kontogiannopoulos K. N., Assimopoulou A. N., Tsivintzelis I., Panayiotou C. and Papageorgiou V. P., (2011). Electrospun fiber mats containing shikonin and derivatives with potential biomedical applications. *Int. J. Pharm.*, **409**, 216-228.

98

References

Koombhongse S., Liu W. and Reneker D. H., (2001). Flat polymer ribbons and other shapes by electrospinning. *Journal of Polymer Science Part B: Polymer Physics*, **39**, 2598-2606.

Kroiss J., Kaltenpoth M., Schneider B., Schwinger M.-G., Hertweck C., Maddula R. K., Strohm E. and Svatoš A., (2010). Symbiotic streptomycetes provide antibiotic combination prophylaxis for wasp offspring. *Nat. Chem. Biol.*, **6**, 261-263.

Kumari A., Yadav S. K. and Yadav S. C., (2010). Biodegradable polymeric nanoparticles based drug delivery systems. *Colloids Surf., B*, **75**, 1-18.

Kumbar S. G., Nukavarapu S. P., James R., Hogan M. V. and Laurencin C. T., (2008). Recent Patents on Electrospun Biomedical Nanostructures: An Overview. *Recent Pat. Biomed. Eng.*, **1**, 68-78.

Lagashetty A. and Venkataraman A., (2005). Polymer Nanocomposites. *Resonance*.

Lannutti J., Reneker D., Ma T., Tomasko D. and Farson D., (2007). Electrospinning for tissue engineering scaffolds. *Materials Science and Engineering: C*, **27**, 504-509.

Lee S. and Obendorf S. K., (2007). Use of Electrospun Nanofiber Web for Protective Textile Materials as Barriers to Liquid Penetration. *Text. Res. J.*, **77**, 696-702.

Leroux F. and Taviot-Gueho C., (2005). Fine tuning between organic and inorganic host structure: new trends in layered double hydroxide hybrid assemblies. *J. Mater. Chem.*, **15**, 3628-3642.

Leung V. and Ko F., (2011). Biomedical applications of nanofibers. *Polym. Adv. Technol.*, **22**, 350-365.

Li D. and Xia Y., (2004). Electrospinning of Nanofibers: Reinventing the Wheel? *Advanced Materials*, **16**, 1151-1170.

Li R., Nie K., Shen X. and Wang S., (2007). Biodegradable polyester hybrid nanocomposites containing titanium dioxide network and poly(ε-caprolactone): Synthesis and characterization. *Mater. Lett.*, **61**, 1368-1371.

Liao G., Jiang S., Xu X. and Ke Y., (2012). Electrospun aligned PLLA/PCL/HA composite fibrous membranes and their in vitro degradation behaviors. *Mater. Lett.*, **82**, 159-162.

Liu H. and Hsieh Y.-L., (2002). Ultrafine fibrous cellulose membranes from electrospinning of cellulose acetate. *Journal of Polymer Science Part B: Polymer Physics*, **40**, 2119-2129.

Liu S.-J., Kau Y.-C., Chou C.-Y., Chen J.-K., Wu R.-C. and Yeh W.-L., (2010). Electrospun PLGA/collagen nanofibrous membrane as early-stage wound dressing. *J. Membr. Sci.*, **355**, 53-59.

Liu Y., He J.-H., Yu J.-y. and Zeng H.-m., (2008). Controlling numbers and sizes of beads in electrospun nanofibers. *Polymer International*, **57**, 632-636.

Mantilla A., Tzompantzi F., Fernández J. L., Góngora J. A. I. D. and Gómez R., (2010). Photodegradation of phenol and cresol in aqueous medium by using Zn/Al + Fe mixed oxides obtained from layered double hydroxides materials. *Catal. Today*, **150**, 353-357.

Mark J. E., (1996). Ceramic-reinforced polymers and polymer-modified ceramics. *Polymer Engineering & Science*, **36**, 2905-2920.

Mathieu L. M., Mueller T. L., Bourban P.-E., Pioletti D. P., Müller R. and Månson J.-A. E., (2006). Architecture and properties of anisotropic polymer composite scaffolds for bone tissue engineering. *Biomaterials*, **27**, 905-916.

Melcher J. R. and Taylor G. I., (1969). Electrohydrodynamics: A Review of the Role of Interfacial Shear Stresses. *Annual Review of Fluid Mechanics*, **1**, 111-146.

Meng Z. X., Xu X. X., Zheng W., Zhou H. M., Li L., Zheng Y. F. and Lou X., (2011). Preparation and characterization of electrospun PLGA/gelatin nanofibers as a potential drug delivery system. *Colloids Surf., B*, **84**, 97-102.

Mi F.-L., Wu Y.-B., Shyu S.-S., Schoung J.-Y., Huang Y.-B., Tsai Y.-H. and Hao J.-Y., (2002). Control of wound infections using a bilayer chitosan wound dressing with sustainable antibiotic delivery. *J. Biomed. Mater. Res.*, **59**, 438-449.

Min B.-M., You Y., Kim J.-M., Lee S. J. and Park W. H., (2004). Formation of nanostructured poly(lactic-co-glycolic acid)/chitin matrix and its cellular response to normal human keratinocytes and fibroblasts. *Carbohydr. Polym.*, **57**, 285-292.

Mojumdar S. C. and Raki L., (2005). Preparation and properties of calcium silicate hydrate-poly(vinyl alcohol) nanocomposite materials. *J Therm Anal Calorim*, **82**, 89-95.

Morton W. J. (1902). Method of dispersing fluids (US, 705691).

Nalawade P., Aware B., Kadam V. J. and Hirlekar R. S., (2009). Layered double hydroxides: A review. *Journal of Scientific & Industrial Research* **68**, 267-272.

Noh H. K., Lee S. W., Kim J.-M., Oh J.-E., Kim K.-H., Chung C.-P., Choi S.-C., Park W. H. and Min B.-M., (2006). Electrospinning of chitin nanofibers: Degradation behavior and cellular response to normal human keratinocytes and fibroblasts. *Biomaterials*, **27**, 3934-3944.

Norton C. L. (1936). Method of and apparatus for producing fibrous or filamentary material (US, 2048651).

References

Oh S. H., Kang S. G., Kim E. S., Cho S. H. and Lee J. H., (2003). Fabrication and characterization of hydrophilic poly(lactic-co-glycolic acid)/poly(vinyl alcohol) blend cell scaffolds by melt-molding particulate-leaching method. *Biomaterials*, **24**, 4011-4021.

Okada M., (2002). Chemical syntheses of biodegradable polymers. *Progress in Polymer Science*, **27**, 87-133.

Patel S. K., Lavasanifar A. and Choi P., (2009). Roles of Nonpolar and Polar Intermolecular Interactions in the Improvement of the Drug Loading Capacity of PEO-b-PCL with Increasing PCL Content for Two Hydrophobic Cucurbitacin Drugs. *Biomacromolecules*, **10**, 2584-2591.

Peng H., Zhou S., Guo T., Li Y., Li X., Wang J. and Weng J., (2008). In vitro degradation and release profiles for electrospun polymeric fibers containing paracetanol. *Colloids Surf., B*, **66**, 206-212.

Peppas N. A., (1985). Analysis of Fickian and non-Fickian drug release from polymers. *Pharm. Acta Helv.*, **60**, 110-111.

Pornsopone V., Supaphol P., Rangkupan R. and Tantayanon S., (2005). Electrospinning of methacrylate-based copolymers: Effects of solution concentration and applied electrical potential on morphological appearance of as-spun fibers. *Polymer Engineering & Science*, **45**, 1073-1080.

Powell H. M., Supp D. M. and Boyce S. T., (2008). Influence of electrospun collagen on wound contraction of engineered skin substitutes. *Biomaterials*, **29**, 834-843.

Prince J., Montoya A., Ferrat G. and Valente J. S., (2009). Proposed General Sol−Gel Method to Prepare Multimetallic Layered Double Hydroxides: Synthesis, Characterization, and Envisaged Application. *Chemistry of Materials*, **21**, 5826-5835.

Pukánszky B., (2005). Interfaces and interphases in multicomponent materials: past, present, future. *European Polymer Journal*, **41**, 645-662.

Qi M., Li X., Yang Y. and Zhou S., (2008). Electrospun fibers of acid-labile biodegradable polymers containing ortho ester groups for controlled release of paracetamol. *Eur. J. Pharm. Biopharm.*, **70**, 445-452.

Qin X.-H. and Wang S.-Y., (2006). Filtration properties of electrospinning nanofibers. *J. Appl. Polym. Sci.*, **102**, 1285-1290.

Raemdonck K., Demeester J. and De Smedt S., (2009). Advanced nanogel engineering for drug delivery. *Soft Matter*, **5**, 707-715.

Ramakrishna S., Fujihara K., Teo W.-E., Yong T., Ma Z. and Ramaseshan R., (2006). Electrospun nanofibers: solving global issues. *Materials Today*, **9**, 40-50.

Reynaud E., Gauthier C. and Perez J., (1999). Nanophases in polymers. *Rev. Metall./Cah. Inf. Tech.*, **92**, 169-176.

Reznik S. N., Yarin A. L., Theron A. and Zussman E., (2004). Transient and steady shapes of droplets attached to a surface in a strong electric field. *Journal of Fluid Mechanics*, **516**, 349-377.

Rho K. S., Jeong L., Lee G., Seo B.-M., Park Y. J., Hong S.-D., Roh S., Cho J. J., Park W. H. and Min B.-M., (2006). Electrospinning of collagen nanofibers: Effects on the behavior of normal human keratinocytes and early-stage wound healing. *Biomaterials*, **27**, 1452-1461.

Rives V., (2001). Layered Double Hydroxides: Present and Future. Nova Science Publishers Inc., New York (US).

Romeo V., Gorrasi G., Vittoria and Chronakis I. S., (2007). Encapsulation and Exfoliation of Inorganic Lamellar Fillers into Polycaprolactone by Electrospinning. *Biomacromolecules*, **8**, 3147-3152.

Rutledge G. C., Li Y., Fridrikh S., Warner S. B., Kalayci V. E. and Patra P., (2000). Electrostatic Spinning and Properties of Ultrafine Fibers. *National Textile Center*, **Annual Report (M98-D01) 2000**, 1-10.

Sabir M. I., Xu X. and Li L., (2009). A review on biodegradable polymeric materials for bone tissue engineering applications. *J. Mater. Sci.*, **44**, 5713-5724.

Said S. S., Aloufy A. K., El-Halfawy O. M., Boraei N. A. and El-Khordagui L. K., (2011). Antimicrobial PLGA ultrafine fibers: Interaction with wound bacteria. *Eur. J. Pharm. Biopharm.*, **79**, 108-118.

Salomon J.-L. and Doelker E., (1980). Formulation des comprimés à libération prolongée. *Pharm. Acta Helv.*, **55**, 174-182.

Sammartino G., Marenzi G., Tammaro L., Bolognese A., Calignano A., Costantino U., Califano L., Mastrangelo F., Tetè S. and Vittoria V., (2005). Anti-inflammatory drug incorporation into polymeric nano-hybrids for local controlled release. *International journal of immunopathology and pharmacology*, **18**, 55-62.

Shin Y. M., Hohman M. M., Brenner M. P. and Rutledge G. C., (2001a). Electrospinning: A whipping fluid jet generates submicron polymer fibers. *Applied Physics Letters*, **78**, 1149-1151

Shin Y. M., Hohman M. M., Brenner M. P. and Rutledge G. C., (2001b). Electrospinning: A whipping fluid jet generates submicron polymer fibers. *Applied Physics Letters*, **78**, 1149-1151.

Sill T. J. and von Recum H. A., (2008). Electrospinning: Applications in drug delivery and tissue engineering. *Biomaterials*, **29**, 1989-2006.

Södergård A. and Stolt M., (2010). Industrial Production of High Molecular Weight Poly(Lactic Acid), In: Poly(Lactic Acid). John Wiley & Sons, Inc., pp. 27-41.

Songsurang K., Pakdeebumrung J., Praphairaksit N. and Muangsin N., (2011). Sustained Release of Amoxicillin from Ethyl Cellulose-Coated Amoxicillin/Chitosan–Cyclodextrin-Based Tablets. *AAPS PharmSciTech*, **12**, 35-45.

References

Sorrentino A., Gorrasi G., Tortora M., Vittoria V., Costantino U., Marmottini F. and Padella F., (2005). Incorporation of Mg-Al hydrotalcite into a biodegradable Poly(ε-caprolactone) by high energy ball milling. *Polymer*, **46**, 1601-1608.

Stevanovic M. and Uskokovic D., (2009). Poly(lactide-co-glycolide)-based Micro and Nanoparticles for the Controlled Drug Delivery of Vitamins. *Curr. Nanosci.*, **5**, 1-14.

Suganya S., Senthil Ram T., Lakshmi B. S. and Giridev V. R., (2011). Herbal drug incorporated antibacterial nanofibrous mat fabricated by electrospinning: An excellent matrix for wound dressings. *J. Appl. Polym. Sci.*, **121**, 2893-2899.

Sun W., Starly B., Nam J. and Darling A., (2005). Bio-CAD modeling and its applications in computer-aided tissue engineering. *Computer-Aided Design*, **37**, 1097-1114.

Sun Z., Zussman E., Yarin A. L., Wendorff J. H. and Greiner A., (2003). Compound Core–Shell Polymer Nanofibers by Co-Electrospinning. *Advanced Materials*, **15**, 1929-1932.

Surendran D., Sarath Kumar R. S., Geetha C. S. and Mohanan P. V., (2012). Long Term Effect of Biodegradable Polymer on Oxidative Stress and Genotoxicity. *BIO*, **2**, 37-46.

Taepaiboon P., Rungsardthong U. and Supaphol P., (2007). Vitamin-loaded electrospun cellulose acetate nanofiber mats as transdermal and dermal therapeutic agents of vitamin A acid and vitamin E. *Eur. J. Pharm. Biopharm.*, **67**, 387-397.

Tammaro L., Costantino U., Bolognese A., Sammartino G., Marenzi G., Calignano A., Tetè S., Mastrangelo F., Califano L. and Vittoria V., (2007). Nanohybrids for controlled antibiotic release in topical applications. *Int. J. Antimicrob. Agents*, **29**, 417-423.

Tammaro L., Costantino U., Nocchetti M. and Vittoria V., (2009a). Incorporation of active nano-hybrids into poly(ε-caprolactone) for local controlled release: Antifibrinolytic drug. *Appl. Clay Sci.*, **43**, 350-356.

Tammaro L., Russo G. and Vittoria V., (2009b). Encapsulation of Diclofenac Molecules into Poly(ε-Caprolactone) Electrospun Fibers for Delivery Protection. *J. Nanomater.*, **2009**.

Tan A., Rajadas J. and Seifalian A. M., (2012). Biochemical engineering nerve conduits using peptide amphiphiles. *J. Controlled Release*, **163**, 342-352.

Taylor G., (1964). Disintegration of Water Drops in an Electric Field. *Proceedings of the Royal Society of London. Series A. Mathematical and Physical Sciences*, **280**, 383-397.

Taylor G., (1966). The Force Exerted by an Electric Field on a Long Cylindrical Conductor. *Proceedings of the Royal Society of London. Series A. Mathematical and Physical Sciences*, **291**, 145-158.

Taylor G., (1969). Electrically Driven Jets. *Proceedings of the Royal Society of London. A. Mathematical and Physical Sciences*, **313**, 453-475.

Teo E. Y., Ong S.-Y., Khoon Chong M. S., Zhang Z., Lu J., Moochhala S., Ho B. and Teoh S.-H., (2011). Polycaprolactone-based fused deposition modeled mesh for delivery of antibacterial agents to infected wounds. *Biomaterials*, **32**, 279-287.

Teo W. E. and Ramakrishna S., (2006). A review on electrospinning design and nanofibre assemblies. *Nanotechnology*, **17**, R89-106.

Tokiwa Y. and Suzuki T., (1977). Hydrolysis of polyesters by lipases. *Nature*, **270**, 76-78.

Valenta C. and Auner B. G., (2004). The use of polymers for dermal and transdermal delivery. *Eur. J. Pharm. Biopharm.*, **58**, 279-289.

Valente J. S., Hernandez-Cortez J., Cantu M. S., Ferrat G. and López-Salinas E., (2010). Calcined layered double hydroxides Mg–Me–Al (Me: Cu, Fe, Ni, Zn) as bifunctional catalysts. *Catal. Today*, **150**, 340-345.

Valente J. S. and Prince J., (2010). Layered Double Hydroxides: Properties, Applications and Synthetic Procedures. *SciTopics. Retrieved November 6, 2012*.

Valente J. S., Tzompantzi F., Prince J., Cortez J. G. H. and Gomez R., (2009). Adsorption and photocatalytic degradation of phenol and 2,4 dichlorophenoxiacetic acid by Mg–Zn–Al layered double hydroxides. *Applied Catalysis B: Environmental*, **90**, 330-338.

Verreck G., Chun I., Peeters J., Rosenblatt J. and Brewster M. E., (2003). Preparation and Characterization of Nanofibers Containing Amorphous Drug Dispersions Generated by Electrostatic Spinning. *Pharmaceutical Research*, **20**, 810-817.

Vittoria V., Tammaro L., Bugatti V. and Bianchi R. (2011). Processo di preparazione di una composizione polimerica comprendente idrotalciti intercalate con molecole attive, composizione così ottenuta e articoli formati comprendenti la stessa, MI2011A001921 (Italy).

Von Werne T. and Patten T. E., (1999). Preparation of Structurally Well-Defined Polymer-Nanoparticle Hybrids with Controlled/Living Radical Polymerizations. *Journal of the American Chemical Society*, **121**, 7409-7410.

Wei A., Wang J., Wang X., Wei Q., Ge M. and Hou D., (2010). Preparation and characterization of the electrospun nanofibers loaded with clarithromycin. *J. Appl. Polym. Sci.*, **118**, 346-352.

References

Whang K., Thomas C. H., Healy K. E. and Nuber G., (1995). A novel method to fabricate bioabsorbable scaffolds. *Polymer*, **36**, 837-842.

Wu C.-S., (2009). Renewable resource-based composites of recycled natural fibers and maleated polylactide bioplastic: Characterization and biodegradability. *Polymer Degradation and Stability*, **94**, 1076-1084.

Wu H., Fan J., Chu C.-C. and Wu J., (2010a). Electrospinning of small diameter 3-D nanofibrous tubular scaffolds with controllable nanofiber orientations for vascular grafts. *J. Mater. Sci.: Mater. Med.*, **21**, 3207-3215.

Wu X.-m., Branford-White C., Zhu L.-m., Chatterton N. and Yu D.-g., (2010b). Ester prodrug-loaded electrospun cellulose acetate fiber mats as transdermal drug delivery systems. *J. Mater. Sci.: Mater. Med.*, **21**, 2403-2411.

Xu J., Jiao Y., Shao X. and Zhou C., (2011). Controlled dual release of hydrophobic and hydrophilic drugs from electrospun poly(l-lactic acid) fiber mats loaded with chitosan microspheres. *Mater. Lett.*, **65**, 2800-2803.

Xu Z. P. and Braterman P. S., (2010). Synthesis, structure and morphology of organic layered double hydroxide (LDH) hybrids: Comparison between aliphatic anions and their oxygenated analogs. *Appl. Clay Sci.*, **48**, 235-242.

Yang Y., Li X., Cheng L., He S., Zou J., Chen F. and Zhang Z., (2011). Core-sheath structured fibers with pDNA polyplex loadings for the optimal release profile and transfection efficiency as potential tissue engineering scaffolds. *Acta Biomater.*, **7**, 2533-2543.

Yarin A. L., Koombhongse S. and Reneker D. H., (2001). Bending instability in electrospinning of nanofibers. *J. Appl. Phys.*, **89**, 3018-3026.

Yoo C. R., Yeo I.-S., Park K. E., Park J. H., Lee S. J., Park W. H. and Min B.-M., (2008). Effect of chitin/silk fibroin nanofibrous bicomponent structures on interaction with human epidermal keratinocytes. *Int. J. Biol. Macromol.*, **42**, 324-334.

Zamani M., Morshed M., Varshosaz J. and Jannesari M., (2010). Controlled release of metronidazole benzoate from poly ε-caprolactone electrospun nanofibers for periodontal diseases. *Eur. J. Pharm. Biopharm.*, **75**, 179-185.

Zeleny J., (1914). The Electrical Discharge from Liquid Points, and a Hydrostatic Method of Measuring the Electric Intensity at Their Surfaces. *Physical Review*, **3**, 69-91.

Zeltinger J., Sherwood J. K., Graham D. A., Müeller R. and Griffith L. G., (2001). Effect of pore size and void fraction on cellular adhesion, proliferation, and matrix deposition. *Tissue Eng.*, **7**, 557-572.

Zeng J., Xu X., Chen X., Liang Q., Bian X., Yang L. and Jing X., (2003). Biodegradable electrospun fibers for drug delivery. *J. Controlled Release*, **92**, 227-231.

Zeng J., Yang L., Liang Q., Zhang X., Guan H., Xu X., Chen X. and Jing X., (2005). Influence of the drug compatibility with polymer solution on the release kinetics of electrospun fiber formulation. *J. Controlled Release*, **105**, 43-51.

Zilberman M. and Elsner J. J., (2008). Antibiotic-eluting medical devices for various applications. *J. Controlled Release*, **130**, 202-215.

Zong X., Kim K., Fang D., Ran S., Hsiao B. S. and Chu B., (2002). Structure and process relationship of electrospun bioabsorbable nanofiber membranes. *Polymer*, **43**, 4403-4412.